AD NUMBER: AD0900415

LIMITATION CHANGES

TO:

Approved for public release; distribution is unlimited.

FROM:

Distribution authorized to U.S. Government agencies only;
Test and Evaluation; 27 Jul 1972. Other requests must be referred to AFAL/AAA, Wright-Patterson AFB, OH 45433.

AUTHORITY

ST-A AFAL LTR, 21 AUG 1975

AFAL-TR-72-49

LIGHTNING PROTECTION TECHNIQUES FOR LARGE CANOPIES ON HIGH SPEED AIRCRAFT

R. Aston, R. Gorton, G. L. Weinstock

MCDONNELL AIRCRAFT COMPANY
MCDONNELL DOUGLAS CORPORATION

TECHNICAL REPORT AFAL-TR-72-49
JANUARY 1972

Air Force Avionics Laboratory
Air Force Systems Command
Wright-Patterson Air Force Base, Ohio

NOTICE

When Government drawings, specifications, or other data are used for any purpose other than in connection with a definitely related Government procurement operation, the United States Government thereby incurs no responsibility nor any obligation whatsoever; and the fact that the government may have formulated, furnished, or in any way supplied the said drawings, specifications, or other data, is not to be regarded by implication or otherwise as in any manner licensing the holder or any other person or corporation, or conveying any rights or permission to manufacture, use, or sell any patented invention that may in any way be related thereto.

Copies of this report should not be returned unless return is required by security considerations, contractual obligations, or notice on a specific document.

LIGHTNING PROTECTION TECHNIQUES FOR LARGE CANOPIES ON HIGH SPEED AIRCRAFT

R. Aston, R. Gorton, G. L. Weinstock

MCDONNELL AIRCRAFT COMPANY
MCDONNELL DOUGLAS CORPORATION

TECHNICAL REPORT AFAL-TR-72-49
JANUARY 1972

FOREWORD

This report was prepared by the McDonnell Douglas Corporation, McDonnell Aircraft Company, Avionics Systems Technology Department under USAF Contract F33615-71-C-1581. The program was administered by the Air Force Avionics Laboratory, Air Force Systems Command, Systems Avionics Division, Wright-Patterson Air Force Base, Ohio. The Air Force project engineer directing the technical aspects of the study was Claude R. Austin AFAL/AAA.

This document is Technical Report AFAL-TR-72-49 and covers work accomplished from July 1971 to December 1971. This work was submitted by the authors January 1972.

This technical report has been reviewed and is approved.

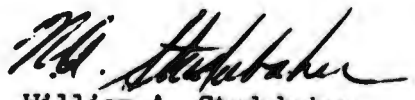

William A. Studabaker
Lt. Colonel, USAF
Chief
Systems Avionics Division

ABSTRACT

The objectives of the work covered by this report were to determine by analysis and experimental evaluation the susceptibility of an F-15 canopy to a lightning strike and to develop lightning protection methods for large canopies.

The primary hazard from a lightning strike to an aircraft canopy occurs if the canopy punctures and the lightning strikes the pilot. This hazard was analyzed mathematically and extensively tested on flat polycarbonate sheets, a simulated canopy and an actual F-15 canopy. Both the analysis and lightning simulation tests showed that the F-15 canopy will not puncture but rather that the lightning would flashover to the canopy frame.

A detailed experimental investigation of corona inside the canopy due to the electric field from a lightning strike was performed. The investigation showed corona not to be a serious hazard but final assessment would require a medical study.

High current tests were performed on the canopy frame and proved that the canopy mounting and frame could withstand 200,000 amp currents. Three lightning diverter systems were designed and tested. Two of the designs proved effective for large canopy application.

The conclusion arrived at as the result of this program is that additional lightning protection for the F-15 canopy is not necessary. Furthermore, it should be noted that although an F-15 canopy was used in this study, the results are general enough that they can be usefully extrapolated to include the canopies and dielectric surfaces on other air vehicles.

TABLE OF CONTENTS

LIST OF ILLUSTRATIONS

LIST OF ILLUSTRATIONS (Continued)

LIST OF ILLUSTRATIONS (Continued)

LIST OF ILLUSTRATIONS (Continued)

LIST OF ILLUSTRATIONS (Continued)

LIST OF TABLES

LIST OF SYMBOLS

A	-	Area
d	-	Material Thickness
ξ	-	Energy
E	-	Electric Field Strength
E_b	-	Breakdown Value of the Electric Field Strength
e	-	Electronic Charge
K	-	Relative Dielectric Constant
l	-	Length
M	-	Mass
R	-	Resistance
r	-	Resistivity
S	-	Specific Heat
T	-	Temperature
V	-	Voltage
w	-	Width of Material
X	-	Coefficient of Thermal Expansion
Y	-	Youngs Modulus
α	-	Temperature Coefficient of Resistance
λ	-	Line Charge Density in a Lightning Strike
ℓ	-	Mass Density
τ	-	Time
MV	-	Megavolts = 1×10^6 Volts
KV	-	Kilovolts = 1×10^3 Volts
Kamps	-	Kiloamperes = 1×10^3 Amperes
MCAIR	-	MCDONNELL AIRCRAFT COMPANY

Section 1

INTRODUCTION AND SUMMARY

The F-15 lightning attach point studies previously conducted by McDonnell Aircraft Company (Reference 1) showed that the canopy can be struck by lightning (Figure 1). A pilot hazard can result if the canopy is punctured or if corona (in large amounts) is induced off the pilot's head.

This program included a detailed analysis of the lightning susceptibility characteristics of the F-15 canopy. Tests were performed on sheets of Lexan (the canopy material) and on a full-size canopy. Investigations of the criteria that determines either surface flashover or canopy material puncture were performed on flat Lexan sheets. An actual F-15 canopy was used for experimental evaluation and verification of the analysis of the primary hazard of canopy puncture and the secondary hazard of corona inside the canopy.

Tests were also performed on three candidate diverter systems to determine the effectiveness of various protective systems. These included both high current and high voltage tests.

The investigation of corona inside the canopy concluded that corona does not present a serious hazard to the crew. Analysis and test show that the canopy will not puncture. Therefore, additional lightning protection for the F-15 canopy is not necessary.

During the program, the services of the Lightning and Transient Research Institute (Mr. J. Stahman) and the lightning protection specialist of the Douglas Aircraft Company Division of McDonnell Douglas Corporation (Mr. M. Amason) were used as consultants. The testing and analysis was performed at McDonnell Aircraft Company facilities in St. Louis, Missouri.

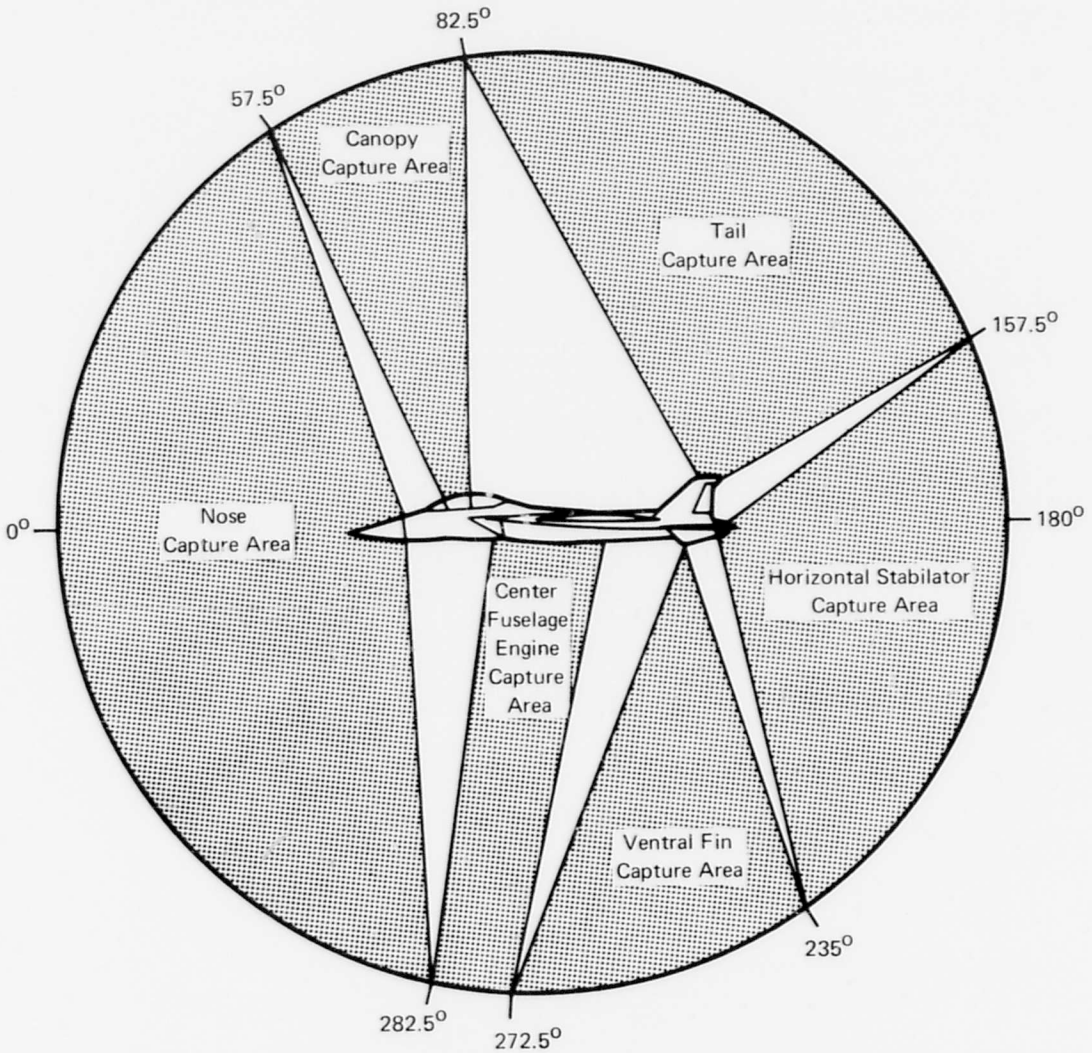

FIGURE 1 F-15 LIGHTNING ATTACHMENT POINTS

Section 2

ANALYSIS AND DESIGN

A review of technical literature revealed that little work had been done on the breakdown of a solid dielectric in air. Due to the difficulties encountered in puncturing a solid dielectric, such as Lexan, plexiglass or other polycarbonates, when air is the ambient medium, most breakdown studies have been performed in a liquid medium (e.g. oil bath). The difficulty of puncturing Lexan was encountered in our laboratory testing and, despite extensive attempts to cause large sheets (48 inch x 96 inch x 1/8 inch) to puncture in air, it never occurred.

As shown in Appendix I , the observed dielectric strength of the material is very dependent upon the method of measurement. Standard American Society for Testing and Materials (A.S.T.M.) tests for "Dielectric Breakdown and Dielectric Strength of Electrical Insulating Materials at Commercial Power Frequencies", (Reference 2), specify "Short Time Test"; "Slow Rate of Rise Test"; and "Step by Step Test", all of which are designed to obtain dielectric breakdown which takes a time span of from 10 seconds to minutes. This type of testing is applicable to insulation testing but not to the relatively rapid lightning stroke. By applying a higher voltage, breakdown is caused in a shorter time. Appendix II extrapolates results of published data on the dielectric breakdown of Lexan polycarbonate material to the requirements of the present application.

2.1 ANALYSIS OF PRIMARY HAZARD - CANOPY PUNCTURE

Appendices III and IV analyze the effect of a uniform field on a canopy and the electric field of a lightning strike.

An analysis which assumes the canopy is equivalent to a dielectric cylinder (Appendix III) in a uniform electric field, and which maintains the inner surface at a reference zero potential, shows that the maximum electric field strength that air can sustain at normal atmospheric pressures cannot cause breakdown of the canopy dielectric in this configuration. At any dielectric boundary, Maxwell's equations require continuity of the normal component of the electric displacement, D

$$D = K_1 E_1 = K_2 E_2$$

where K and E are the dielectric constant and electric field strengths respectively in medium 1 (air) $K_1=1$ and medium 2 (Lexan) $K_2=3$. Solving the above for the electric field in Lexan yields

$$E_2 = \frac{K_1}{K_2} E_1 .$$

Since, the minimum electric field necessary to cause breakdown in 0.29 inch (the F-15 canopy thickness) Lexan is about 350 Kv per inch, it would be necessary to maintain a field in air of three times this figure, i.e., over 1×10^6 V per inch. Air is able to maintain such a high electric field only at high pressure (of several atmospheres or more) and over very short distances (fractions of an inch). Before

the Lexan breaks down, air breakdown occurs which restricts the value of the applied electric field to a level below that required to cause breakdown in Lexan.

2.2 SIGNIFICANT SECONDARY EFFECTS

Although canopy puncture by the lightning stroke was considered the primary hazard, the study also considered the following secondary effects of a lightning strike:

a) Corona hazard to pilot.

b) Danger of activation of the canopy ejection device.

c) Conduction of the high current causing welding of the aircraft frame to the canopy frame.

2.2.1 Corona

Investigations, including analysis and testing, were conducted to assess the magnitude of the corona that would be induced under the canopy by a lightning strike. Photographs of corona streamers from the top of the simulated pilot's seat were obtained. Section 3 of this report gives the results of that study.

2.2.2 Canopy Ejection Mechanism

The positioning of the explosive mechanism used for the ejection of the canopy and the pilot seat was investigated. The triggering device is mechanical rather than electrical, and the explosive cable is situated where it is not exposed to induced corona streamers and is not in the conductive path of a lightning strike from the canopy to the airframe. Therefore, the ejection mechanism will not be affected by a lightning strike.

2.2.3 Conduction of Canopy Strike to Airframe

High current tests of 200,000 amperes from the arches to the canopy metal frame were performed. The conduction path from the canopy frame to the airframe is through a number of parallel paths. There are four separate canopy stainless steel retaining hooks which are clamped to the canopy frame by the canopy counterbalance actuator pressure. Each provides a conductive path between the canopy frame and the airframe. In addition, two canopy hinges behind the pilot seat also provide a high current conductive path. The high current test results are discussed in Section 3.

2.3 LIGHTNING PROTECTION

The mechanical design of the F-15 canopy is such that the maximum surface distance to a metallic point capable of carrying a 200 KA strike is approximately 31 inches. The maximum voltage on the canopy is proportional to this distance times the maximum flashover electric field on the surface. The maximum voltage can therefore be reduced by either reducing the flashover distance or the electric field required for surface breakdown. Thus, protective devices are designed to reduce the flashover distance to divert a lightning strike, and to reduce the electric field required to initiate flashover. Appendix V contains design information used in the evaluation of various lightning diverter systems.

The designs of various diverter systems were studied with regard to the specific requirements of this program. The main criteria involved were:

a) Crew lightning protection
b) Safety
c) Crew ejection capability
d) Visibility
e) Crew performance
f) Cost, maintenance and ease of retrofit
g) Aerodynamic effects.

2.3.1 External Solid Bar Diverter

The first diverter system considered was that of a solid aluminum bar 3/8 inch X .124 inch X 40 inches long. It would extend from above the back of the pilot's head to the canopy arch. The temperature rise due to a high current strike or aerodynamic heating causes considerable differential expansion between the metal bar and the Lexan canopy. Appendix V analyzes the effects of the physical properties of a solid bar diverter made of copper or aluminum caused by temperature rise as a function of the cross-sectional area when struck by a 200K amp peak and 43 microsecond duration lightning strike.

Appendix V also shows the difference in the thermal expansion rates of Lexan (3.75×10^{-5}/°F) and copper ($.89 \times 10^{-5}$/°F) or aluminum (1.59×10^{-5}/°F) to be a problem. In this case, the expansion problem cannot be minimized by increasing the cross-sectional area of the diverter. Such a large difference in expansion places a considerable strain upon the bond between the diverter and the canopy. In laboratory bond tests, none of the adhesives were found capable of bonding metal to Lexan at the high temperatures anticipated by worst case aerodynamic heating.

High magnetic forces are produced in a 200K amp lightning strike. Diverter damage caused by these magnetic forces compound the temperature problem. A report of the method of magnetic force calculation is presented in Appendix VI.

Since adhesive attachment of a bar diverter is not feasible, other methods of attachment were examined. Attaching the external metal bar diverter by means of a sliding mechanism, allowing the rod to move longitudinally, could solve the differential expansion problem. However, the sliding mechanism would have to be capable of withstanding the high magnetic forces and would be undesirable because the total system cross-sectional area would be large and would increase aerodynamic drag and reduce visibility.

Any screw fastening method is also undesirable because a metal screw would introduce the electric field directly into the canopy and a dielectric screw of adequate strength would be too large.

For the reasons discussed in this section, it is therefore considered impractical to use an external solid bar on the canopy for lightning protection.

2.3.2 Ionizing Button Strip Diverter Outside the Canopy

This type of diverter was originally designed and developed by Douglas Aircraft Company for use on commercial aircraft. The button strip diverter is

shown in Figure 103 of Appendix V. It is constructed of a thin insulating strip with a resistive film coating on the underside and metal buttons (about ten per inch) along the entire length on the top side, with small air gaps between each button. The buttons are connected through the strip to the resistive film on the other side. Due to the high resistance between individual buttons, a high current does not flow in the strip itself.

The metal buttons act as a "catalyst" in ionizing the air adjacent to the row of buttons. The low prestrike current causes a high voltage between adjacent buttons leading to ionization and corona current over the surface of the strip. This leads to breakdown in the air at a reduced voltage, providing a low impedance air path to the end of the strip, which is attached to the metal canopy frame.

Differential expansion problems can be circumvented by use of Lexan as the base material in which the buttons are mounted. Since the high current does not flow in the diverter, the magnetic forces do not act on the diverter and available adhesives can be used to attach it to the canopy.

2.3.3 Metal Strip Diverter Under the Canopy

A thin metal strip inside the canopy, extending from a point above the back of the pilot's head to the canopy arch, is also a practical alternative. Since it is inside the canopy, it does not have the aerodynamic problems associated with an external diverter. The low current conducted by the internal diverter means that a small cross-section can be used, so that the mechanical forces (due to differential expansion) are small; thus, the strip can be held by available adhesives. Since the strip is narrow, visibility restrictions are also less than the other two candidate diverters. The internal metal strip is rated as a second choice for protection in Table I (a) since it is not as effective as the button strip in reducing the surface flashover voltage. Tests results (see Section 3) have shown that the electric field required for flashover is 5 KV per inch with the internal diverter compared to 1.2 KV per inch for the button strip, and 19 KV per inch without any form of protection.

To determine the probability of puncture, laboratory tests were performed using both flat Lexan sheets and an actual F-15 canopy. Since puncture did not occur, additional tests were performed using a simulated canopy of 1/8 inch thick Lexan sheet (approximately 1/2 the canopy thickness). The sheet was formed into a flat bottom hollow cylinder with a greater diameter than the actual canopy in order to establish a minimum safety factor. Again, external surface flashover occurred when a high-voltage arc was forced to strike the canopy and no punctures were found. Laboratory tests (described in Section 3) were performed with the strip exposed and with it coated with an insulating material.

In order to evaluate the relative protection effectiveness of the two methods regarded as most feasible (button strip and inside diverter), a simultaneous test of the two diverters was performed by mounting the two strips on a flat Lexan sheet, on parallel axes spaced 12 inches apart. High-voltage breakdown tests to the diverters were then performed at various distances and positions to establish the relative "attraction" each had upon the breakdown path (Section 3). At a distance from the surface greater than 6 inches, the button diverter had a greater attraction. After

considering all the criteria listed in Section 2.3, and the ramifications of each device, the preferred diverter for this application is a metal strip inside the canopy extending from a point above the back of the pilot's head to the canopy arch.

2.3.4 Diverter Comparison

The three candidate diverters are rated for various requirements in Table I:

TABLE I

COMPARISON OF CANDIDATE DIVERTERS

Criteria	Diverter Type: External Solid Bar	External Button Strip	Internal Metal Strip
a Protection (1)	3 (U)	1 (A)	2 (A)
b Safety (2)	3 (U)	2 (A)	1 (A)
c Ejection (3)	No effect	No effect	No effect
d Visibility (4)	3 (A)	2 (A)	1 (A)
e Cost/Retrofit (5)	2 (A)	3 (A)	1 (A)
f Aerodynamics (6)	2 (A)	3 (A)	1 (A)
g Thermal (7)	3 (U)	2 (A)	1 (A)

Numbers (1, 2, 3) refer to the order of effectiveness

(A) = Acceptable (U) = Unacceptable

Criteria Notes:

(1) Although classified in order of effectiveness, all three diverters cause a significant reduction in flashover voltage.

(2) The external solid bar was considered potentially dangerous due to attachment problems and resultant whipping of the canopy if partial detachment occurred.

(3) None of the diverters were considered deleterious to the crew ejection capability since no interference is involved in the physical mounting method.

(4) Visibility was considered a potential problem with the external solid bar if a sliding mechanism were used.

(5) Cost and retrofit could be a problem if a sliding mechanism were used for mounting the external solid bar.

(6) Aerodynamic effects with a sliding mechanism may move the external solid bar to third choice.

(7) Thermal expansion problems due to aerodynamic heating of the canopy are unacceptable for the external bar (See Section 2.3.1).

Section 3

LABORATORY TESTS

3.1 GENERAL TEST DESCRIPTION

Laboratory tests were performed to investigate surface flashover on a Lexan-air interface and the possibility of dielectric breakdown. These were accomplished on flat Lexan sheets, a simulated F-15 canopy and an actual F-15 canopy. Tests were also performed to investigate corona inside the canopy caused by a simulated lightning strike both with and without lightning protection.

Laboratory testing of the following three candidate diverters was performed:

a) A solid bar on the outside of the canopy extending from above the back of the pilot's head to the canopy frame.

b) A metal strip inside the canopy extending from above the back of the pilot's head to the canopy frame.

c) A system of metal buttons on the outside of the canopy extending from above the back of the pilot's head to the canopy frame.

All tests described in this report were performed in the MCAIR Lightning Simulation Laboratory in St. Louis. The principal facilities used were a 200K amp high current generator and a 1.6 MV high voltage Marx generator. A smaller, 250 KV Marx generator was used for the flat sheet surface flashover measurements. A complete description of the MCAIR Lightning Simulation facility is presented in Appendix VII.

3.2 DISPOSITION OF TEST ITEMS

All test articles are stored at the McDonnell Aircraft Company facility in St. Louis.

3.3 VALIDITY OF TESTING

Serious consideration was given to the question as to how valid long laboratory sparks are in simulating a lightning strike. This is discussed in F.A.A. Report No. NA-69-27 (Reference 3). The report states that the long laboratory spark can simulate most of the properties of the electric field associated with a lightning strike, but not the continuing current phase nor the shock pressure wave. It is also believed that the spark adequately simulates the temporal characteristics of lightning discharges. In laboratory tests the long laboratory spark has been used only to simulate the electric field effects. Magnetic field effects have been simulated by a separate high current generator and are considered valid for the local effects investigated.

3.4 SURFACE FLASHOVER AT LEXAN-AIR INTERFACE (ANALYSIS VERIFICATION)

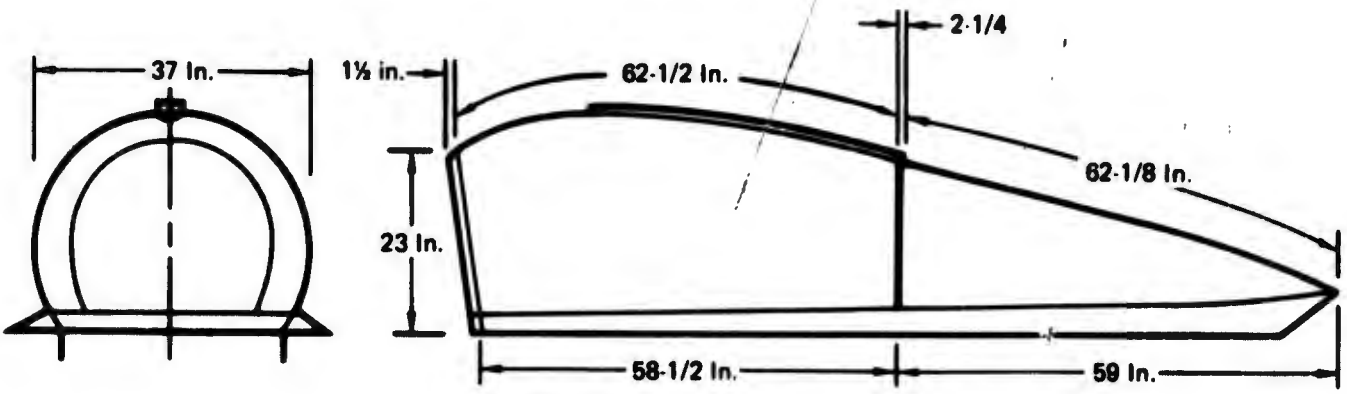

FIGURE 2 CANOPY SURFACE DIMENSIONS

The dimensions of the F-15 Lexan canopy are as shown in Figure 2. The maximum distance to metal from any point on the transparency surface is 31-1/4 inches.

Since the canopy thickness is 0.29 inch, the punch-through versus surface flashover criteria lies in comparing surface breakdown over 31 inches of air with dielectric breakdown through 0.29 inch of Lexan. (See Appendix I.) The conditions at the surface must be considered since the field causing surface flashover is the component parallel to the surface whereas the field in the Lexan involves the normal component as well. For this reason, the simplified analysis of a cylindrical canopy in a uniform field (Appendix III) was made. As stated in Appendix III, the configuration analyzed is more likely to puncture than the F-15 canopy.

The maximum potential difference between inner and outer surfaces, just before air breakdown, is 14,700 volts. This is equivalent to an average value of 50 volts per mil in the Lexan, which is insufficient to cause the Lexan to break down (see Appendix II).

An extension of this reasoning when applied to the Lexan sheet tests explains why puncture did not occur in the presence of an air gap.

In order to verify this analysis, differing thicknesses of Lexan sheet down to 1/8 inch thick were tested for puncture. As the applied voltage was increased air breakdown and resulting surface flashover always occurred. In order to use increased voltages large sheets, 1/8 inch thick, were used up to a maximum size of 48 x 84 inches. The electrodes were placed in the center of this sheet on opposite sides, giving a maximum surface distance to any edge of 24 inches.

The following significant results were obtained:

- Surface flashover on a Lexan surface between two rod electrodes on the same side (Figure 3) was 19 KV per inch
- Surface flashover on a Lexan surface with two rod electrodes on opposite sides (Figure 4) was 5 KV per inch
- Surface flashover on Lexan sheet with two rod electrodes on opposite sides, both normal to surface, was 5.4 KV/inch (2.75 KV/inch accounting for both surfaces) (Figure 5).

NOTE: Although surface tracking leaves an optically detectable path on the surface, this does not appear to affect the path of any subsequent discharge.

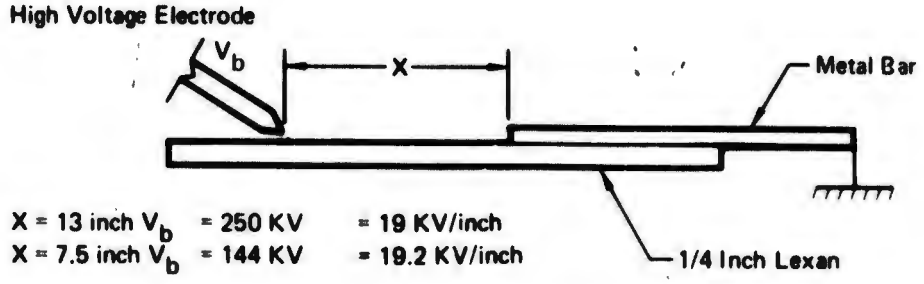

FIGURE 3 LEXAN-AIR SURFACE FLASHOVER

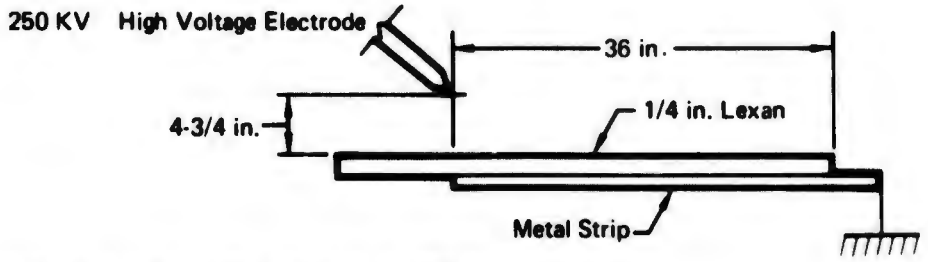

4-3/4 in. Air Gap + 36 in. Flashover = 250 KV
4-3/4 x 15 KV + 36 x E_b = 250 KV
Average Field E_b = 5 KV Per in.

FIGURE 4 LEXAN SURFACE FLASHOVER WITH DIVERTER BELOW THE LEXAN SHEET

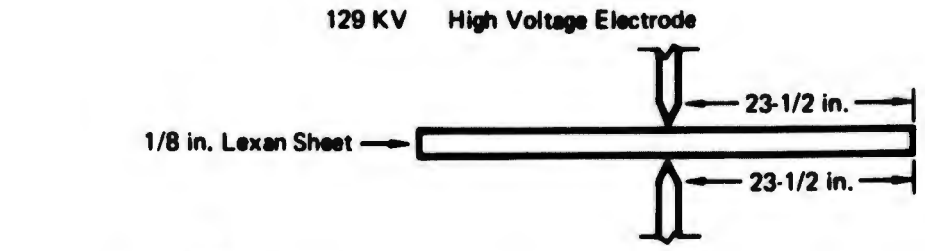

$$\text{Average Field} = \frac{129}{47} = 2.7 \text{ KV Per in.}$$

FIGURE 5 LEXAN SURFACE FLASHOVER WITH ANTITHETICAL ELECTRODES

The F-15 canopy material is coated with a very thin hardening coat. In order to determine the effect of the hardening coat on the surface breakdown, the flashover tests were repeated using the coated aft canopy section. No significant difference was found between the results using the coated canopy and the results obtained for uncoated flat Lexan sheets.

3.5 COMPARISON OF THE DIVERTER EFFECTIVENESS OF THE BUTTON STRIP OUTSIDE THE CANOPY AND A METAL STRIP INSIDE THE CANOPY

First the ionizing potential of the button strip was determined as shown in Figure 6. To evaluate the relative efficiency of the button strip outside the canopy and a metal strip on the interior surface of the canopy, 30 inch samples of each were mounted parallel, 12 inches apart, on a flat Lexan sheet as shown in Figure 7.

An electrode at a voltage high enough to cause breakdown was placed in different positions (coordinates x, y of Figure 7) at the ungrounded end of the diverters, and the resultant breakdown to one or the other diverter paths noted.

With the electrode touching the Lexan surface ($x = 0$) the breakdown path divided between the two paths when the electrode was at the mid point ($y = 6$ inches) (Figure 10). When the electrode was displaced from the center position, breakdown was to the nearest diverter.

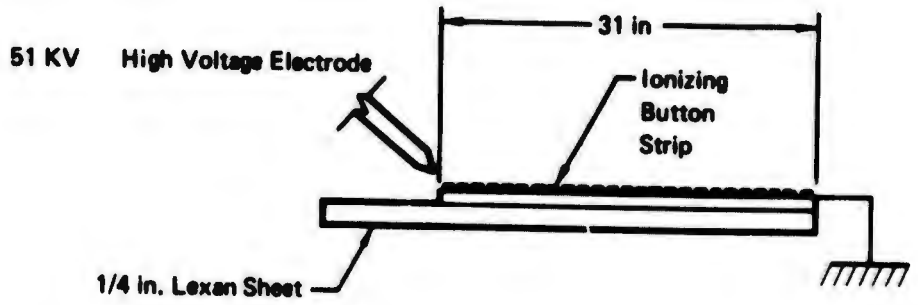

1 in. Air Gap + 31 in. Strip = 51 KV
31 in. Strip = (51-15) KV
1.16 KV Per in.

FIGURE 6 IONIZING POTENTIAL OF BUTTON STRIP

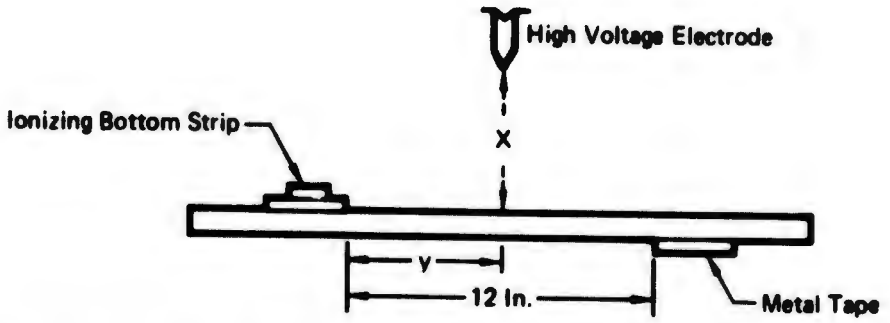

FIGURE 7 CONFIGURATION FOR COMPARISON OF RELATIVE DIVERTER EFFECTIVENESS

Experimental Data

x = 0	V_b = 215 KV	
y = 5"	Figure 8	Breakdown to ionizing strip
y = 5-3/4"	Figure 9	Breakdown to ionizing strip
y = 6"	Figure 10	Breakdown to both diverters
y = 8"	Figure 11	Breakdown to tape diverter

When the high voltage electrode was more than six inches from the surface of the Lexan sheet the breakdown path showed a distinct preference for the ionizing button strip, mounted on the upper surface, rather than breaking down to the path above the metal tape attached to the undersurface of the Lexan sheet.

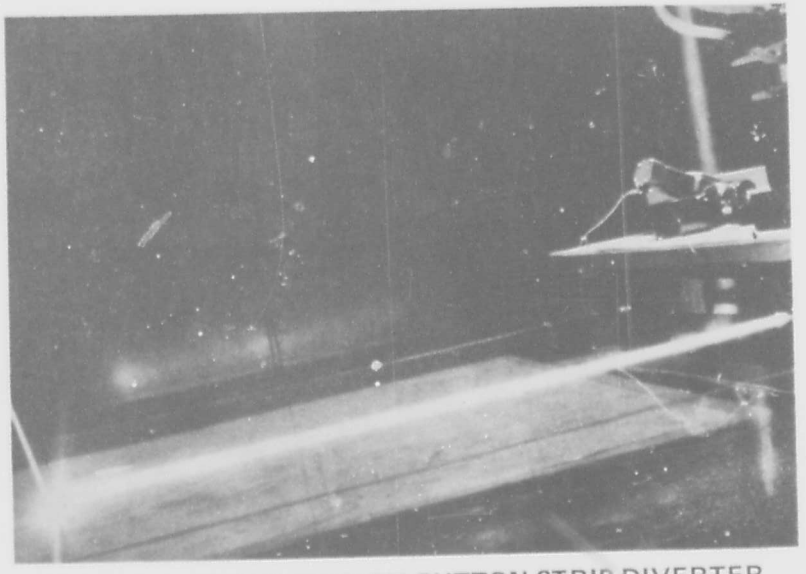

FIGURE 8 IONIZATION BY BUTTON STRIP DIVERTER
Y = 5 INCHES

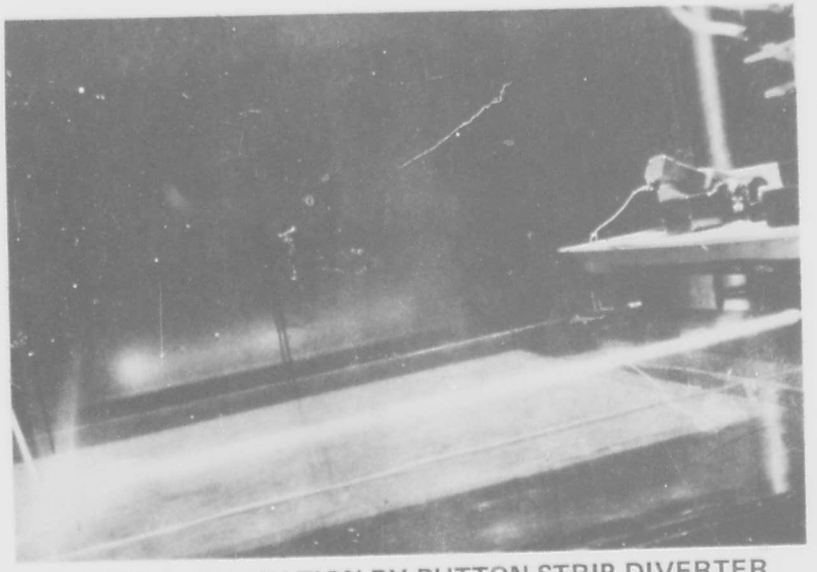

FIGURE 9 IONIZATION BY BUTTON STRIP DIVERTER
Y = 5-3/4 INCHES

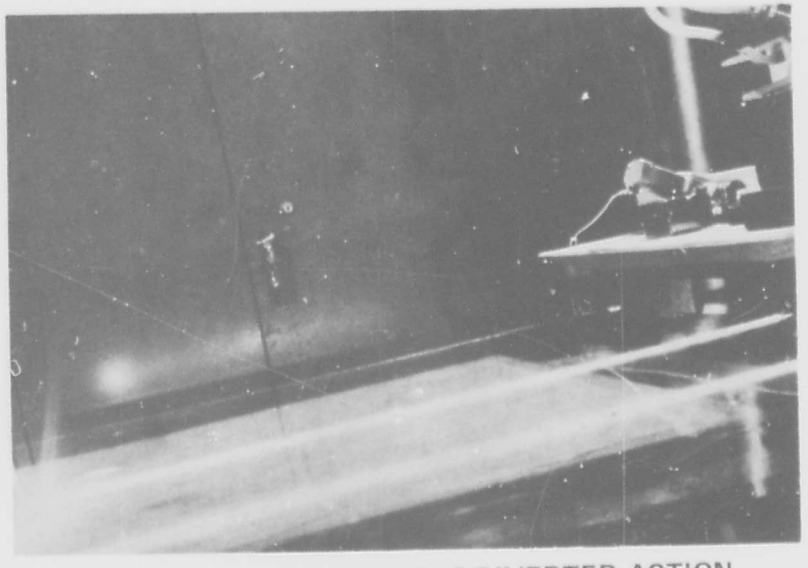

FIGURE 10 SIMULTANEOUS DIVERTER ACTION
Y = 6 INCHES

FIGURE 11 IONIZATION BY INTERNAL DIVERTER
Y = 8 INCHES

The more significant data points were as follows:

Figure	x	y	V_b	
12	1 inch	6 inches	220 KV	Critical points for breakdown to ionizing button strip rather than above the metal tape
13	5 inches	6 inches	220 KV	
14	5 inches	6 inches	220 KV	
15	9 inches	11 inches	250 KV	

3.6 HIGH VOLTAGE CORONA TESTS

3.6.1 Test Setup

An F-15 canopy was used to determine the magnitude of corona streamering current inside the canopy just before a lightning strike hits the canopy. The upper part of a simulated pilot seat was fixed inside the canopy and a pilot's helmet was attached to it. The earphones and microphone were grounded, but the seat frame was not. Three cameras were used. One with high speed roll film was used to photograph low intensity corona inside the canopy; the other two were Polaroid type cameras from two different angles. These were used to photograph the high intensity spark breakdown, and corona outside the canopy.

Figures 16 through 19 show the facility layout for simulating lightning strikes to the canopy transparency.

The transparency was mounted on a manual hydraulic lift. The forks of the hydraulic lift were extended about 6 feet by two wooden 6 inch x 6 inch beams in order to minimize the effects of the lift and forks on the local electric field.

The height of the high voltage probe was at 124 inches above floor level. The top of the canopy was about 40 inches above floor level.

Corona was studied under two circumstances:

1) With the high voltage generator set at slightly lower than the breakdown value so that a discharge would not occur

2) With the high voltage generator set above breakdown so that a spark to some part of the canopy occurred.

Under the transparency an actual pilot's helmet was located (see Figure 17) with the usually grounded parts connected to the metal frame and generator return. The seat was simulated by a simple metal framework insulated from the metal canopy frame by a 1/16 inch thick insulator to which it was attached mechanically. Photographs (Figures 19 and 20) show the layout and camera angles used. The camera used for photographing the corona under the canopy used high speed roll film and can be seen mounted on a tripod pointing towards the helmet and seat. Two polaroid cameras were used to photograph the long spark discharge.

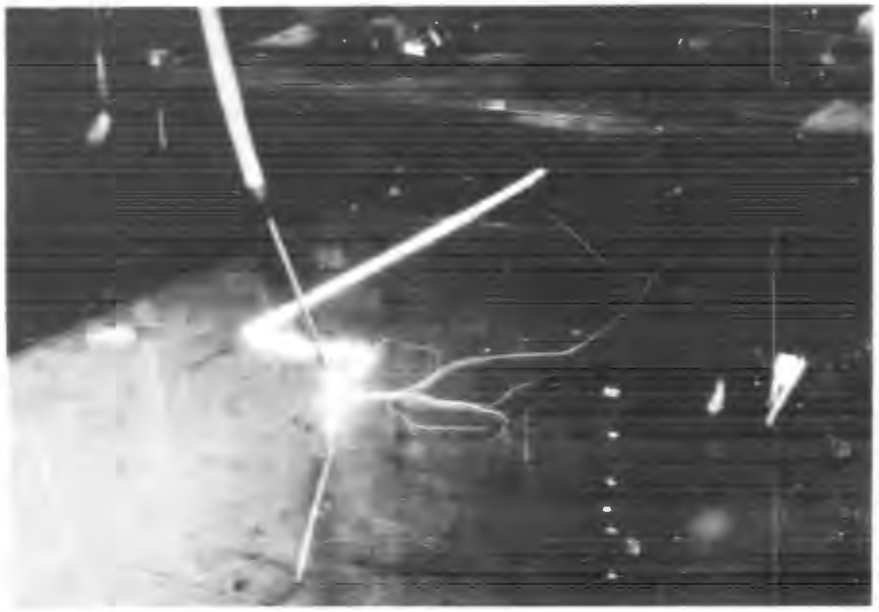

FIGURE 12 RELATIVE DIVERTER EFFECTIVENESS: ELECTRODE 1 INCH FROM SURFACE

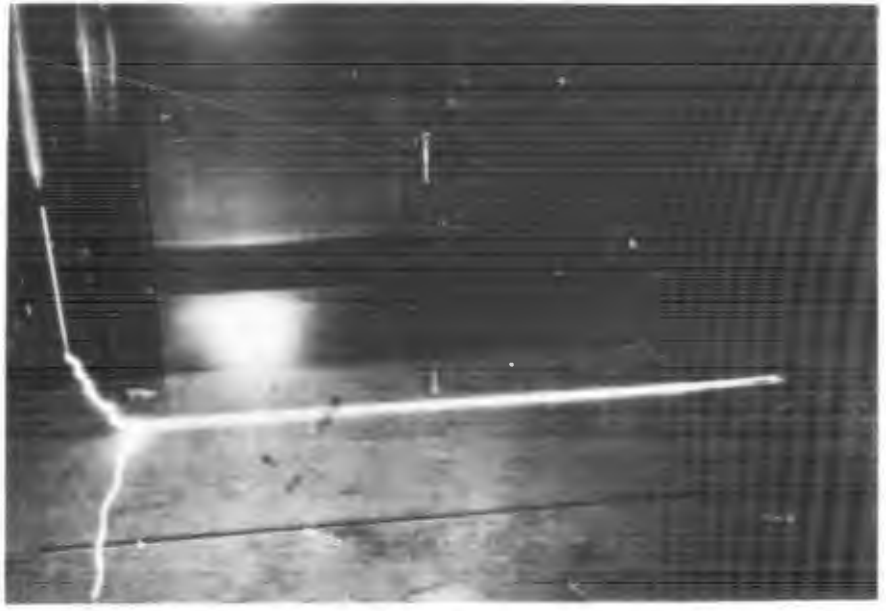

FIGURE 13 RELATIVE DIVERTER EFFECTIVENESS: ELECTRODE 5 INCHES FROM SURFACE

FIGURE 14 RELATIVE DIVERTER EFFECTIVENESS: ELECTRODE 9 INCHES FROM SURFACE

FIGURE 15 RELATIVE DIVERTER EFFECTIVENESS: ELECTRODE 9 INCHES FROM SURFACE

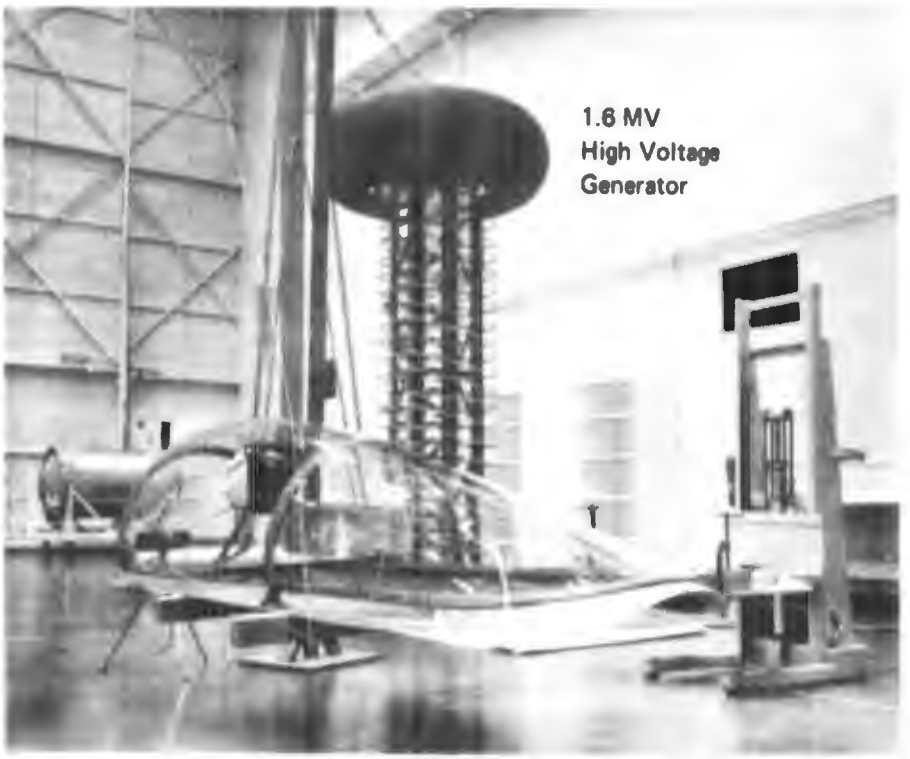

FIGURE 16 HIGH VOLTAGE GENERATOR AND CANOPY - SIDEVIEW

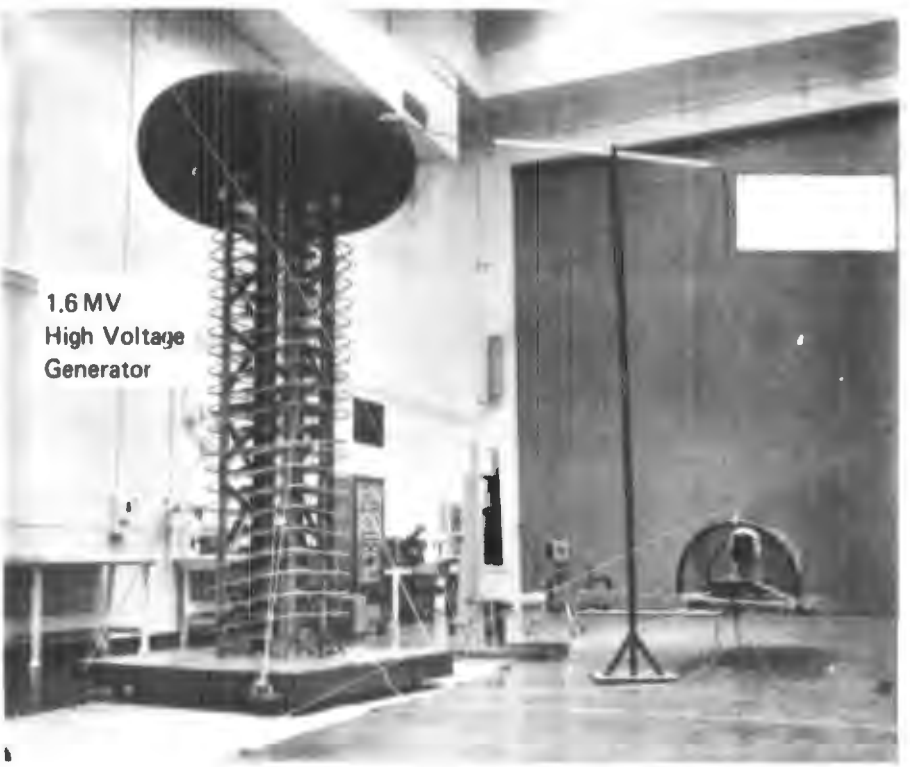

FIGURE 17 HIGH VOLTAGE GENERATOR AND CANOPY - ENDVIEW

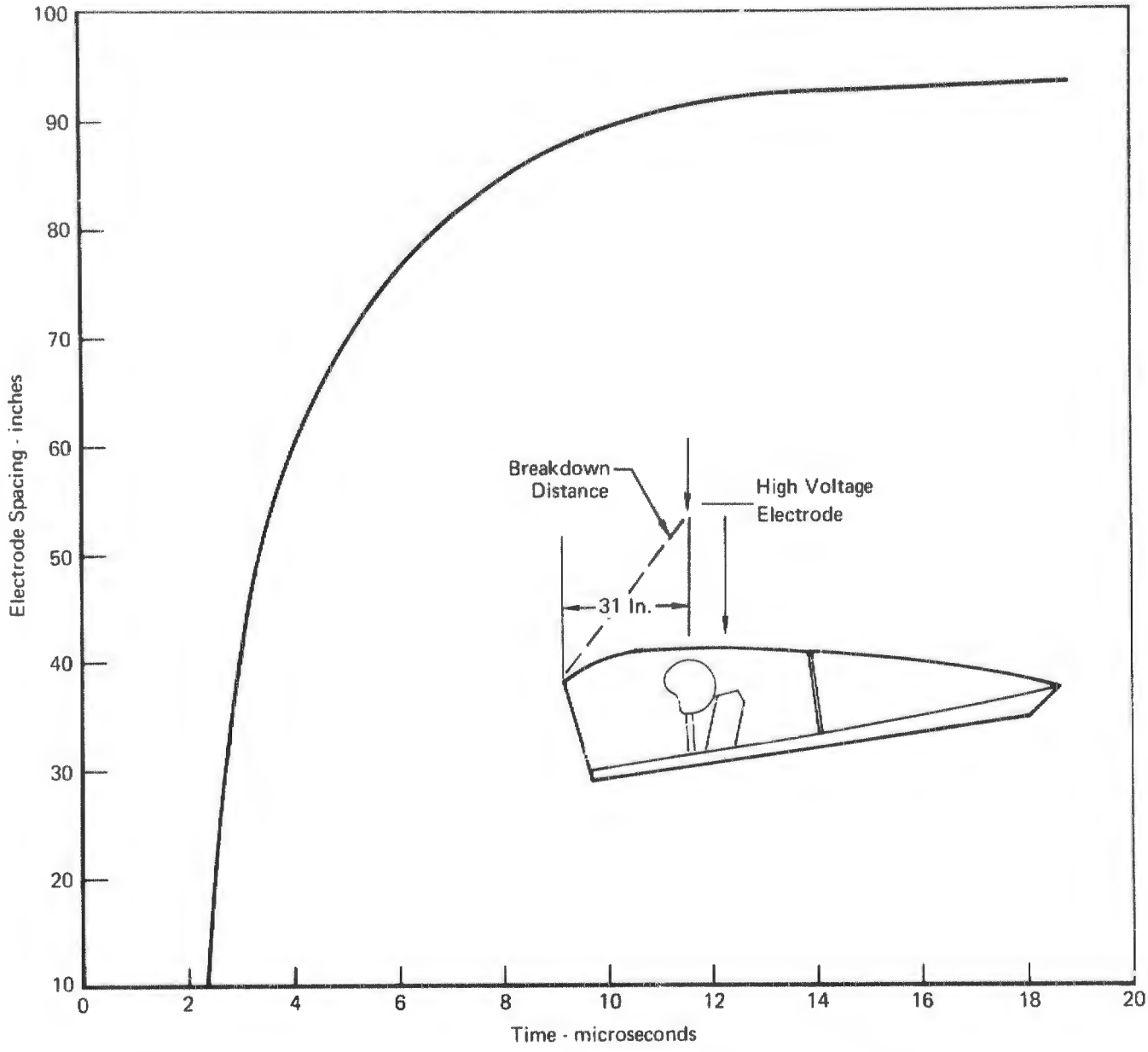

FIGURE 18 DISTANCE vs TIME TO BREAKDOWN AT 1.2 MV

FIGURE 19 CORONA CAMERA AND CANOPY

FIGURE 20 SIMULATED HELMET AND SEAT ARRANGEMENT

The high voltage generator was set for 1.2 MV to 1.3 MV amplitude and the high voltage electrode was placed approximately 86 inches above the top of the canopy (see Figures 21 through 35). Photographs were taken during the strike of corona streamering.

3.6.2 Photographic Technique

When the polaroid cameras were stopped down sufficiently to eliminate fogging, the spark gave insufficient illumination of the canopy. To overcome this difficulty, a double exposure, first of the canopy with general lighting, then a second exposure of the discharge was made at a smaller aperture without overhead lighting. Unfortunately, reflection from overhead fluorescent lighting at the canopy surface degraded some photographs. Reflection of the spark from the canopy surface also occurred in some photographs.

In order to prevent fogging of the high speed film, the tests were run in a darkened room and a shroud placed over the canopy to reduce direct light from the bright spark breakdown. Sequence shots (Figures 22 through 28) show the presence of weak corona streamering from the top of the pilot's seat behind helmet. In order to obtain breakdown to the center arch support, the high voltage electrode was moved to 13-1/2 inches behind a point directly above the pilot position. (Figure 21.) Corona was not visible in this configuration (Figure 29). Figures 30 through 35 show additional pictures of the corona study.

3.6.3 Results

Photographs of internal corona during a simulated lightning strike show that most corona originates from the top of the pilot seat. No intense sparking was noticeable. Comparison with a reproducible source (a model Van de Graf generator) indicates that the corona is too small to represent a serious hazard even without protection. If desired, either of the recommended diverters can be added to reduce or eliminate the small amount of corona that will be present under the canopy due to a lightning strike.

3.7 High Voltage Tests on F-15 Canopy

High voltage tests at 1.4 MV were performed on the F-15 canopy in a close simulation to the actual conditions to determine if the canopy would puncture.

Lightning attachment was always to the metallic canopy arch when an approaching strike was simulated by a long spark from the electrode located 80 inches above the canopy. The high voltage electrode was then brought progressively closer to the transparency surface of the canopy (Figures 36 through 51), while maintaining a high voltage. When the electrode was at about 36 inches above the transparency (Figure 45) attachment to the forward part of the transparency occurred. The attachment point gradually moved aft as the electrode was brought nearer to the transparency surface (Figures 46 through 51) until it was only 1 inch from the surface. Figure 51 shows how air breakdown, in all directions will occur, at electric field values too low to puncture the Lexan. These conditions might occur in the case of a swept stroke starting from a strike to the forward canopy arch. In none of these configurations did puncture of the canopy occur. This included deliberate "overstressing" by forcing the simulated strike to go to the canopy transparency.

FIGURE 21 1.3 MV BREAKDOWN TO CANOPY FROM 83 INCHES

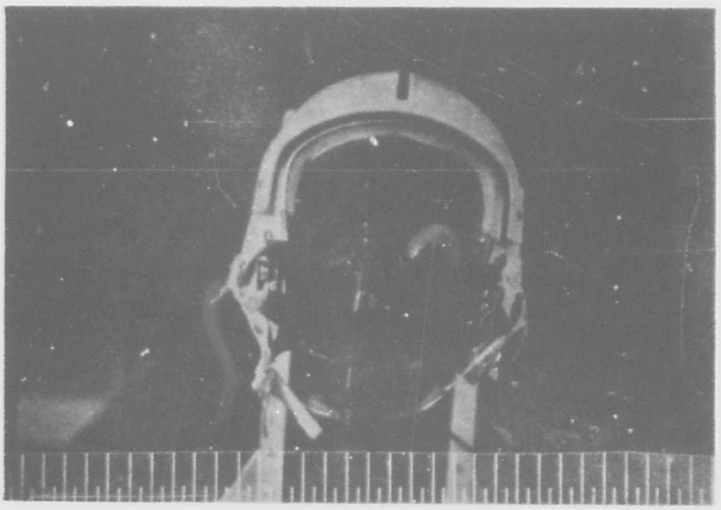

FIGURE 22 1.3 MV BREAKDOWN TO CANOPY FROM 83 INCHES - CORONA STREAMERS

The High Voltage Electrode is 83 inches Above the Canopy and Slightly Forward of the Pilot Position. The Visible Corona Originates from the Simulated Pilot's Seat.

The high voltage electrode is 83 inches above the canopy and slightly forward of the pilot position. The visible corona originates from the simulated pilot's seat.

FIGURE 23 1.3 MV BREAKDOWN TO CANOPY FROM 83 INCHES - CORONA STREAMERS

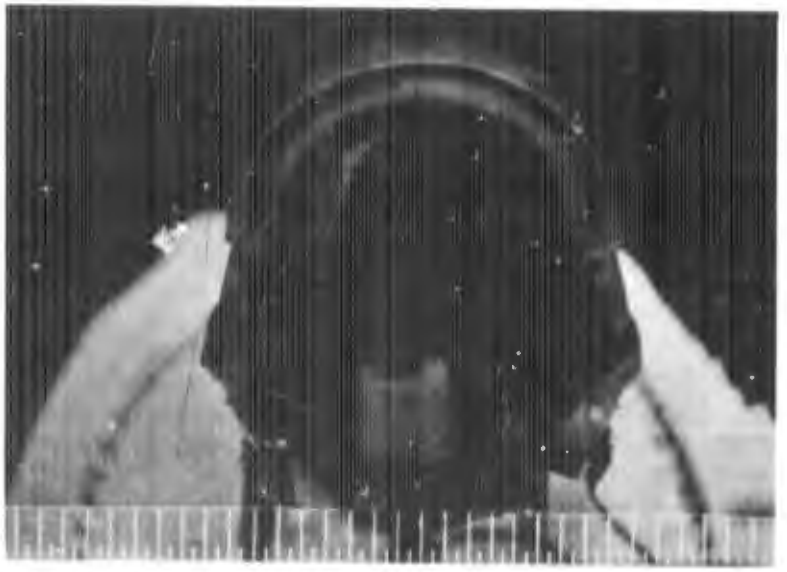

The high voltage electrode is 86 inches above the canopy and slightly forward of the pilot position. The visible corona originates from the simulated pilot seat.

FIGURE 24 1.3 MV BREAKDOWN TO CANOPY FROM 86 INCHES - CORONA STREAMERS

The high voltage electrode is 86 inches above the canopy and directly above the pilot position. The visible corona originates from the simulated pilot seat.

FIGURE 25 1.3 MV BREAKDOWN TO CANOPY FROM 86 INCHES - CORONA STREAMERS

FIGURE 26 CORONA STREAMERS CORRESPONDING TO FIGURE 27

Note:
The high voltage electrode is 86 inches above the canopy and 7 inches aft of the pilot position. The visible corona originates from the simulated pilot's seat.

FIGURE 27 1.4 MV BREAKDOWN TO CANOPY FROM 86 INCHES AND 38 INCHES AFT

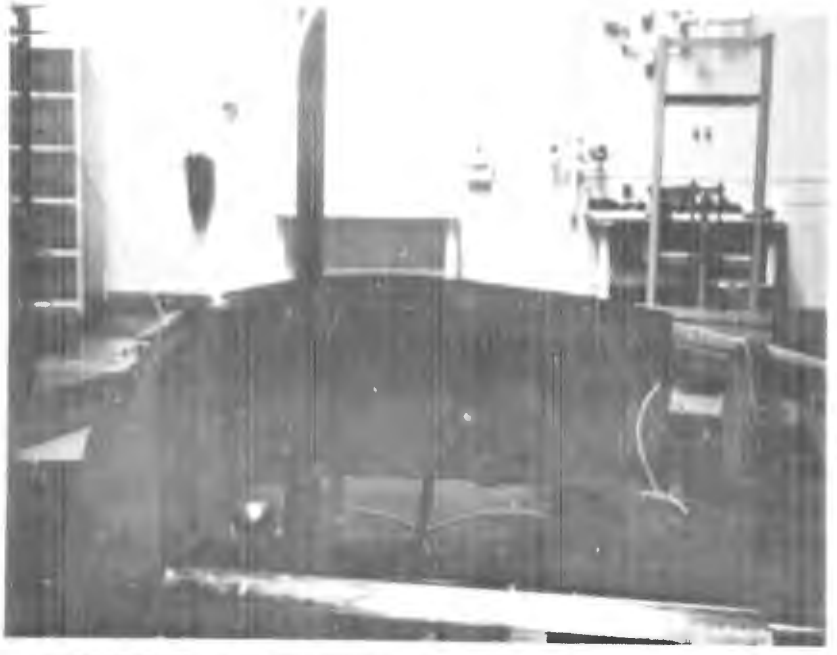

FIGURE 28 1.4 MV BREAKDOWN TO CANOPY FROM 86 INCHES AND 38 INCHES AFT SIDEVIEW

FIGURE 29 1.4 MV STRIKE TO AFT CANOPY - NO CORONA

The High Voltage Electrode is 86 inches Above the Canopy and 14 5 inches Aft of the Pilot Position The Breakdown Occurred to the Center Arch.

FIGURE 30 1.4 MV STRIKE TO AFT CANOPY ARCH

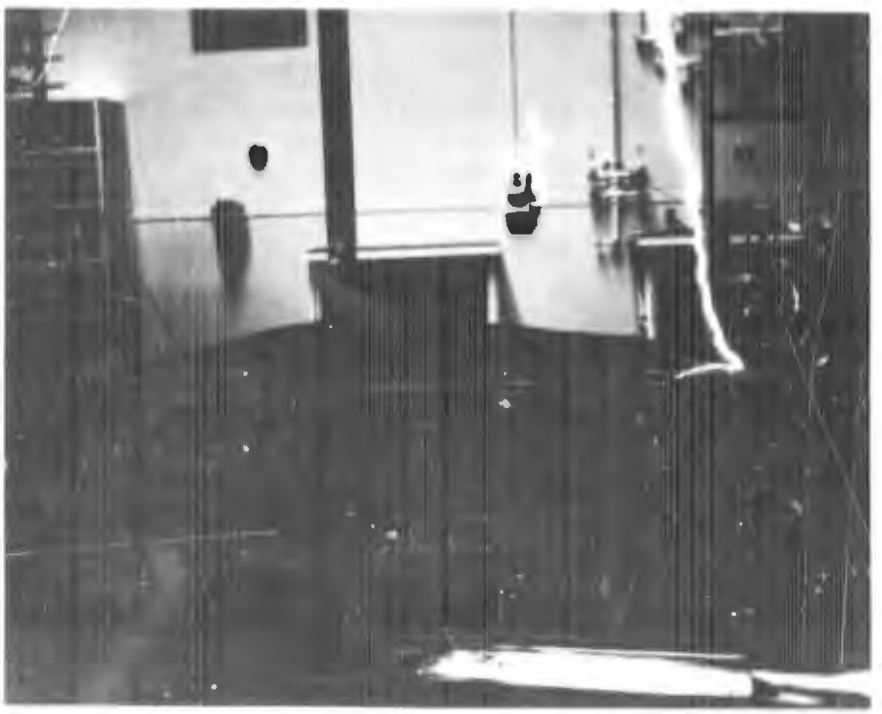

FIGURE 31 1.4 MV STRIKE TO AFT CANOPY ARCH - SIDEVIEW

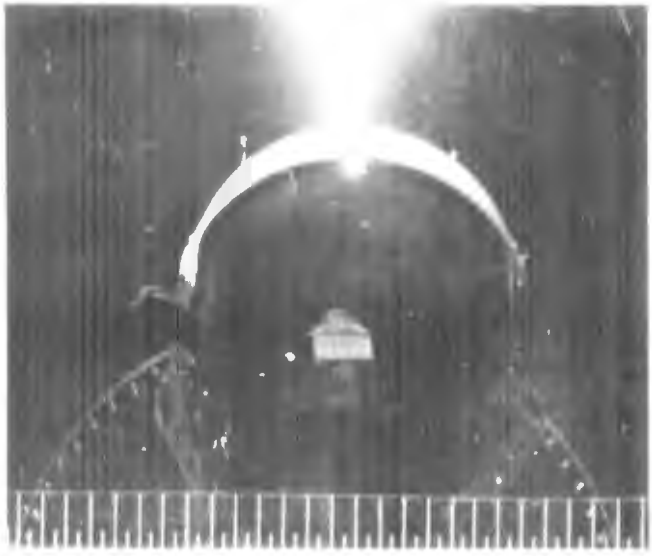

FIGURE 32 NO CORONA STREAMERS APPEAR WHEN THE DIVERTER IS FITTED

Note:
The high voltage electrode is 86 inches above the canopy and 27 inches aft of the forward arch

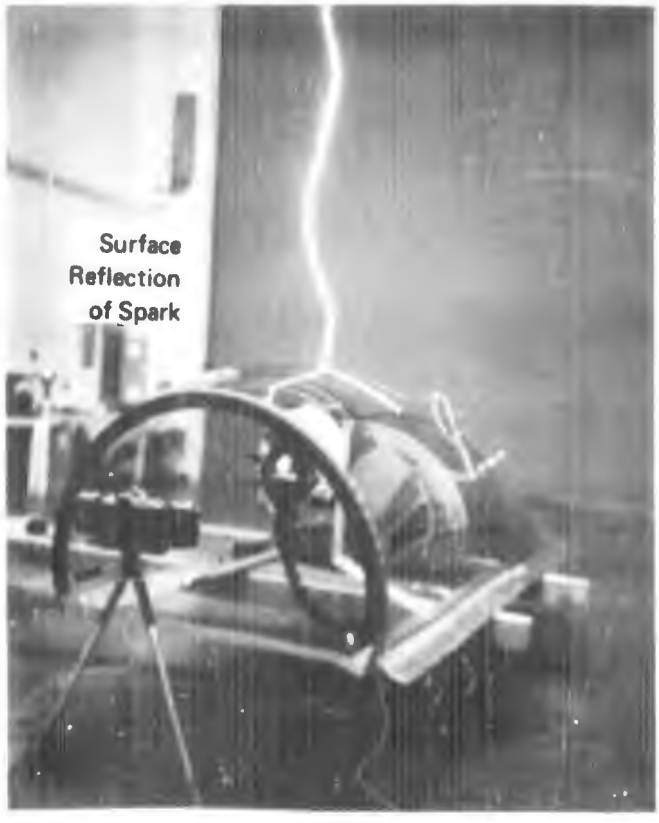

FIGURE 33 1.3 MV BREAKDOWN TO THE IONIZING DIVERTER FITTED TO THE CANOPY

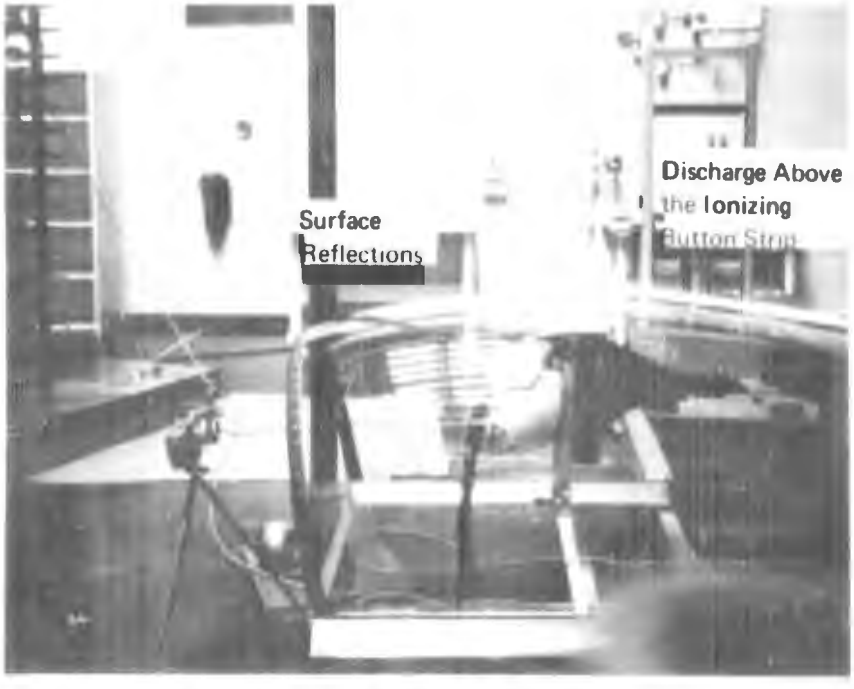

FIGURE 34 1.3 MV BREAKDOWN TO THE IONIZING DIVERTER FITTED TO THE CANOPY - SIDEVIEW

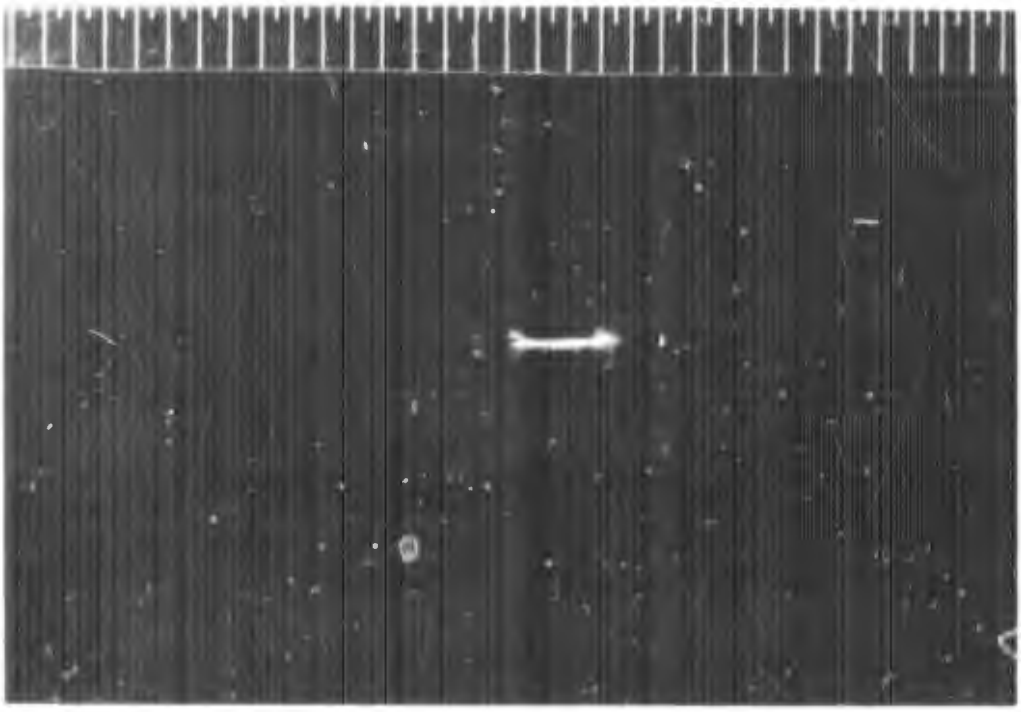

FIGURE 35 DISCHARGE FROM A MODEL VAN DE GRAF GENERATOR

FIGURE 36 1.4 MV STRIKE TO UNPROTECTED CANOPY FROM 80 INCHES

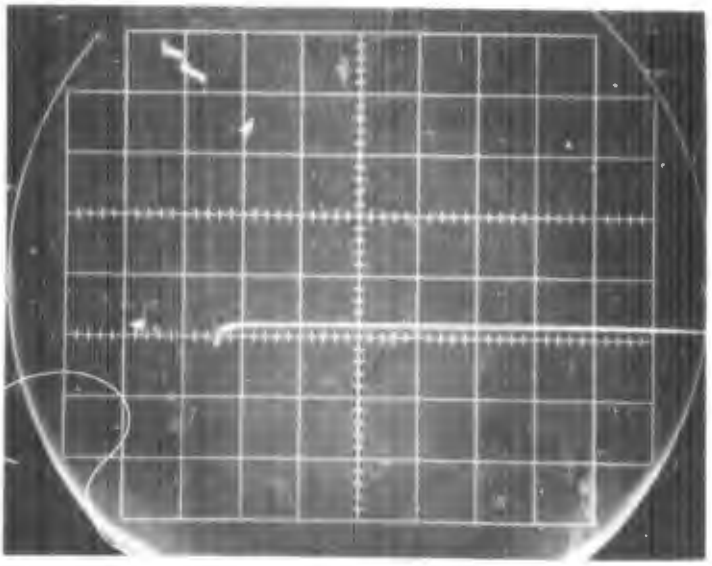

FIGURE 37 OSCILLOSCOPE TRACE FOR FIGURE 36 10 MICROSECS PER DIVISION

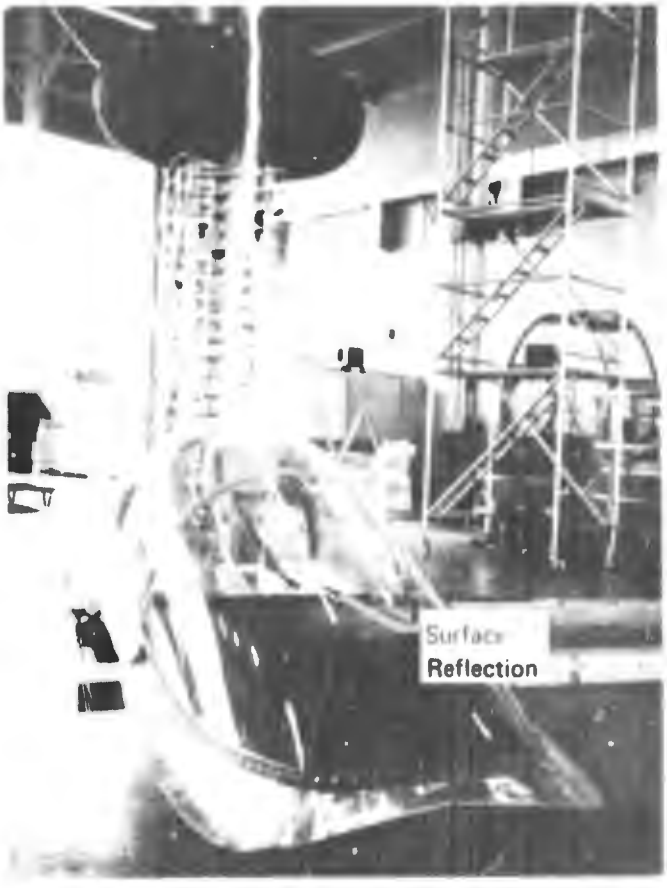

FIGURE 38 1.4 MV STRIKE TO UNPROTECTED CANOPY FROM 72 INCHES

FIGURE 39 1.4 MV STRIKE TO UNPROTECTED CANOPY FROM 72 INCHES - SIDEVIEW

Note:
Reflections on canopy surface are reflections of spark and also roof lights. This is typical of many canopy photographs.

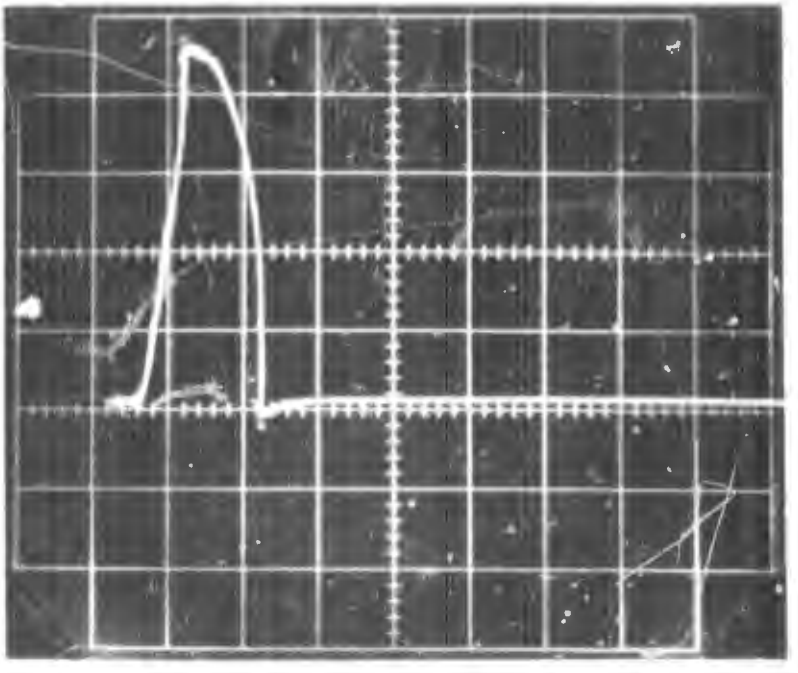

FIGURE 40 OSCILLOSCOPE TRACE FOR FIGURE 38 - 5-MICROSECS PER DIVISION

FIGURE 41 1.4 MV STRIKE TO UNPROTECTED CANOPY FROM 60 INCHES

FIGURE 42 1.4 MV STRIKE TO UNPROTECTED CANOPY FROM 60 INCHES - SIDEVIEW

FIGURE 43 1 4 MV STRIKE TO UNPROTECTED CANOPY FROM 48 INCHES

FIGURE 44 1.4 MV STRIKE TO UNPROTECTED CANOPY FROM 48 INCHES SIDEVIEW

FIGURE 45 1.4 MV STRIKE TO UNPROTECTED CANOPY FROM 36 INCHES

FIGURE 46 1.4 MV STRIKE TO UNPROTECTED CANOPY FROM 24 INCHES

FIGURE 47 1.4 MV STRIKE TO UNPROTECTED CANOPY FROM 12 INCHES

FIGURE 48 1.4 MV STRIKE TO UNPROTECTED CANOPY FROM 12 INCHES - SIDEVIEW

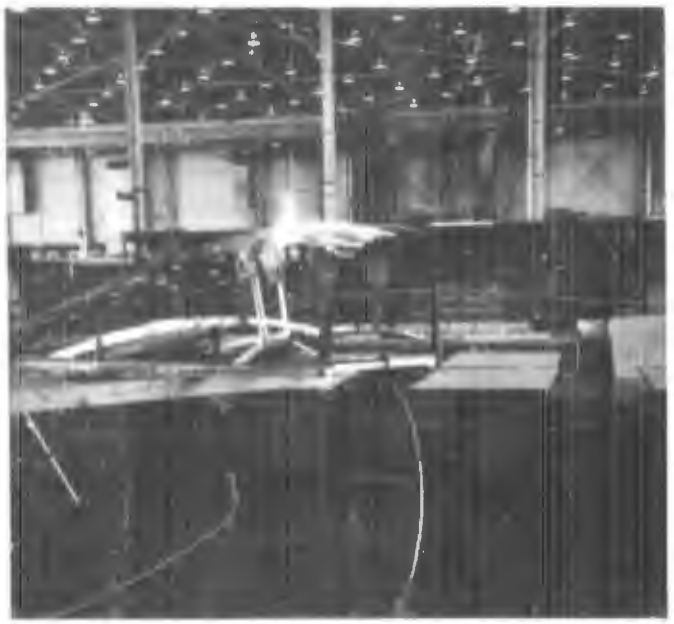

FIGURE 49 1.4 MV STRIKE TO
UNPROTECTED CANOPY FROM 6 INCHES

FIGURE 50 1.4 MV STRIKE TO
UNPROTECTED CANOPY FROM 4 INCHES

FIGURE 51 1.4 MV STRIKE TO
UNPROTECTED CANOPY FROM 1 INCH

These Photographs are Not Typical of Lightning Attachment. These Conditions May Occur in "Swept Strokes." After Attachment to Front Arch.

3.8 High Voltage Tests on 1/8 Inch Thick "Canopy"

In order to establish the existence of a large safety margin (against puncture) a simulated canopy was constructed with a transparency thickness of 0.125 inch (compared to the 0.29 inch thickness of the F-15 canopy), and a diameter of about 40 inches (compared to 37 inches for the F-15 canopy).

A series of high voltage strikes (Figures 52 through 78) to the simulated thin canopy were carried out using approximately 1.3 MV and with a rod electrode at gap distances of 88 inches to 1 inch above the canopy. The experimental conditions and results are presented in Table II. In none of these configurations did canopy puncture occur.

The output waveshape of the generator for the case when breakdown does not occur is shown in Figure 54. The rise time is approximately 1 microsecond and duration is 250 microseconds. Figure 56 shows that when breakdown does occur, at 88 inches gap length, the duration is limited to about 20 microseconds due to the spark breakdown time. With shorter gaps this time is reduced due to the higher field in the smaller gap. See Figure 18 for distance-breakdown time relationship with a constant generator voltage of 1.2 MV.

In order to check the effect of the internal diverter on the probability of puncture, two series of high voltage tests were carried out. For the first series a thin narrow aluminum tape was bonded to the internal surface of the canopy on the longitudinal center line. Care was taken to ensure that the adhesive did not cover the exposed surface. The results of the high voltage tests in this configuration are presented in Table III.

For the second series, the exposed surface of the diverter tape was completely covered by spraying a thick layer of acrylic adhesive over it. The same high voltage tests were repeated. The results are recorded in Table IV. Neither series of tests resulted in canopy puncture.

3.9 High Current Tests - External Metal Bar Diverter

An evaluation of adhesives for bonding the metal bar diverter was accomplished using high current tests on aluminum alloy and copper strips (see Table V). Three different adhesives were selected for test based on published data of bond strength at a temperature of 250°F, and compatibility with the Lexan material. The selected adhesives were:

a) Epon 828 with Diethylene Triamine hardener, manufactured by Shell Chemical Company

b) Epon 913 with Part 3 hardener manufactured by Shell Chemical Company

c) R.T.V. 630 manufactured by General Electric Company

Temperature sensitive color paint was used to assess temperature changes in 25°F increments in the range from 250°F to 500°F.

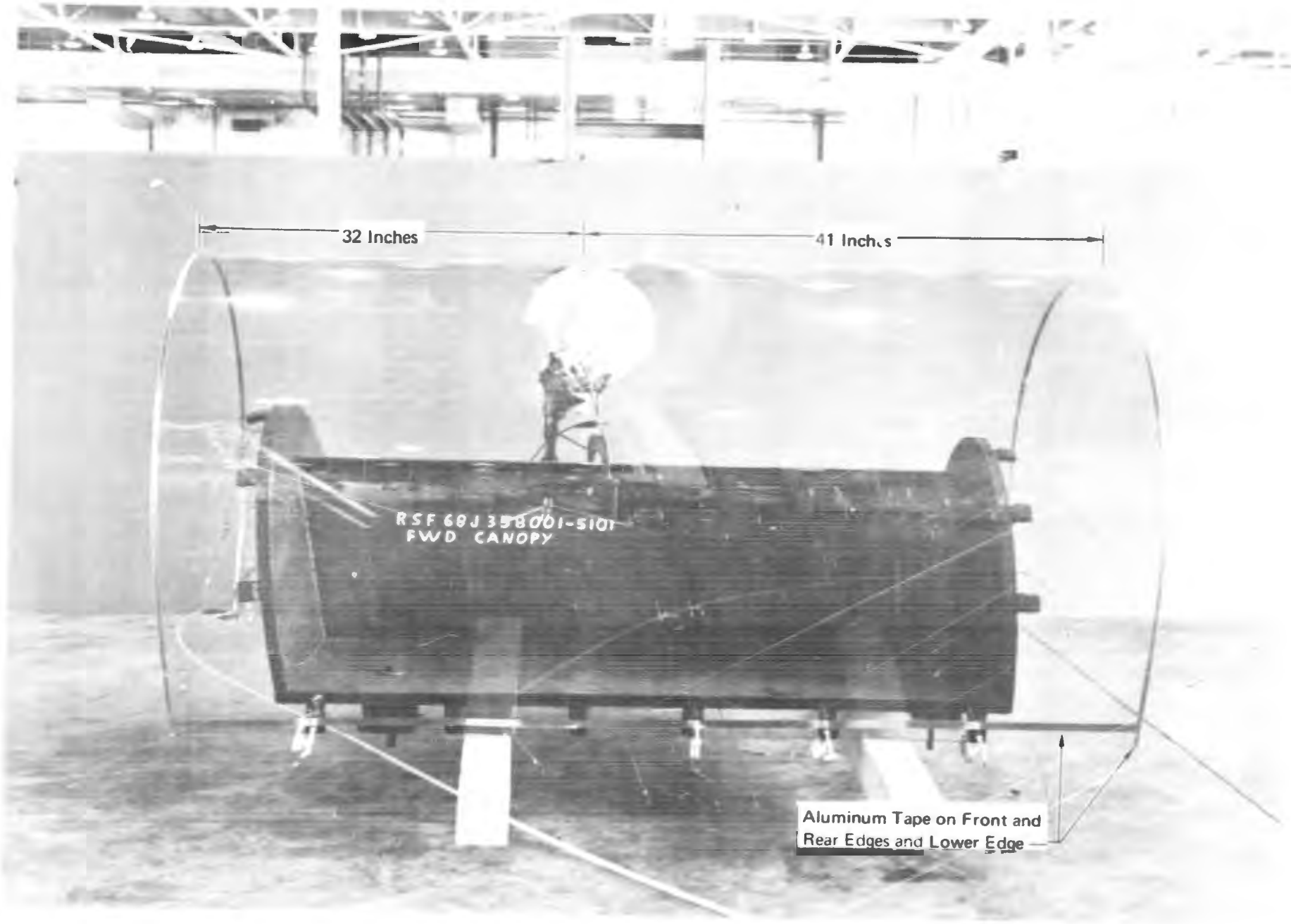

FIGURE 52 SIDEVIEW OF 1/8 INCH THICK LEXAN SIMULATED CANOPY

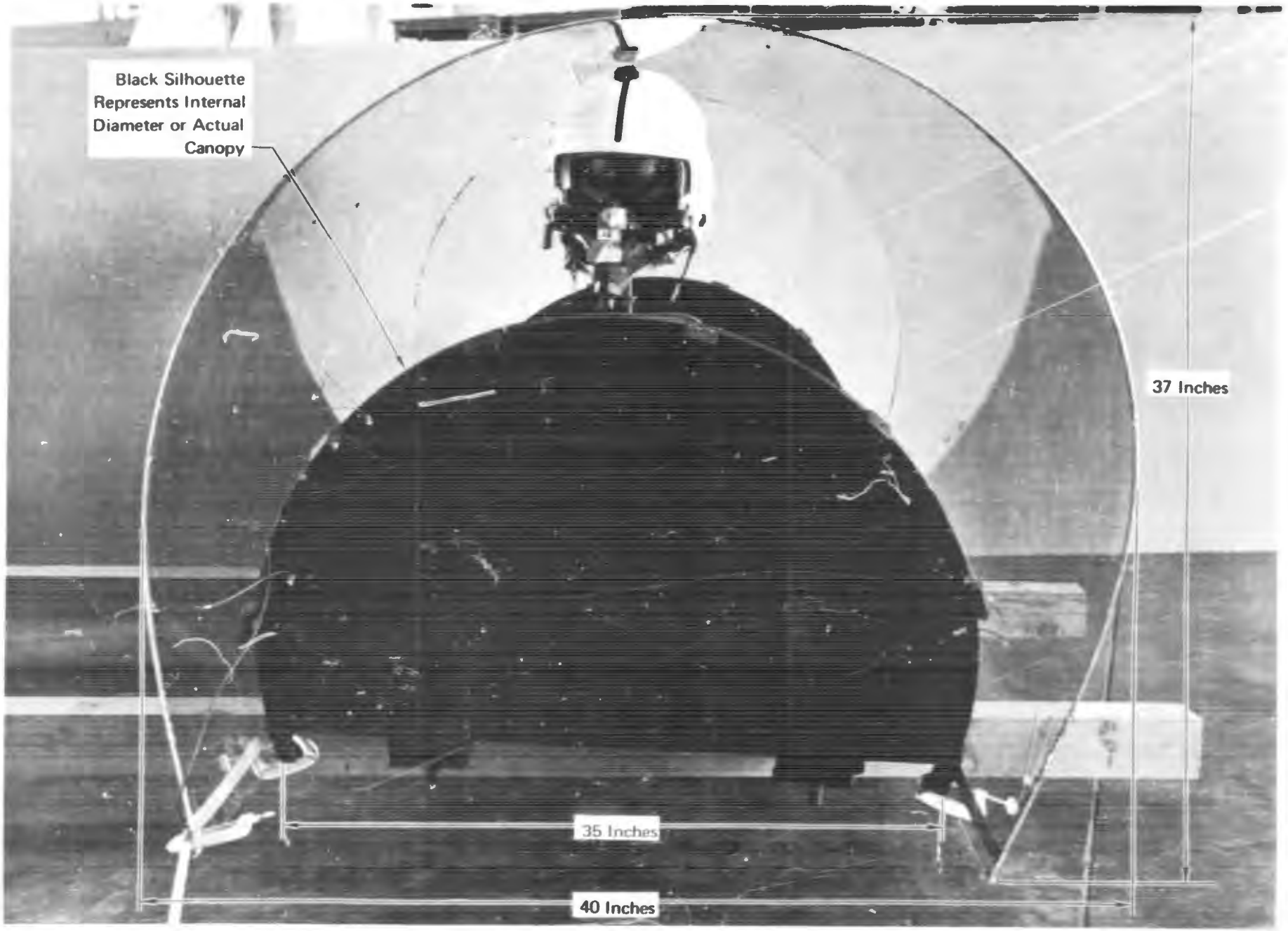

FIGURE 53 ENDVIEW OF 1/8 INCH THICK LEXAN SIMULATED CANOPY

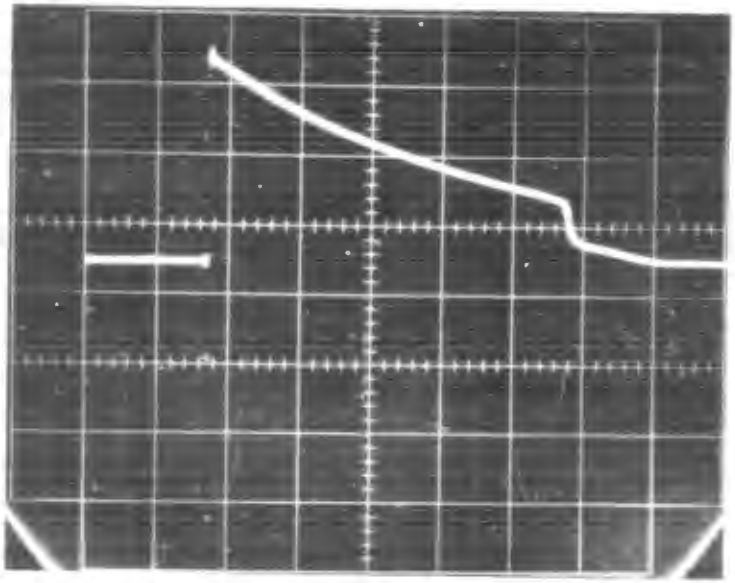

FIGURE 54 OSCILLOSCOPE VOLTAGE TRACE FOR "HOLD OFF" CONDITION - 50 MICROSECS PER DIVISION

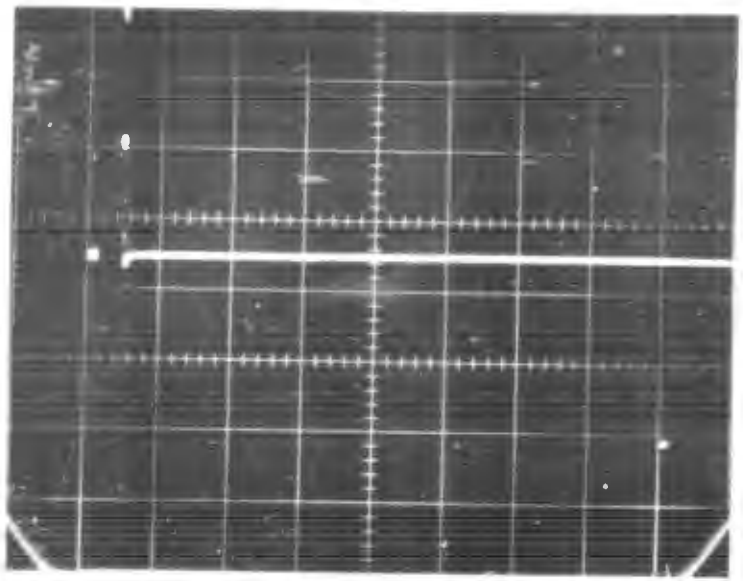

FIGURE 56 OSCILLOSCOPE VOLTAGE TRACE FOR FIGURE 55 - 50 MICROSECS PER DIVISION

FIGURE 55 1.4 MV STRIKE TO SIMULATED CANOPY FROM 88 INCHES

FIGURE 57 1.4 MV STRIKE TO SIMULATED CANOPY FROM 12 INCHES

FIGURE 58 1.4 MV STRIKE TO SIMULATED CANOPY FROM 6 INCHES

FIGURE 59 1.4 MV STRIKE TO SIMULATED CANOPY FROM 4 INCHES

FIGURE 60 1.4 MV STRIKE TO SIMULATED CANOPY FROM 1 INCH

FIGURE 61 1.2 MV STRIKE TO 1/8 INCH CANOPY WITH INTERNAL DIVERTER FROM 80 INCHES

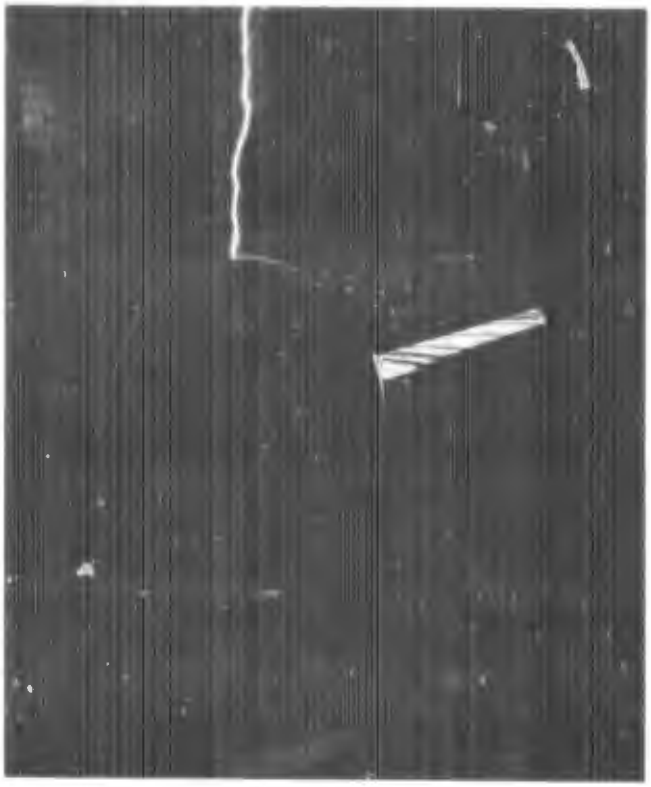

FIGURE 62 1.2 MV STRIKE TO 1/8 INCH CANOPY WITH INTERNAL DIVERTER FROM 72 INCHES

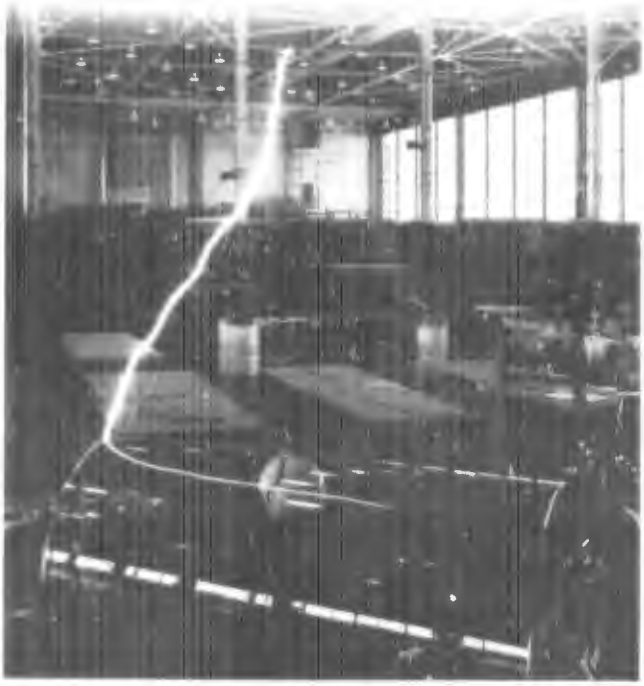

FIGURE 63 1.4 MV STRIKE TO 1/8 INCH CANOPY WITH INTERNAL DIVERTER FROM 60 INCHES

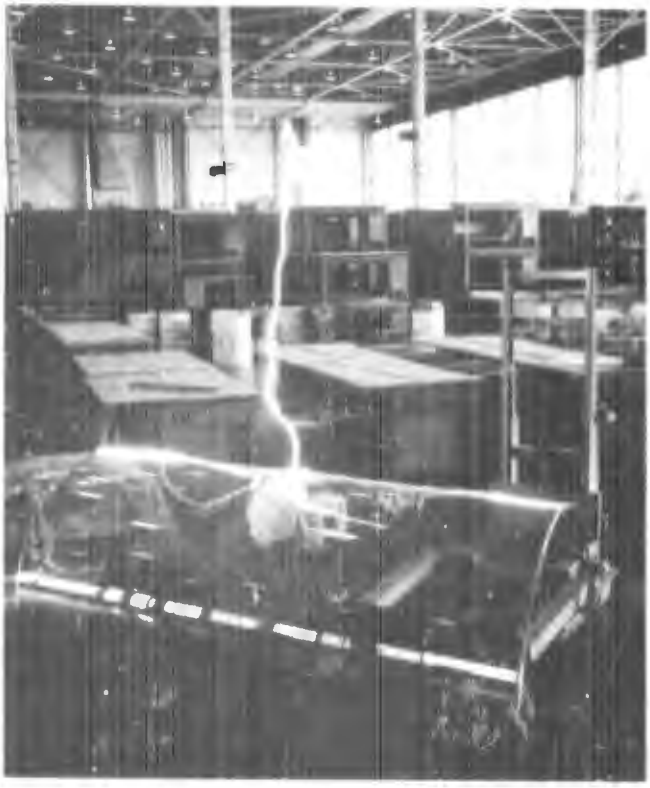

FIGURE 64 1.4 MV STRIKE TO 1/8 INCH CANOPY WITH INTERNAL DIVERTER FROM 48 INCHES

FIGURE 65 1.4 MV STRIKE TO 1/8 INCH CANOPY WITH INTERNAL DIVERTER FROM 36 INCHES

FIGURE 66 1.4 MV STRIKE TO 1/8 INCH CANOPY WITH INTERNAL DIVERTER FROM 24 INCHES

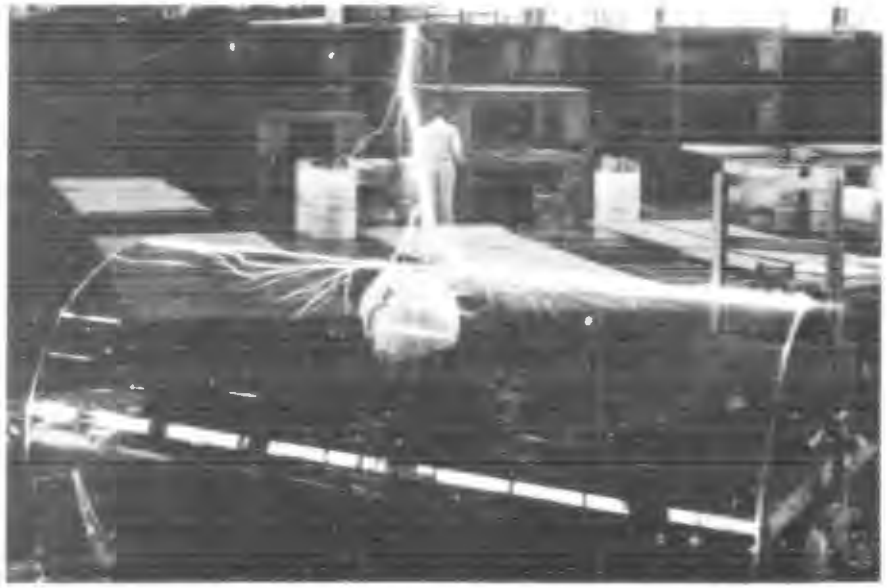

FIGURE 67 1.4 MV STRIKE TO 1/8 INCH CANOPY WITH INTERNAL DIVERTER FROM 24 INCHES

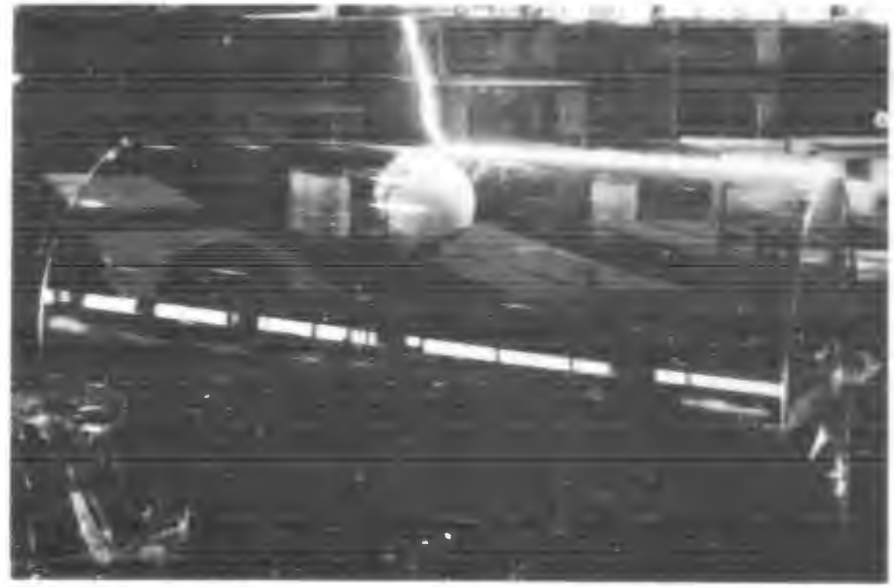

FIGURE 68 1.4 MV STRIKE TO 1/8 INCH CANOPY WITH INTERNAL DIVERTER FROM 12 INCHES

FIGURE 69 1.4 MV STRIKE TO 1/8 INCH CANOPY WITH INTERNAL DIVERTER FROM 6 INCHES

FIGURE 70 1.4 MV STRIKE TO 1/8 INCH CANOPY WITH INTERNAL DIVERTER FROM 4 INCHES

FIGURE 71 1.4 MV STRIKE TO 1/8 INCH CANOPY WITH INTERNAL DIVERTER FROM 1 INCH

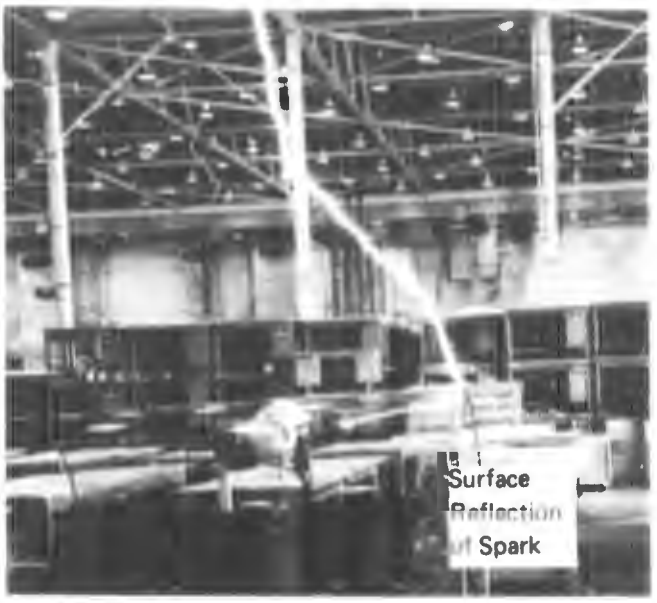

FIGURE 72 1.4 MV STRIKE TO 1/8 INCH CANOPY WITH INSULATED INTERNAL DIVERTER FROM 60 INCHES

FIGURE 73 1.4 MV STRIKE TO 1/8 INCH CANOPY WITH INSULATED INTERNAL DIVERTER FROM 36 INCHES

FIGURE 74 1.4 MV STRIKE TO 1/8 INCH CANOPY WITH INSULATED INTERNAL DIVERTER FROM 24 INCHES

FIGURE 75 1.4 MV STRIKE TO 1/8 INCH CANOPY WITH INSULATED INTERNAL DIVERTER FROM 12 INCHES

FIGURE 76 1.4 MV STRIKE TO 1/8 INCH CANOPY WITH INSULATED INTERNAL DIVERTER FROM 6 INCHES

FIGURE 77 1.4 MV STRIKE TO 1/8 INCH CANOPY WITH INSULATED INTERNAL DIVERTER FROM 4 INCHES

FIGURE 78 1.4 MV STRIKE TO 1/8 INCH CANOPY WITH INSULATED INTERNAL DIVERTER FROM 1 INCH

TABLE II

1/8 INCH CANOPY TESTS - NO DIVERTER

FIGURE	DISTANCE ABOVE SURFACE	ELECTRODE VOLTAGE KV	REMARKS
-	88"	1300	Held off
55	88"	1450	Breakdown to Front Arch
-	88"	1450	Breakdown to Front Arch
-	80"	1220	Breakdown to Front Arch
-	80"	1435	Breakdown to Front Arch
-	72"	1420	Breakdown to Front Arch
-	60"	1420	Breakdown to Front Arch
-	48"	1420	Breakdown to Front Arch
-	36"	1420	Breakdown to Front Arch
-	24"	1420	* Breakdown to Forward Transparency
57	12"	1420	* Breakdown to Center of Transparency
58	6"	1420	** Sparks over all the Surface
59	4"	1420	** Sparks over all the Surface
60	1"	1420	** Sparks over all the Surface

- Indicates that tests were performed but pictures were not included in this report due to similarity.

* Breakdown occurred to the canopy transparency external surface and then surface flashover occurred to the metal canopy arch.

** After striking the canopy transparency, intense streamering spread out in all directions over the external transparency surface. Puncture of the transparency did not occur.

TABLE III

1/8 INCH CANOPY TESTS - METAL TAPE DIVERTER INSIDE CANOPY
(FROM CENTER ARCH 36-1/2 INCHES FORWARD)

FIGURE	DISTANCE ABOVE SURFACE INCHES	ELECTRODE VOLTAGE KILOVOLTS	REMARKS
-	88	1420	Breakdown to Forward Arch
-	88	1320	Breakdown to Forward Arch
-	80	1290	Breakdown to Forward Arch
61	80	1220	Breakdown to Forward Arch
-	80	1188	Held Off
62	72	1188	Breakdown to Forward Arch
63	60	1420	Breakdown to Forward Arch
64	48	1420	Breakdown to Forward Arch
-	36	1420	*Breakdown to Diverter
65	36	1420	*Breakdown to Diverter
66	24	1420	**Breakdown to Transparency
67	24	1420	**Breakdown to Everything
68	12	1420	*Breakdown to Diverter
69	6	1420	Breakdown to Everything
70	4	1420	*Breakdown to Diverter
71	1	1420	*Breakdown to Diverter
-	48	1420	"Seat" Simulated **Breakdown to Transparency
-	12	1420	* Breakdown to Diverter
-	6	1420	"Seat" Ungrounded * Breakdown to Diverter
-	6	1420	"Seat" Grounded * Breakdown to Diverter
-	1	1420	* Breakdown to Diverter
-	48	1420	** Breakdown to Everything

TABLE IV

1/8 INCH CANOPY TEST - 36 1/2 INCH METAL DIVERTER INSIDE CANOPY

TAPE INSULATED AGAINST INTERNAL CORONA

FIGURE	DISTANCE ABOVE SURFACE	TIME μSEC	VOLTAGE KV	REMARKS
-	88"		1420	Breakdown to Forward Arch
72	60"	5.5	1420	Breakdown to Forward Arch
73	36"	4	1420	Breakdown to Forward Arch
74	24"		1420	Breakdown to Transparency
-	24"		1420	Breakdown to Transparency
-	24"		1420	*Breakdown to Diverter
-	12"		1420	**Breakdown to Everything
75	12"		1420	**Breakdown to Everything
76	6"	2.8	1420	*Breakdown to Diverter
-	6"		1420	*Breakdown to Diverter
77	4"	2.8	1420	*Breakdown to Diverter
78	1"		1420	*Breakdown to Diverter

- Indicates that tests were performed but pictures were not included in this report due to similarity.

* Breakdown occurred to the canopy transparency surface directly above the internal diverter. The discharge then traversed the external surface directly above the internal diverter until it reached the center canopy arch. Puncture of the canopy did not occur.

** After striking the canopy transparency surface, intense streamering spread out in all directions over the external surface. Puncture of the canopy did not occur.

TABLE V

HIGH CURRENT TESTS - DIVERTER ADHESIVE BONDING TO LEXAN

NO.	FIGURE	MATL X SECT	LENGTH	ADHESIVE	I_{PK} (K AMPS)	MICROSECS 1/2 J_{PK} WIDTH	REMARKS
1	84	Alum. Alloy .375" x .051"	24"	EPON 828 + DTA	190	43	Ambient Temperature = 75°F. Bond Failed over Entire Length.
2	--	Alum. Alloy .375" x .051"	24"	RTV 630	197	43	Ambient Temperature = 75°F. Bond o.k. except 1" at Strike Point.
3	--	Alum. Alloy .375" x .051"	24"	EPON 913	197	50	Ambient Temperature = 75°F. Bond Failed over Entire Length.
4	82c	Copper .5" x .032"	24"	RTV 630	198	42	Ambient Temperature = 75°F. Bond Failed over Entire Length. Pinch Effect Caused Narrowing and Thickness Increase.
5	82a	Alum. Alloy .5" x .062"	24"	RTV 630	204	43.5	Ambient Temperature = 75°F. Bond did not Appear to Have Deteriorated with Visual Inspection.
6	82a	Diverter No. 5 used for Oven High Temperature Soak Test			-	-	Ambient Temperature 250°F for 30 Minutes. No Visual Evidence of Bond Deterioration.
7	83b	Copper .5" x .032"	36"	RTV 630	-	-	Ambient Temperature 250°F for 30 Minutes. Evidence of Partial Bond Failure at each End.
8	83a	Alum. Alloy .5" x .063"	36"	RTV 630	-	-	Ambient Temperature 250°F for 30 Minutes. Bond Failed at Both Ends.
9	--	Alum. Alloy .5" x .063"	24"	RTV 630	-	-	Ambient Temperature 200°F. Current Test at Elevated Temperature.
10	--	Copper .375" x .063"	9"	RTV 630	206	43	Ambient Temperature = 75°F Attachment Test. Attachment Bolt Melted. Diverter Completely Detached.
11	--	Copper .375" x .063	9"	RTV 630	209	28	Ambient Temperature = 75°F.Attachment Test. Attachment Bolts Failed. Diverter Completely Detached.

-- Indicates that tests were performed but pictures were not included in this report due to similarity.

The tests (Figures 79 through 89) were made to evaluate adhesive bonding under the following specific circumstances:

a) Temperature rise due to a lightning strike (Figure 82)

b) Temperature effects due to worst case aerodynamic heating (Figure 83)

c) Lightning current generated magnetic field effects (Figures 87 through 89)

Peak currents greater than 200K amps with a duration at the half amplitude points greater than 40 microseconds were used in these tests. This exceeds the requirements of MIL-B-5087.

A special jig (See Figure 79) was constructed to give cancellation of the magnetic field of the current return conductors. The solid bar diverter failed these tests due to differences in thermo expansion between the solid bar and the Lexan.

Additional tests for 200K amp strikes directly to the F-15 canopy metal arches showed them to be capable of withstanding such strikes (Figures 90 through 93). Subsequent examination of the screws at the point showed evidence of slight damage to the thread of the ones carrying the current. (Figure 92.)

3.10 TEST RESULT SUMMARY

3.10.1 Primary Hazard - Puncture

Experimental validation of the analysis result, that "air cannot support a sufficiently high electric field to cause puncture of Lexan", has been achieved.

Tests for the experimental validation of the analysis were made in several configurations. These tests included attempts to puncture 1/4 inch flat Lexan sheets and 1/8 inch flat Lexan sheet. Puncture did not occur when using either thickness.

Tests made on a 1/8 inch thick simulated canopy with voltages of 1.4 MV did not cause "canopy" puncture nor did tests made on the actual 0.29 inch thick F-15 canopy.

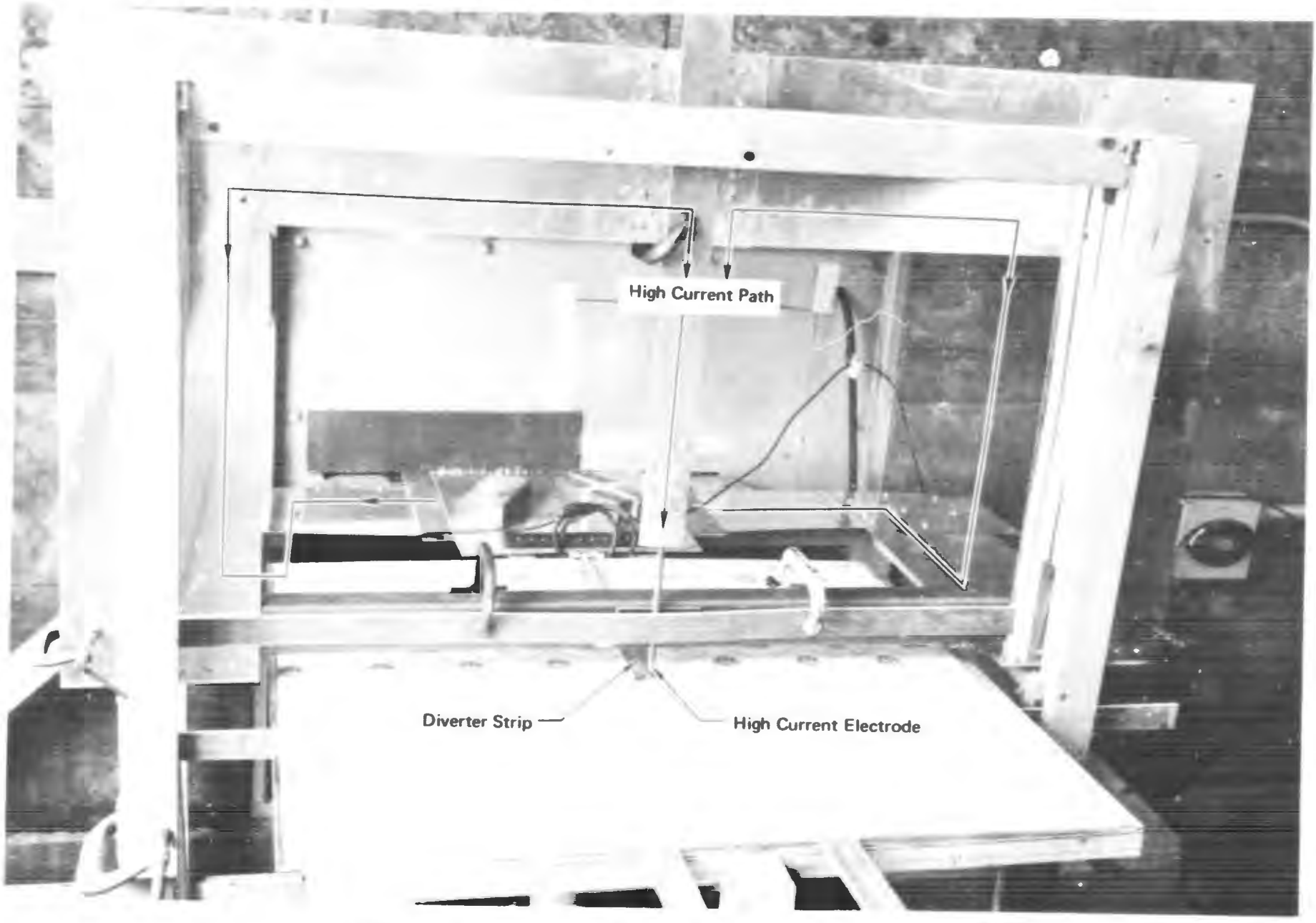

FIGURE 79 HIGH CURRENT JIG FOR 200,000 AMP TESTS

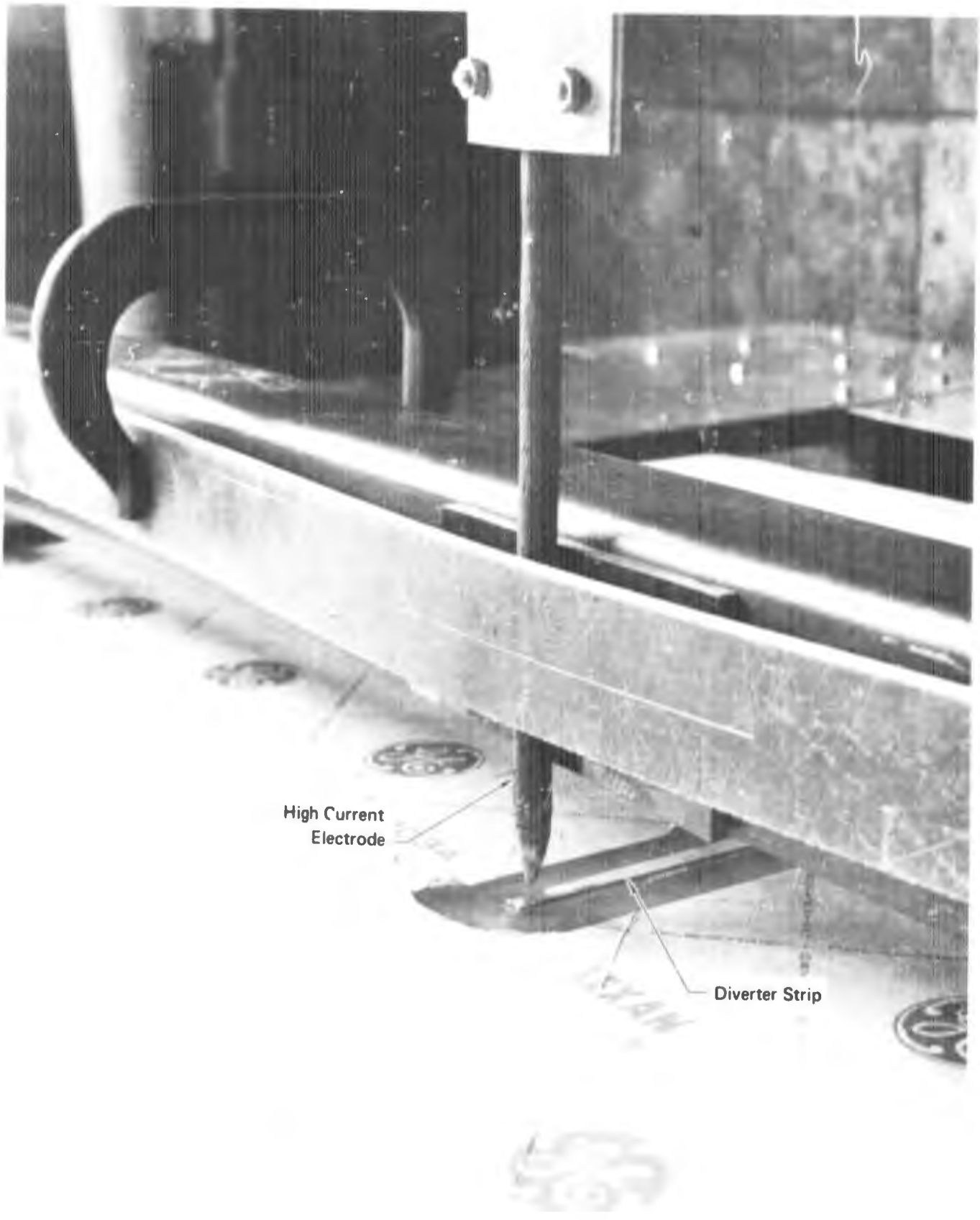

FIGURE 80 CLOSE-UP OF DIVERTER AFTER 200,000 AMP TEST

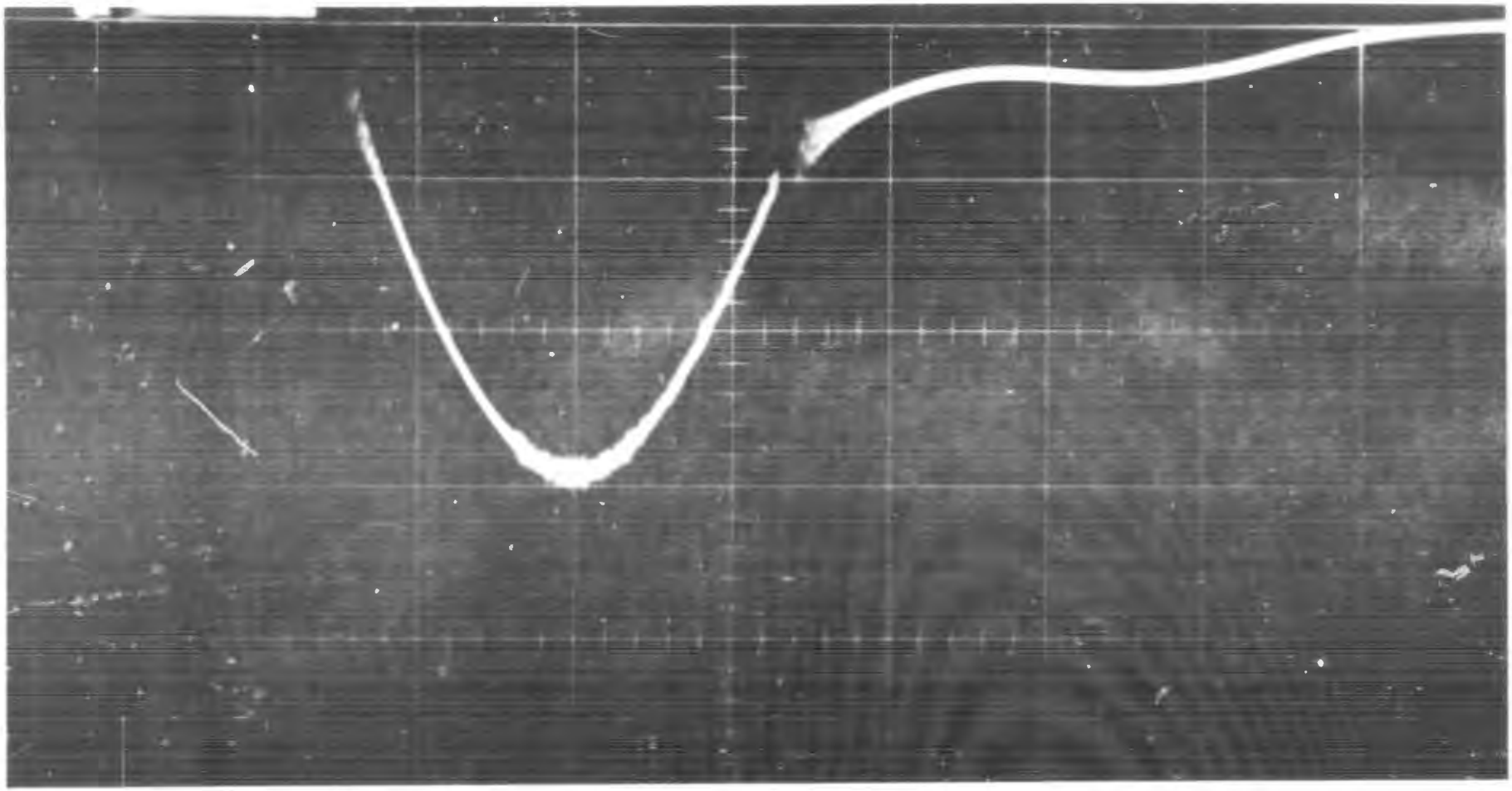

I_p = 197 KA T_p = 35 μ sec $T_{1/2}$ = 43

FIGURE 81 200,000 AMP CURRENT WAVEFORM

FIGURE 82 DIVERTER RODS AFTER 200,000 AMP CURRENT TESTS

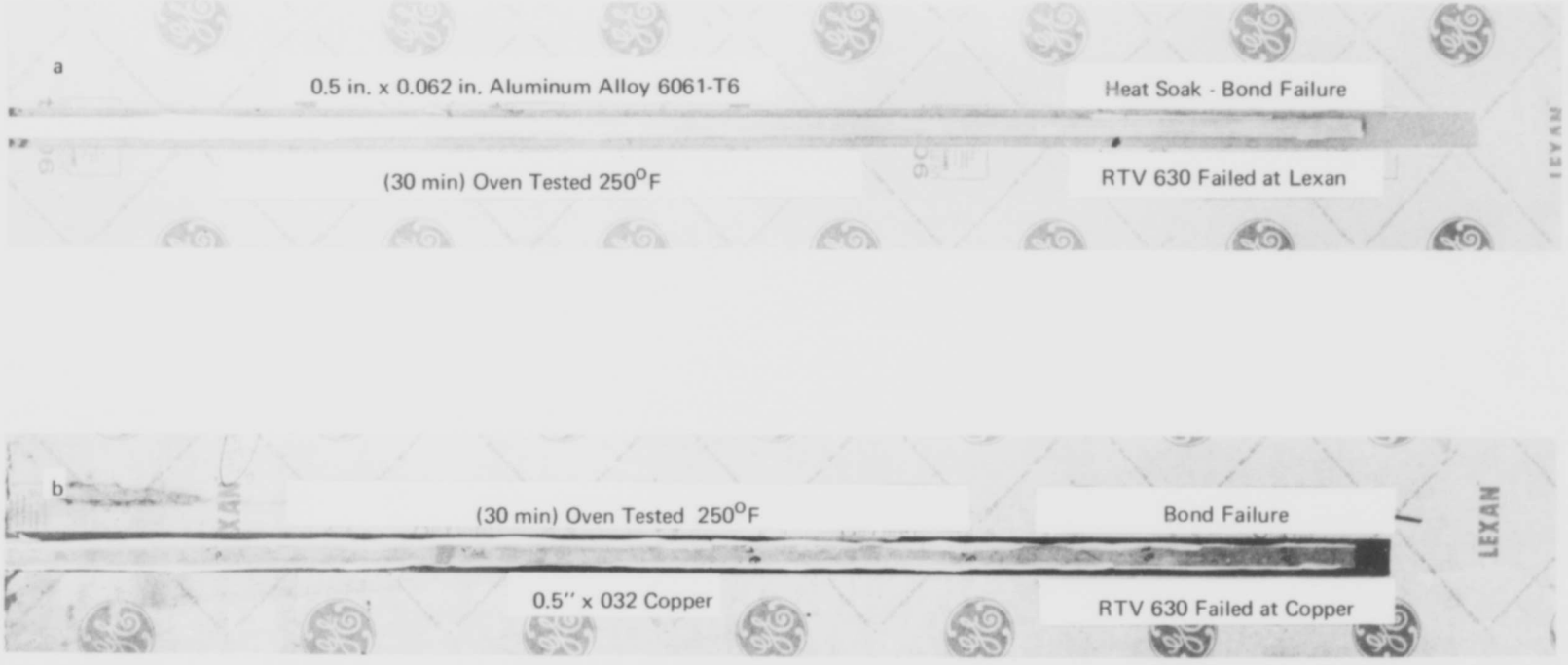

FIGURE 83 DIVERTER RODS AFTER 250°F TEMPERATURE SOAK TEST

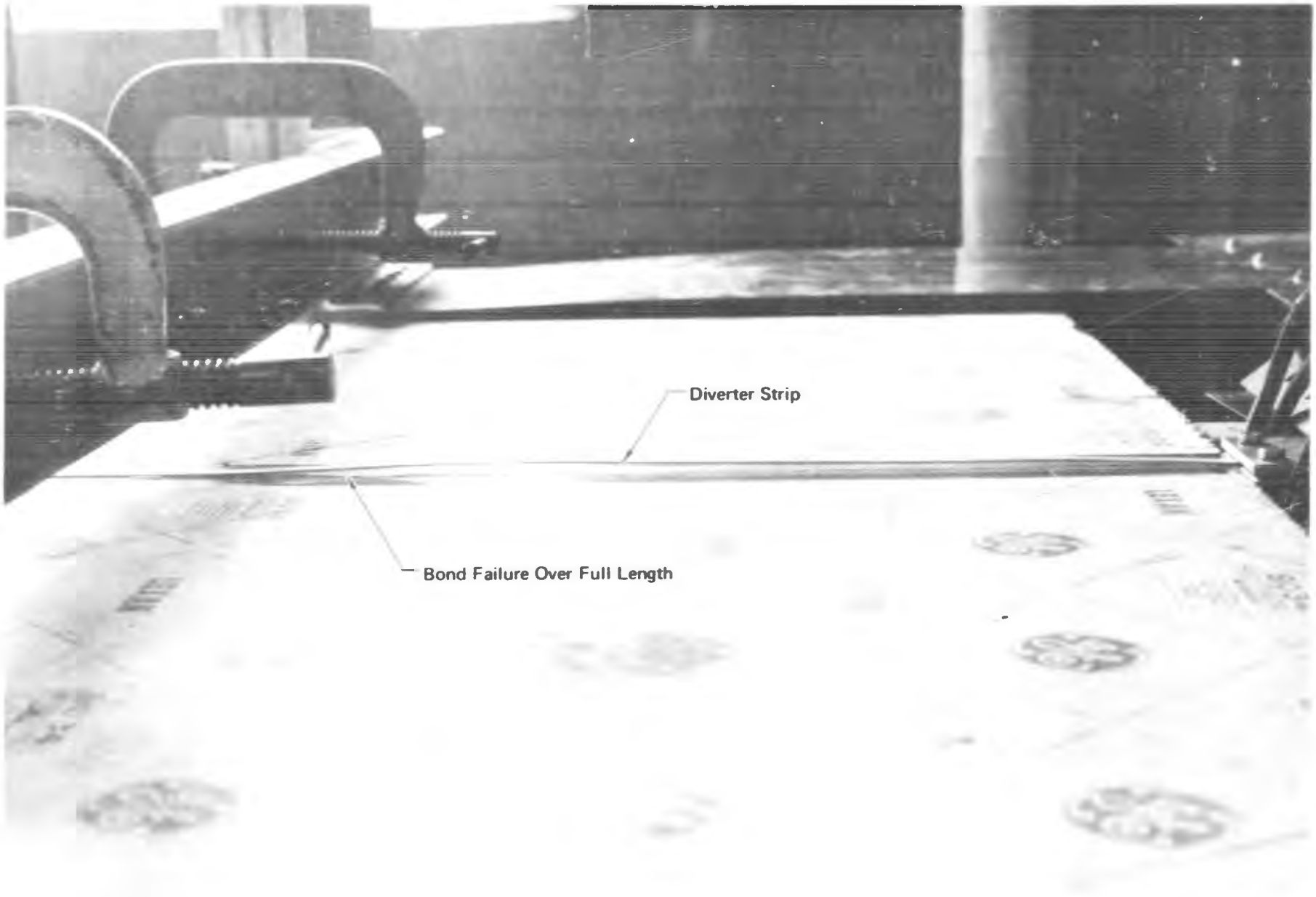

FIGURE 84 DIVERTER DETACHED AFTER HIGH CURRENT TEST 1

FIGURE 85 TEST JIG FOR SIMULTANEOUS HIGH TEMPERATURE AND CURRENT TEST

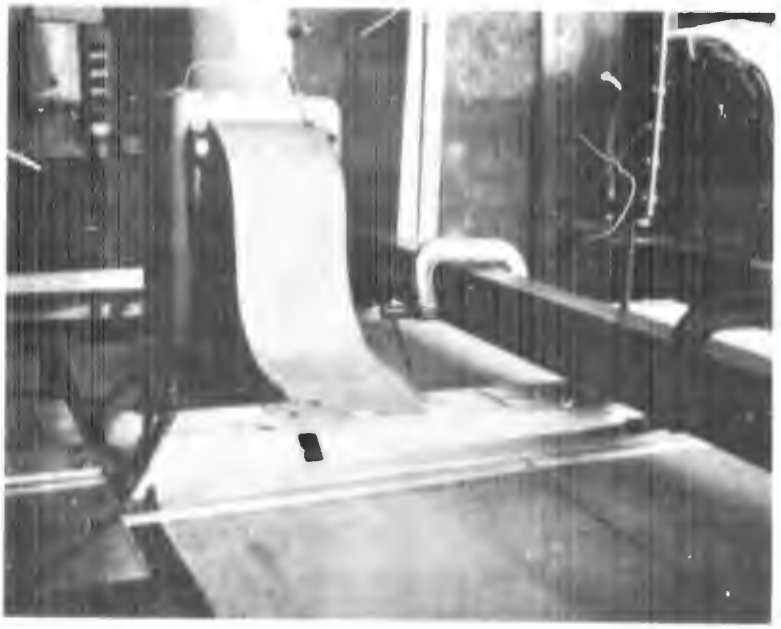

FIGURE 86 AIR HEATER AND BLOWER

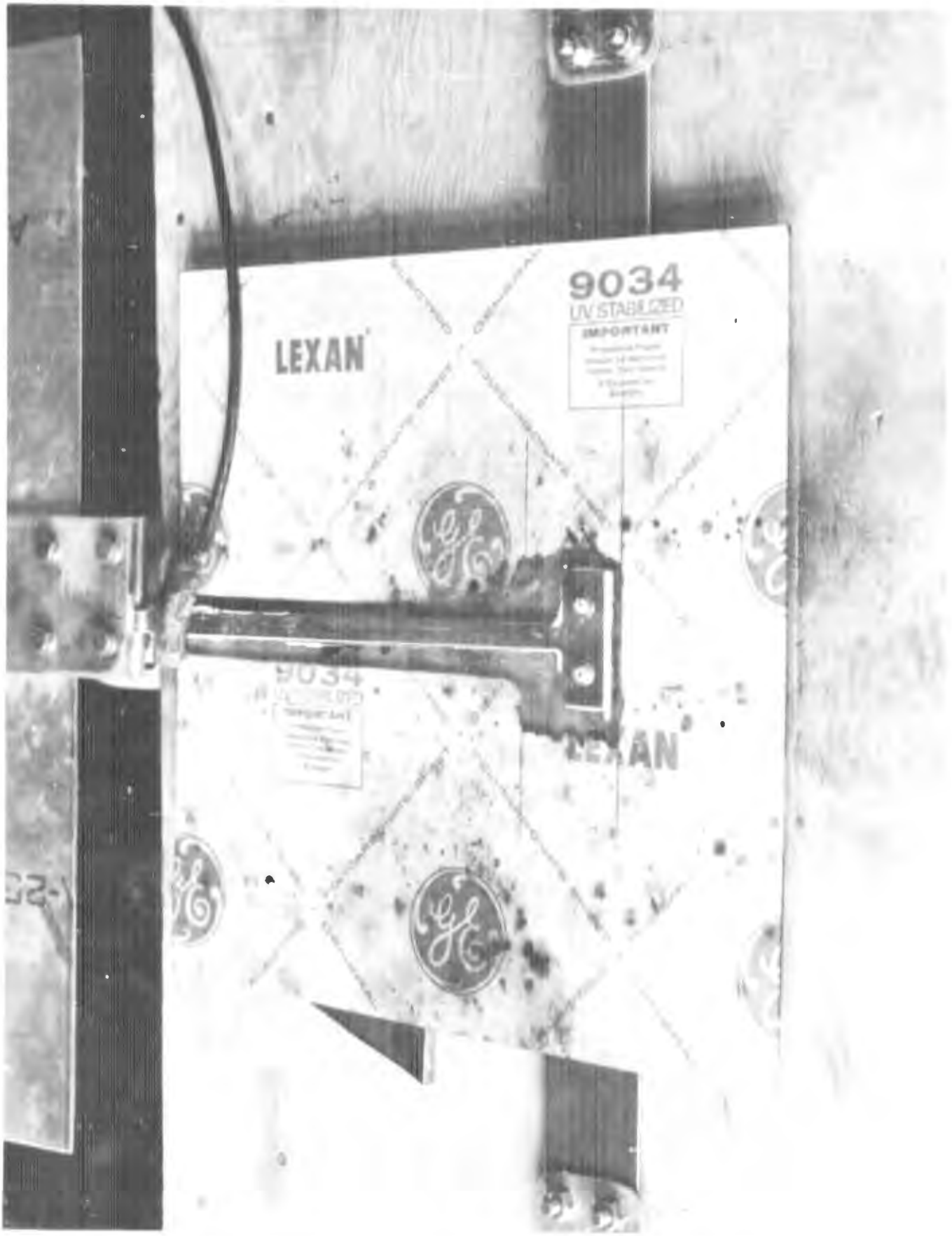

FIGURE 87 DIVERTER ATTACHMENT TEST ITEM BEFORE STRIKE

FIGURE 88 DIVERTER ATTACHMENT TYPE 1 AFTER 200,000 AMP TEST

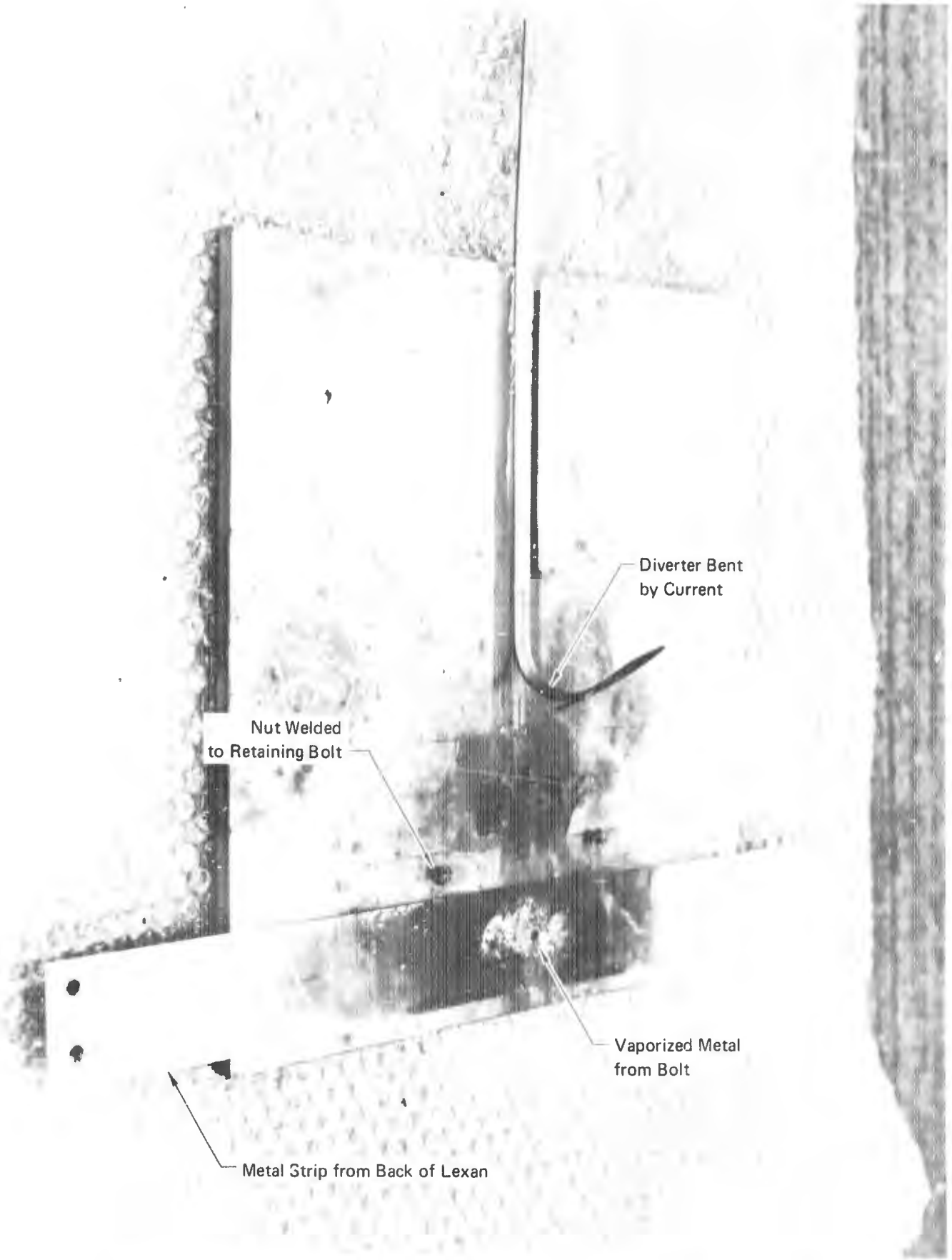

FIGURE 89 DIVERTER ATTACHMENT TYPE 2 AFTER 200,000 AMP TEST

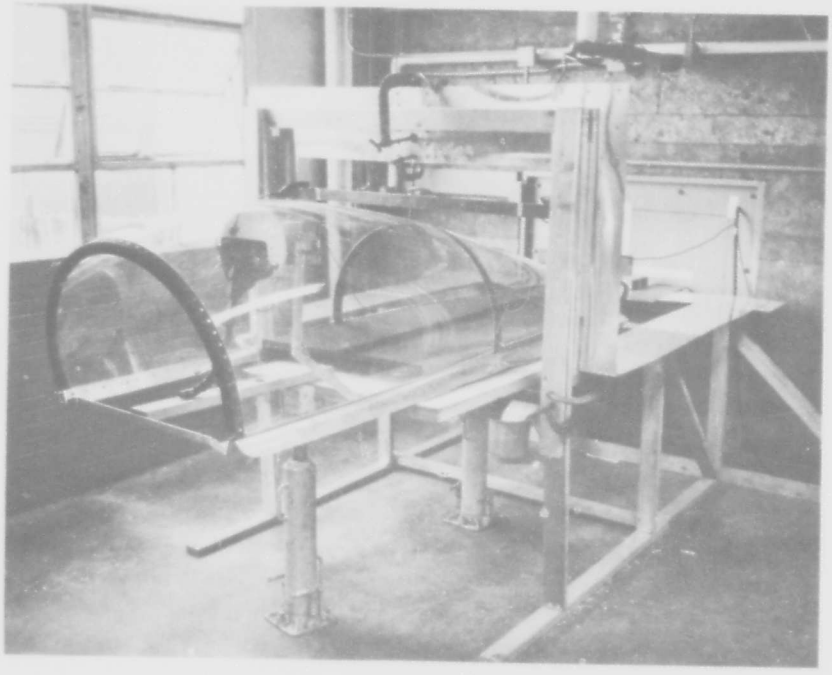

FIGURE 90 CANOPY TEST JIG FOR 200,000 AMP STRIKE TO JOINT

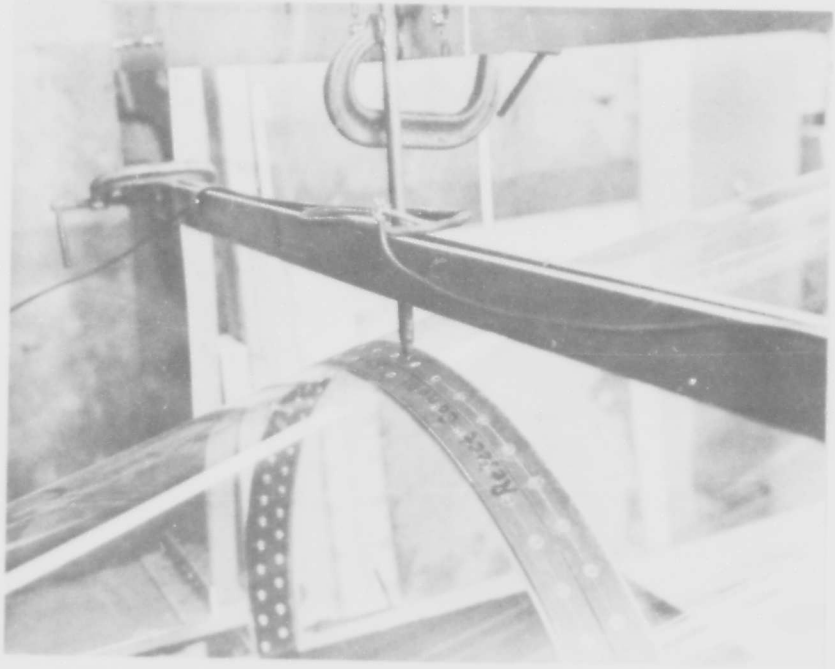

FIGURE 91 CANOPY JOINT AFTER 200,000 AMP TEST

FIGURE 92 JOINT SCREWS DAMAGED BY 200,000 JOINT TEST

FIGURE 93 200,000 AMP CURRENT WAVESHAPE APPLIED TO CANOPY JOINT

3.10.2 Secondary Hazard - Corona Current

The electric field from the lightning strike will cause a high electric field inside the canopy. Our tests have shown that under these circumstances a corona discharge will originate from the top of the pilot seat (Figures 22 through 25) but, no corona discharge originating from the pilot helmet was detected. Comparison with a photograph of the discharge from a small model Van de Graf generator indicates the magnitude of the corona current from the seat back was smaller than the Van de Graf current. When tested on laboratory personnel the discharge from the model Van de Graf generator was judged by the laboratory personnel to have only a minor effect.

3.10.3 Diverter Tests

Laboratory tests on the three diverter systems show that all three offer adequate protection against corona. The tests also show that canopy puncture will not occur when equipped with any of these diverter systems (See Appendix V).

The results of analysis and tests show that the problem of high current heating of the external metal bar can be limited sufficiently with a cross sectional area greater than .023 square inches. The thermal expansion due to aerodynamic heating does not seem to have a satisfactory answer.

Laboratory tests performed on the other two diverter systems show an adequate level of protection against corona (Figure 32) and that the internal diverter does not cause canopy puncture (Figures 61 through 78).

Section 4

CONCLUSIONS

Both analysis and laboratory tests show that puncture of the canopy will not occur.

Although the previous attachment model tests indicate the possibility of a lightning strike to the canopy, the present attachment point tests show that it attaches to the metallic canopy supports, and either the front arch or the canopy center arch support will be struck. Attachment to the canopy transparency will not normally occur. When a strike attaches to the front canopy arch, a swept stroke may occur. Under these conditions, the strike may sweep aft over the transparancy surface and re-attach to the center canopy arch support.

The limiting effect of air upon the maximum electric field will protect the transparency against puncture, and high current tests show that either canopy arch is capable of conducting over 200,000 amperes. Replacement of some of the screws attaching the transparency to the arch supports may be necessary after strikes of 200,000 amperes.

A final judgement of the physiological effects of corona current on the pilot requires a detailed medical study. The engineering conclusions reached in Section 3 are that such corona streamering as exists appears too small to represent a serious hazard to the pilot.

Both the analysis and laboratory tests support the conclusion that additional protection of the F-15 canopy is not necessary. The margin of safety against canopy puncture established by the high voltage tests on a simulated canopy made of 1/8 inch thick Lexan sheet and the failure of tests to puncture large flat sheets also support this conclusion.

The crew may feel slight effects of corona from a direct strike, but this effect will be much less discomforting than the blinding flash and noise which will occur at the same time. (The crew may also receive an electrical shock as the result of physically touching two portions of the cockpit, e.g., the cockpit sill with one arm and the throttle with the other hand during a lightning strike, but the canopy has no bearing on this effect.)

Our final recommendation is that additional lightning protection for the F-15 canopy is not necessary. Furthermore, it should be noted that although an F-15 canopy was used in this study, the results are general enough that they can be usefully extrapolated to include the canopies and dielectric surfaces on other air vehicles.

Appendix I

CRITERIA FOR THE PUNCTURE OR SURFACE FLASHOVER OF A LEXAN SHEET IN AIR

1.0 CANOPY FLASHOVER AND AIR BREAKDOWN

The breakdown of both solid and gaseous dielectrics is a function of both the electric field strength and duration of its application.

For gaseous dielectrics, the Townsend mechanism (Reference 4) is used for very small gaps. For larger gaps, theory is based on a non-uniform electric field moving with corona streamers. These streamers originate at local points of a highly divergent electric field, which move outwards at the end of each corona streamer, thereby causing local breakdown or ionization of the gas ahead of the streamer. The values of breakdown in a divergent electric field are much lower than those required in equivalent gaps with uniform electric fields.

The time dependence in small gaps is explained by the requirement of a free electron to initiate the Townsend mechanism. An additional delay is required for larger gaps due to the finite velocity of propagation of the corona streamers.

The present theory of solid dielectric breakdown attributes an "Intrinsic Dielectric Strength" to solid dielectrics which is considered to be electronic breakdown of the molecular structure initiated by free electrons (References 5, 6, & 7). Free electrons exist even in the best insulators. These are analogous to the free electrons in gases required by the Townsend Mechanism. Under the acceleration of high electric fields, they cause "ionization" within the solid dielectric. If the field is sufficiently high, intrinsic breakdown can occur within 10^{-8} seconds, and the value is temperature dependent (Figure 94).

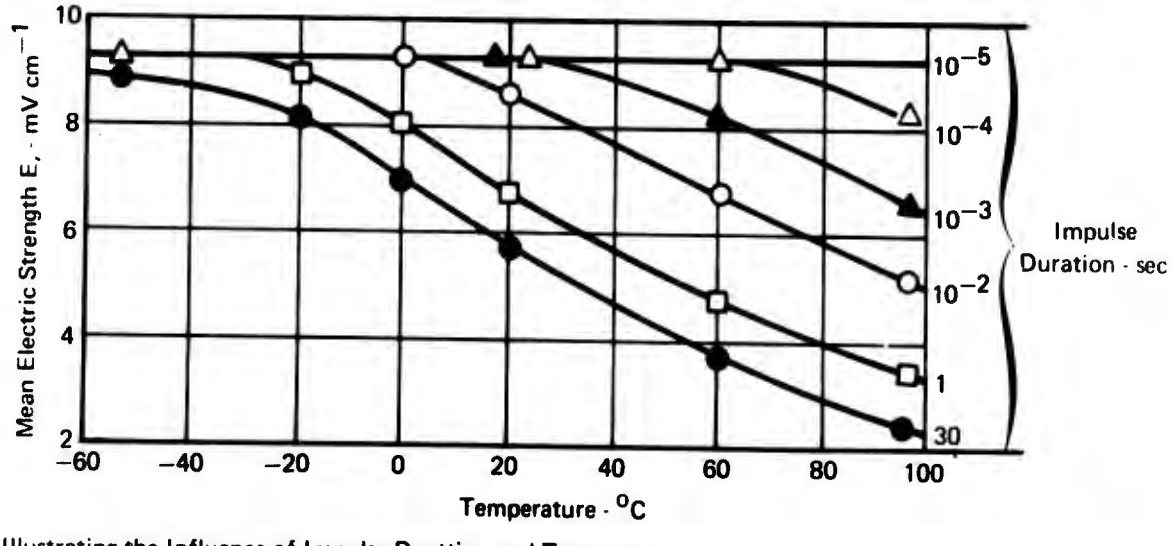

Illustrating the Influence of Impulse Duration and Temperature on the Electric Strength of Glass (Vermeer 1956)

FIGURE 94 DIELECTRIC STRENGTHS IN SOLID DIELECTRICS

The above graph illustrates the way in which the intrinsic strength is degraded by variation of temperature and duration of application of the electric field. It clearly shows the upper limit of the dielectric strength to be approximately 3.5 MV/cm for this particular dielectric. This graph is illustrative of impulse and thermal dielectric strength.

"Thermal Dielectric Strength" is the dielectric strength usually quoted and tested by either the "Step by Step" or "Short Time" dielectric breakdown of ASTM D149-64, "Standard Method of Test of Dielectric Strength", (Reference 2). It is usually very temperature dependent. The thermal dielectric strength is also dependent upon the thickness of the sample. The usually accepted explanation of thermal breakdown is that local heating resulting from the dielectric conduction current, causes generation of heat faster than the thermal conductivity can reduce it, and at the same time, the electrical conductivity is increased. This results in a thermal runaway condition. At the same time, the temperature dependent intrinsic strength decreases and eventual breakdown occurs.

Impulse dielectric breakdown voltage is higher than the thermal value since a shorter time is available for thermal heating to reduce the dielectric strength. Two other effects which degrade the intrinsic dielectric strength are "Discharge Breakdown" and "Electromechanical Breakdown". (Reference 8).

Discharge breakdown is caused by imperfections or voids in the dielectric. Augmentation of the electric field in the dielectric is caused by a change in dielectric constant. Premature local breakdown at higher electric field strengths initiates gradual but growing erosion of the parent dielectric leading to its total breakdown.

Electromechanical breakdown is related to mechanical deformation or fracture caused by electric stress in the materials. Many polymers soften with an increase in temperature and easily deform. The mechanical pressure owing to attraction between surface charges may amount to an atmosphere or greater when the electric field approaches the intrinsic electric strength (Figure 95).

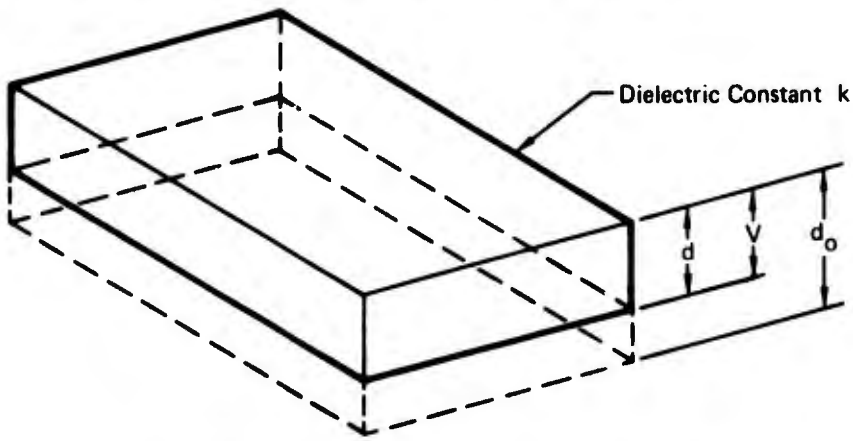

FIGURE 95 ELECTRO-MECHANICAL BREAKDOWN

Consider a plane slab of dielectric material with electrodes free to follow the movement of the dielectric material (Reference 9).

The compressive forces = $\frac{K\ V^2}{8\pi d^2} \times 1.1 \times 10^{-4}$ Dynes.

The initial thickness 'd_o' is reduced to d in accordance with Hookes Law.

$$\frac{K V^2}{8\pi d^2} = Y \log_e\left(\frac{d_o}{d}\right) \times 9 \times 10^4 \qquad (1)$$

Y = Youngs Modulus

K = Relative dielectric constant

Failure then occurs at an apparent stress of $E_A = V/d_o$, which is less than the true intrinsic strength $E_I = V/d$.

The product $d^2 \log_e (d_o/d)$ has a maximum value when $\log \left(\frac{d_o}{d}\right) = .5$

Substituting this value in Equation 1

$$E_b = \sqrt{\frac{V^2}{d^2}} = \sqrt{\frac{4\pi Y}{K}} \times 300 \text{ volts/cm} \qquad (2)$$

which is the maximum field strength the dielectric can withstand. Any further increase in the applied voltage will result in a mechanical collapse.

Since the relative dielectric constant, K, for Lexan is 3.17, then Equation 2 becomes

$$\underline{E = 597 \sqrt{Y} \text{ volts per cm.}} \qquad (3)$$

As shown in the graphs of Figure 96, Youngs Modulus is a function of temperature for dielectric materials. The relationship between electric strength and temperature can be seen to be similar. (As Equation (2) illustrates). Excellent agreement has been achieved in experimental tests at higher temperatures, verifying the relationship between electric field and mechanical breakdown (References 10, 11, & 12). The value of "Y" for Lexan varies between 4×10^5 psi at 80° F and 1.4×10^5 psi at 300° F. (The equivalent cgs values for Equation 3 are 2.75×10^{10} dyne cm^{-2} at 80° F and 96.5×10^8 dynes cm^{-2} at 300° F.) (Reference 13)

Inserting these values into Equation (3) gives the following values for electromechanical breakdown of Lexan.

$$E_{80} = 597\sqrt{2.75 \times 10^{10}} \qquad (4)$$

$$= \underline{\underline{99 \times 10^6}} \text{ volts per cm at 80° F.}$$

(or 252 MV per inch)

$$E_{300} = 597\sqrt{96.5 \times 10^8} \qquad (5)$$

$$= 58.6 \times 10^6 \text{ volts per cm at 300° F.}$$

(or 149 MV per inch)

The value at 300° F shows that electromechanical breakdown value at 300° F is considerably higher than the thermal or impulse values (See Appendix II).

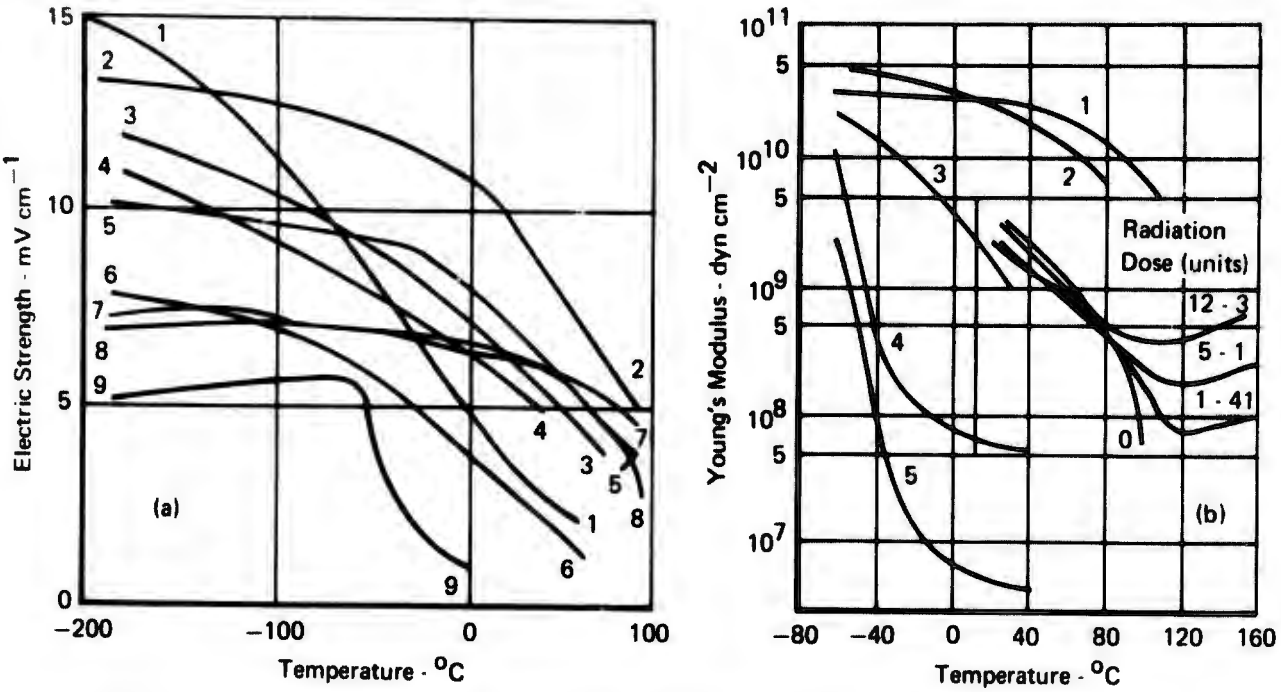

Comparison of effect of temperature on the electric strength of some polymers, and its effect on their elasticities. (a) Electric strength according to Ball (1951) and Oakes (1949): 1, polyvinyl alcohol; 2, polymethyl methacrylate; 3, polyvinyl chloride-acetate; 4 and 5, chlorinated polythene (55 and 8% Cl); 6, clear baking oil-varnish; 7, polystyrene: 8, polythene; 9, polyisobutylene; materials 1-5, polar; materials 7-9, non-polar. (b) Young's modulus according to Moll and leFevre (1948): 1, polystyrene; 2, polymethyl methacrylate; 3, unirradiated polythene; 4, natural rubber vulcanizate; 5, polysubutylene; insert (Charlesby and Hancock 1953), irradiated polythene (unit radiation does is a flux of 10^{12} slow neutrons/cm^2 plus associated fast neutrons and gamma rays).

FIGURE 96 EFFECT OF TEMPERATURE ON THE ELECTRIC STRENGTH OF POLYMERS

2.0 CANOPY PUNCTURE VERSUS AIR BREAKDOWN CRITERIA

Whatever the method of dielectric failure is, the dielectric strength is a function of both voltage and duration of the voltage in both solid and gaseous dielectrics.

It is, therefore, reasonable that the duration, as well as the actual magnitude of the applied voltage, will determine which method of puncture will occur. The resultant breakdown will then reduce the applied voltage to a level below the breakdown voltage of the other.

The breakdown-time curve of the air gap around a canopy, is dependent upon many accountable factors (such as the geometrical shape, the air pressure and temperature). Other external factors (such as the shape of the applied electric field and the existence of a static electric field due to thunderstorm clouds before the application of the field due to an incident lightning strike) are not predictable in a deterministic sense.

Data for the breakdown strength of air in an electric field is usually extrapolated from the equivalent value in a uniform field.

Appendix II

DIELECTRIC STRENGTH OF LEXAN

1.0 THERMAL DIELECTRIC STRENGTH

Thermal dielectric strength of Lexan is not constant but is a function of material thickness.

Since it is important to know at what value various thicknesses should break down, five measured values at various thicknesses were obtained (Reference 14).

Values given are:

Thickness (T mils)	1.5	3.0	4.7	23	125
D. Strength (E_b V/mil)	3190	3080	2560	1130	400

When plotted, these values appear to resemble points on a rectangular hyperbola:

$$E_B = \frac{27950}{T + 6.66} + 187.69 \text{ Volts/Mil} \qquad (6)$$

This is plotted in the accompanying graph, Figure 97. The voltage breakdown curve is plotted in Figure 98. An approximation for this, to within ± 5%, for $T \geq 85$ mils, is

$$V_B = 28{,}000 + 188T \text{ Volts} \qquad (7)$$

2.0 IMPULSE DIELECTRIC STRENGTH OF POLYCARBONATE

The impulse dielectric strength of polycarbonate is not constant but is a function of material thickness as is the thermal dielectric strength.

Due to the high dielectric strength and limited size of test samples, it is difficult to cause breakdown in air, and tests are usually performed in a high dielectric strength liquid, such as oil.

Values obtained from "Lexan" material by the manufacturer give the following values, under oil:

Sample Thickness (mils)	30	82	132
Dielectric Strength (volts/mil)	1993	1250	1010
Breakdown Voltage (volts)	9790	102500	133320

Assume impulse dielectric strength is similar in form to thermal (rectangular hyperbola)

T = Thickness E_B = Dielectric Strength Volts/Mil

$(T - A)(E_B - B) = K$

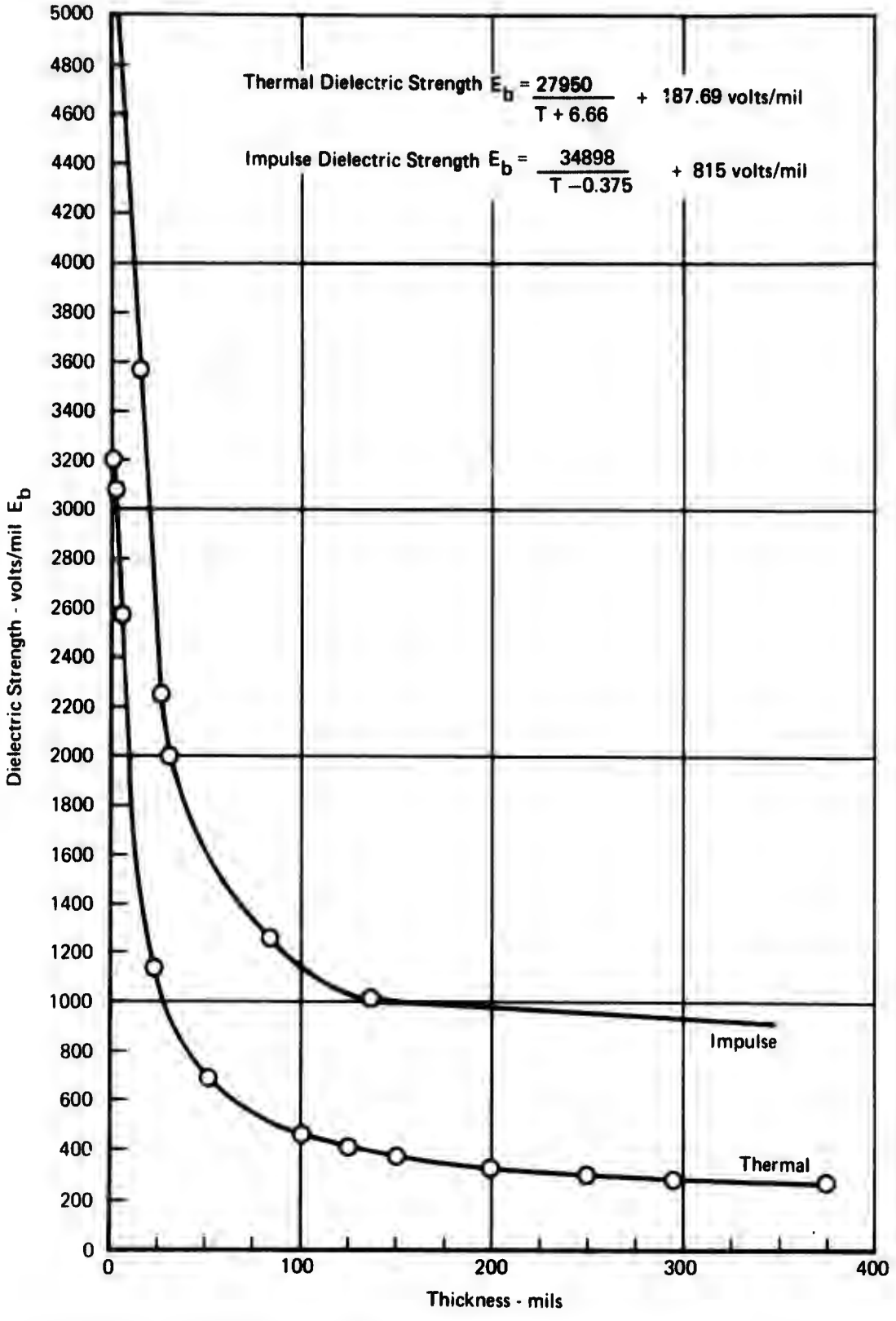

FIGURE 97 THERMAL AND IMPULSE DIELECTRIC STRENGTH OF LEXAN

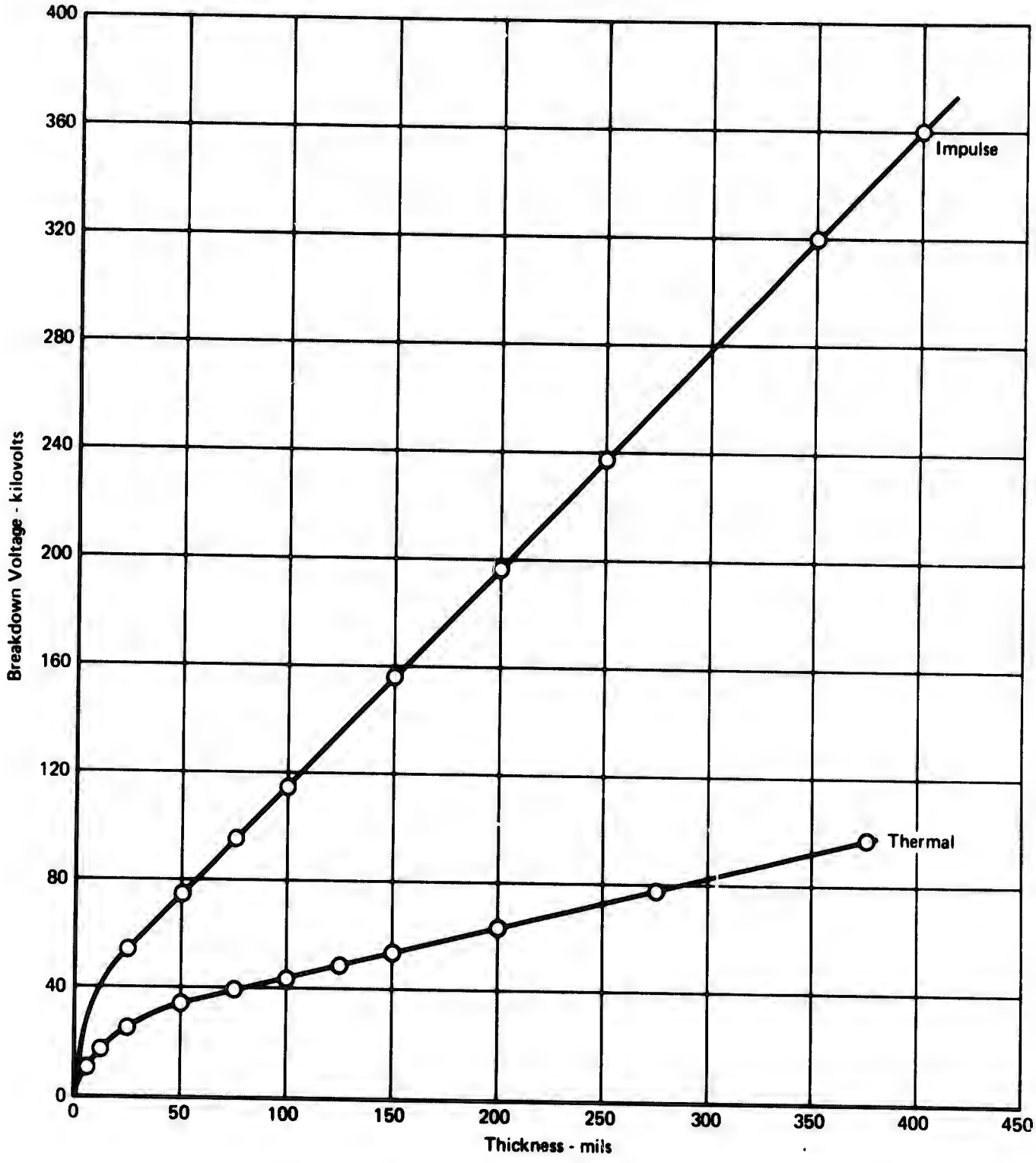

FIGURE 98 LEXAN BREAKDOWN VOLTAGE

Solving as above derivation for the thermal values:

$$E_B = \frac{34898}{T-.375} + 815 \text{ Volts/Mil} \tag{8}$$

and above T = 25 mils

$$V_b = 35000 + 815\ T \tag{9}$$

to within ± 5%.

Appendix III

THE ELECTRIC FIELD IN A DIELECTRIC CYLINDER IN A UNIFORM ELECTRIC FIELD

The following model is used to illustrate the breakdown characteristics of a dielectric canopy in air. For the purpose of this analysis the canopy is taken to be adequately represented by a hollow dielectric cylinder (Figure 99).

In order to investigate the "worst case" conditions the internal surface is set to an equipotential surface. Mathematically this means that the electric field component normal to the surface of the cylinder is greater than it would be in any other configuration. The normal component is the component causing dielectric breakdown and the tangential component is the field causing surface flashover.

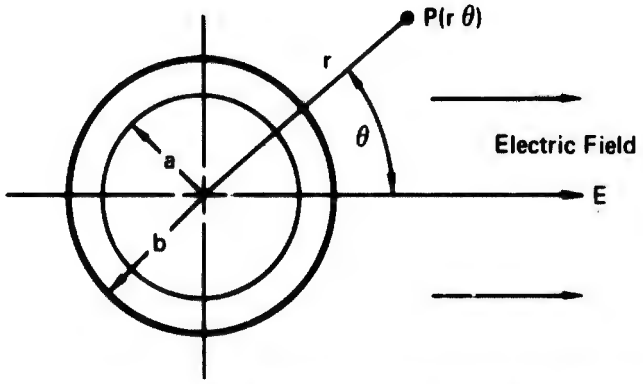

FIGURE 99 DIELECTRIC CYLINDER IN A UNIFORM ELECTRIC FIELD

The solution for the potential at point "P" is (Reference 15):

$$V_o = \left(r - \frac{A}{r}\right) E \cos\theta \qquad r > b \tag{10}$$

$$V_i = \left(Br - \frac{C}{r}\right) E \cos\theta \qquad a < r < b \tag{11}$$

where

$$A = b^2 \frac{[(K+1)a^2 + (K-1)b^2]}{(K+1)b^2 + (K-1)a^2} \quad cm^2 \tag{12}$$

$$B = \frac{2b^2}{(K+1)b^2 + (K-1)a^2} \tag{13}$$

$$C = \frac{2\,a^2b^2}{(K+1)b^2 + (K-1)a^2} \quad cm^2 \tag{14}$$

a = inner radius of cylinder (cm)

b = outer radius of cylinder (cm)

K = relative dielectric constant

Inserting the canopy values:

a = 93.98 cm	A = 8924 cm^2
b = 94.72 cm	B = .335
K = 3	C = 2960 cm^2

The Equations (9) and (10) become

$$V_o = \left(r - \frac{8924}{r}\right) E \cos\theta \tag{15}$$

$$V_i = \left(.335r - \frac{2960}{r}\right) E \cos\theta \tag{16}$$

The voltage across the dielectric is the value of V_i at r = b = 94.72 cm,

$$V_i = .49\ E \cos\theta$$

which is a maximum when cos θ = 1.

Conclusion

The above analysis shows that the maximum voltage across the canopy thickness is approximately half the external field value, i.e., for E = 30 KV per cm, the maximum potential across the dielectric is 14,700 volts and the average electric field is 20 KV per cm (50.73 KV per inch).

The value for long-term thermal breakdown of .29 inches of Lexan is 83 KV, as derived in Appendix II, which is six times greater than the maximum value obtainable in a uniform field. The impulse value is 272 KV.

This result shows that the electric field strength in the Lexan will never reach its punch through value when subjected to the electric field of a lightning strike.

Appendix IV

PHYSICAL MODEL OF LIGHTNING STRIKE

1.0 GENERAL DISCUSSION

The physical model of a lightning strike used throughout the analytical portions of the contract are discussed herein. The model has been validated in light of spectroscopic measurements performed by others in lightning work. (Ref. 16.)

An advancing spark is a very highly ionized column of gas. The electric field may be analyzed by assuming it to be a net line charge λ. The net charge will give a radial electric field (Figure 100) which maintains the intense ionization necessary to replace the loss due to recombination within the discharge.

The net line charge density is derived by assuming the diameter of the discharge to be the envelope of the electric field required to cause ionization of air (30KV per cm).

Calculations of the volume density of total charge can then be calculated and compared to spectroscopic measurements which have been made in actual lightning strikes. The correlation is extremely close. (1.26×10^{23} per cubic meter derived compared with values of 1 to 2×10^{23} per cubic meter or from spectroscopic measurements. (Ref. 17.)

2.0 FIELD DUE TO LINE CHARGE

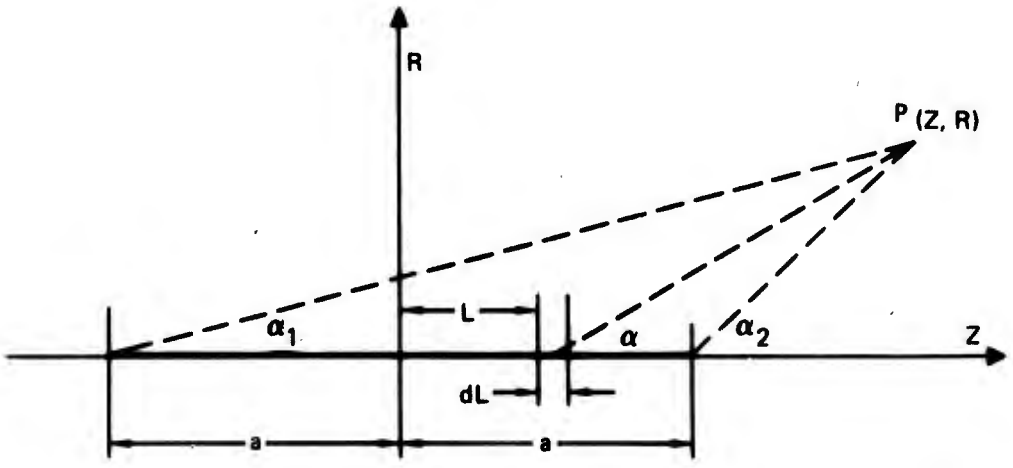

FIGURE 100 FIELD AT P DUE TO A LINE CHARGE λ COULOMB PER METER

If charge lies on Z axis length 2a, field at P due to element dL 'F charge per unit length = λ, then $|dE| = \dfrac{\lambda R L}{4\pi E_o [R^2 + (z-L)^2]}$ (18)

The field at a point P due to the line change can be resolved into the perpendicular components E_z and E_R. (Ref. 17)

$$E_z = \frac{\lambda}{4\pi\varepsilon_o R}\left[\frac{R}{[R^2 + (z-a)^2]^{1/2}} - \frac{R}{[R^2 + (z+a)^2]^{1/2}}\right] \quad (19)$$

$$= \underline{\underline{\frac{\lambda}{4\pi\varepsilon_o R}\ [\sin \alpha_2 - \sin \alpha_1]}} \quad (20)$$

$$E_R = \frac{\lambda}{4\pi\varepsilon_o R}\left[\frac{z+a}{[R^2 + (z+a)^2]^{1/2}} - \frac{z-a}{[R^2 + (z-a)^2]^{1/2}}\right] \quad (21)$$

$$= \underline{\underline{\frac{\lambda}{4\pi\varepsilon_o R}\ [\cos \alpha_1 - \cos \alpha_2]}} \quad (22)$$

For infinite line $a \to \infty$ $E_z \to 0$

and $$E_R = \frac{\lambda}{2\pi\varepsilon_o R} \quad (23)$$

3.0 CALCULATION OF LINE CHARGE DENSITY

Reported values of the diameter of lightning for high current strikes vary from 1-2mm to 1-2cm. If the field for air breakdown is 30,000 volts per cm., this gives a net line charge (if R = 1mm)

$\lambda_e = E_b\ 2\pi\varepsilon_o R$ (From Equation 23)

$$= \frac{3.10^6\ 2\pi \times 10^{-3}}{36\pi \times 10^9}$$

$$= \underline{\underline{16.6 \times 10^{-8}}} \text{ coulombs per meter.}$$

Assuming the velocity of charges is $v = 3 \times 10^6$ meter/second (typical velocity of lightning) and a high current strike of 200K amps occurs, the value of the line current charge density $\lambda_i = I/v$

$$= \frac{2.10^5}{3.10^6}$$

$$= \underline{\underline{66 \times 10^{-3}}} \text{ coulombs per meter}$$

The difference between these two values must indicate that positive ions are present which neutralize the external field but contribute to the current.

Suppose that only singly ionized molecules are present and N_+ and N_- are the number of positive ions and electrons, respectively

λ_e must be due to excess charge of one sign = $(N_+ - N_-)e$

$$\lambda_e = 16.6 \times 10^{-8} = (N_+ - N_-)\ 1.6 \times 10^{-19} \text{ coulomb per meter} \qquad (24)$$

$$(N_+ - N_-) = \underline{\underline{1 \times 10^{12}}} \text{ per meter}$$

where e = electronic charge = 1.6×10^{-19} coulomb.

If

V_+ is velocity of positive ions

V_- is velocity of negative electrons, which is oppositely directed to V_+

e is the electronic charge

$$I = (V_+N_+ + V_-N_-)e = \left(\frac{V_+N_+}{V_-N_-} + 1\right) N_-V_-e \qquad (25)$$

$$\text{Current change density } \lambda_i = \frac{I}{v} = \left(\frac{V_+N_+}{V_-N_-} + 1\right) \frac{N_-V_-e}{v} \qquad (26)$$

Because of the higher mass and scattering cross section of the positive ions they have much lower mobility than electrons and therefore their current contribution in the discharge must be much smaller than the electron current thus Equation 26 may be written

$$\lambda_i = eN_- = 66 \times 10^{-3} \text{ coulombs per meter} \qquad (27)$$

and

$$N_- = \underline{\underline{39.6 \times 10^{16}}} \qquad (28)$$

Using the previous value for the discharge diameter (R=1mm)

$$\text{Electron Volume density} = \frac{N_-}{\pi R^2} \text{ per cubic meter} \qquad (29)$$

$$= \underline{\underline{1.26 \times 10^{+23}}}$$

The positive ion volume density from Equation 24 is given by $(N_+ - N_-)$

$$= \frac{1 \times 10^{12}}{\pi . 10^{-6}} = .32 \times 10^{18} \text{ per cubic meter} \qquad (30)$$

$$N_+ = N_- + .32\ 10^{18} \qquad (31)$$

$$= \underline{1.26 \times 10^{23} + .32 \times 10^{18}}$$

which shows that although the difference $(N_+ - N_-) = .32 \times 10^{18}$ is large, the ratio $\frac{N_+}{N_-} = 1.0000025$ is very nearly unity.

Appendix V

DIVERTER DESIGN

1.0 TEMPERATURE RISE OF A METAL CONDUCTOR DUE TO A HIGH IMPULSE CURRENT FLOW

A conductor subject to a high current flow will generate heat due to the I^2R losses. In the case of a short impulse current, it may be assumed that heat losses during the conduction period are negligible compared to the heat gained.

The following derivation accounts for the resistance change due to the temperature coefficient of resistance. The derivation is specifically related to a square cross section metal diverter (Figure 101).

The differential energy rate $\frac{d\varepsilon}{d\tau}$ is due to a lightning current I flowing in a length of the lightning conductor having a resistance R.

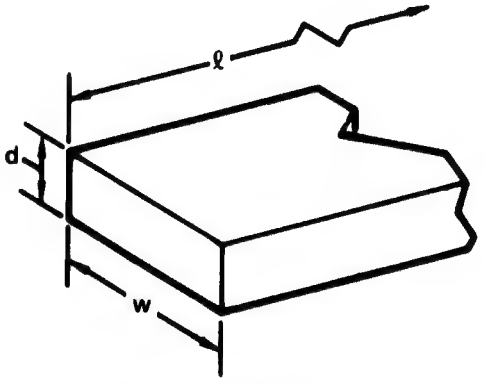

FIGURE 101 DIVERTER DIMENSIONS

Let $T_F - T_o$ = Temperature rise of lightning conductor	^oC
Let d = Thickness of lightning conductor	cm
w = Width of lightning conductor	cm
A = Cross sectional area of lightning conductor	cm^2
ℓ = Length of lightning conductor	cm
ρ = Mass density	$gm\ cm^{-3}$
s = Specific heat	$cal\ gm^{-1}$
r = Resistivity	ohm cm
R = Resistance/cm length = r/A	ohm/cm
R_o = Resistance at T_o	
I = Current in lightning strike	Amps.
$\tau_2 - \tau_1$ = Time duration of strike	seconds

α = Temperature coefficient of resistance

Mass of conductor = M = Apℓ

Differential energy input $d\varepsilon = .238\ I^2 R d\tau = M\ S d\tau$

The bar resistance, R, is a function of the temperature rise.

$$R = R_o\ (1 + \alpha(T - T_o))$$

$$\int_{T_o}^{T_F} \frac{dT}{1 + \alpha(T - T_o)} = \int_{\tau_1}^{\tau_2} \frac{.238\ I^2}{A\ \rho\ S\ \ell}\ \frac{r}{A}\ d\tau \qquad (32)$$

When integrated this leads to:

$$(T_F - T_o) = \frac{1}{\alpha}\ \exp.\left[\frac{.238\ I^2\alpha}{\rho.\ S.\ A^2}\ (\tau_2 - \tau_1)\right] - \frac{1}{\alpha} \qquad (33)$$

The following physical constants were used:

MATERIAL COEFFICIENT	ANNEALED COPPER	99% ALUMINUM	HARD COPPER	LEXAN
S	.093	.214	.093	.3
r	1.7241×10^{-6}	2.82810^{-6}	1.776×10^{-6}	2.1×10^{16}
α	3.93×10^{-3}	3.9×10^{-3}	3.82×10^{-3}	
ρ	8.89	2.7	8.94	1.2

Applying these values to the equation for the temperature rise, the two curves shown in Figure 102 were obtained for copper and aluminum diverters.

2.0 DIFFERENTIAL EXPANSION OF A LIGHTNING STRIP AND THE F-15 LEXAN CANOPY

Thermal expansions of the metal diverter rod mounted on the F-15 canopy may be caused either by the high temperature rise of the diverter when subject to a lightning strike, aerodynamic heating, or ambient temperature when on the ground.

The temperature range encountered by the canopy will be from 275°F, under the worst case aerodynamic heating, down to -35°F due to ambient temperature conditions.

Differential Expansion of Lightning Strip and Canopy

Due to thermal expansion differences the lightning diverter will expand at a different rate than the polycarbonate canopy.

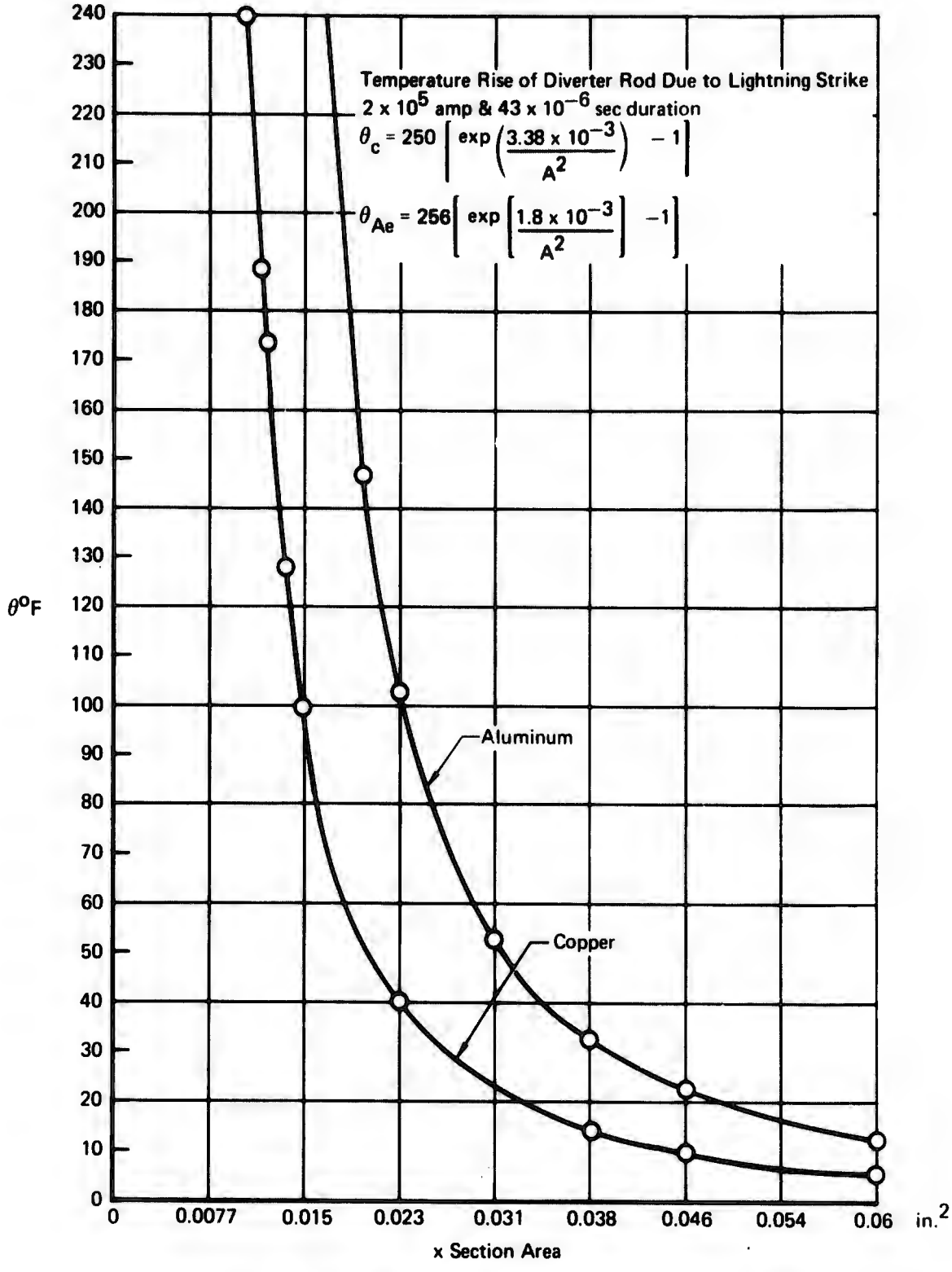

FIGURE 102 TEMPERATURE RISE OF A DIVERTER ROD

Coefficient of Thermal Expansion

LEXAN	$3.75 \times 10^{-5}/°F$
ALUMINUM	$1.59 \times 10^{-5}/°F$
COPPER	$0.89 \times 10^{-5}/°F$

These figures show that Lexan will expand 4.2 times as much as a copper diverter rod and 2.4 times as much as an aluminum rod.

The differences in expansion for a 40 inch copper diverter (attached at 75°F) using the above values are:

.229 inch for a 200°F rise, and

.125 inch for a 110°F fall.

The equivalent values for a 40 inch aluminum diverter are:

.173 inch for a 200°F rise, and

.095 inch for a 110°F fall.

3.0 RECOMMENDED DIVERTER DESIGN

The two diverter designs proven feasible for installation on the F-15 Canopy are the ionizing button strip and the thin metal strip inside the canopy. Figure 103 shows the detail design parameters of the ionizing button strip diverter and Figures 104 and 105 show photographs of an actual strip. Figure 106 shows the canopy installation for both diverters and detail design information for the metal strip inside the canopy.

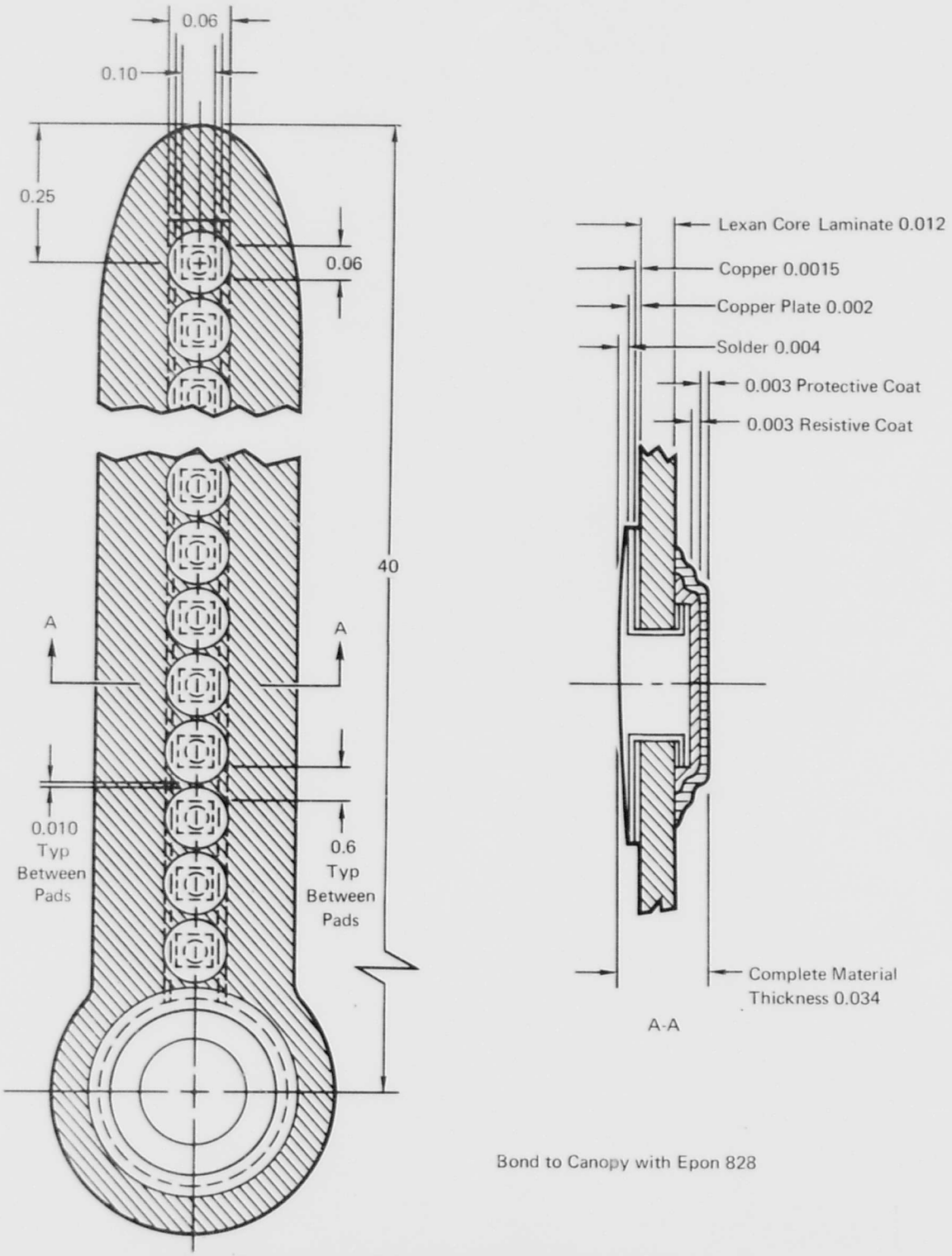

FIGURE 103 IONIZING BUTTON STRIP DIVERTER

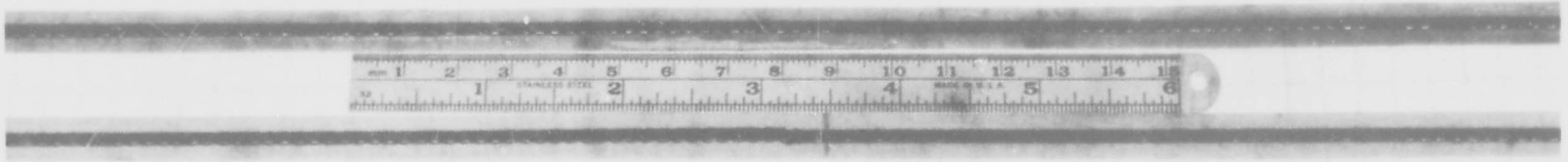

FIGURE 104 RESISTIVE FILM ON REAR OF TWO IONIZING BUTTON STRIPS

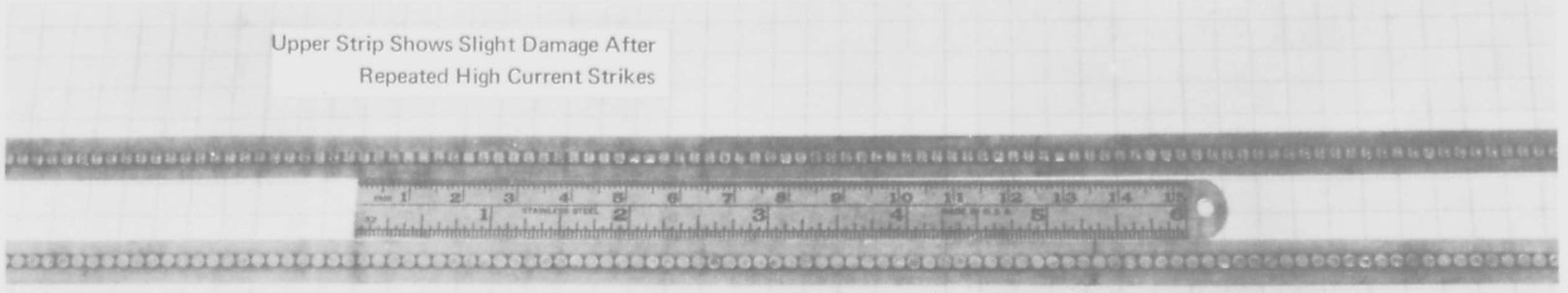

FIGURE 105 BUTTONS ON THE EXPOSED SIDE OF TWO IONIZING BUTTON STRIPS

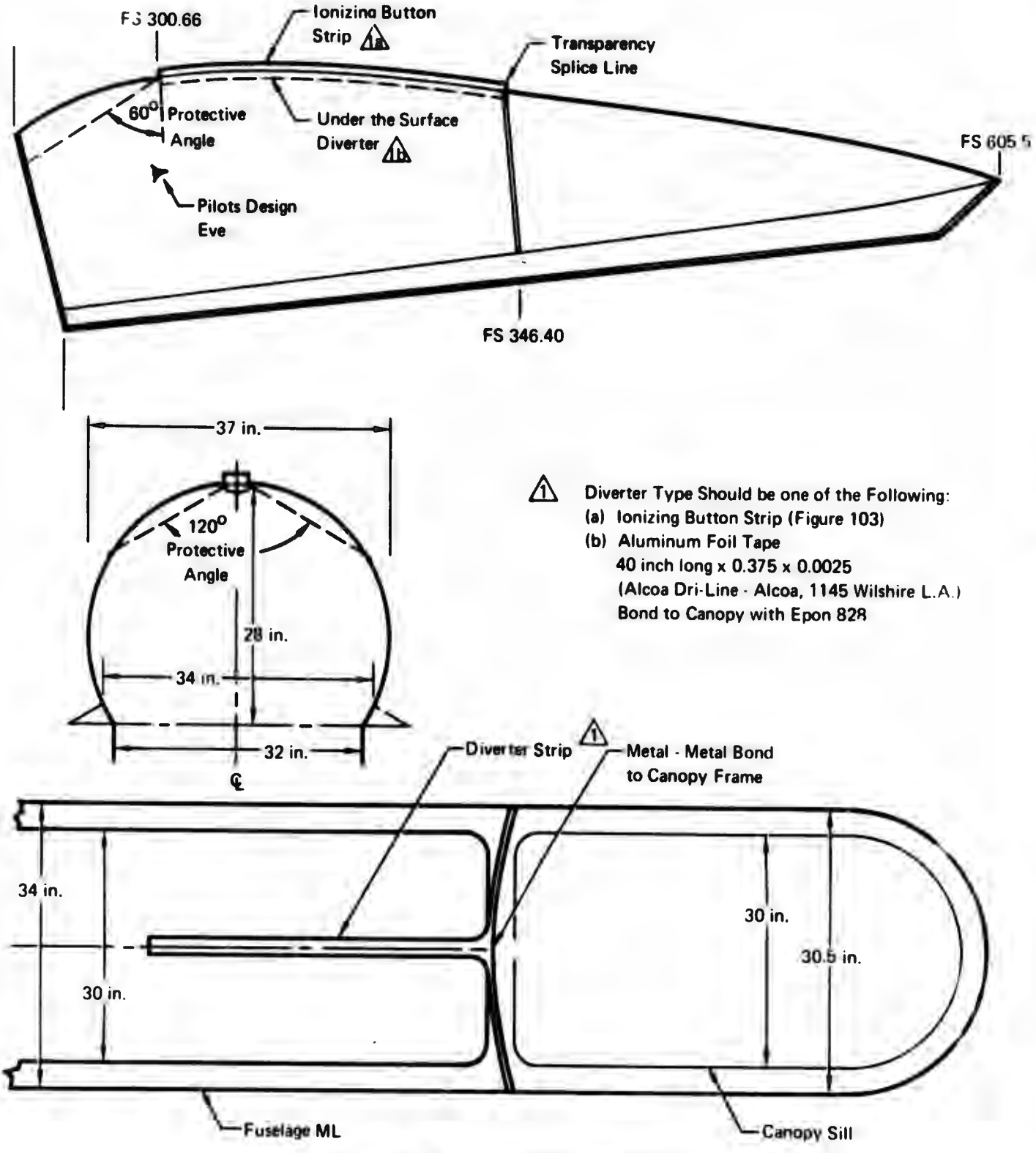

FIGURE 106 DIVERTER POSITION

Appendix VI

SELF FORCE ON A CURVED CURRENT CONDUCTOR

One of the factors to be considered in the design of lightning diverter systems is the mechanical force due to the large currents. This appendix discusses the self force on a curved current conductor.

A model for the outward self force on a curved current conductor has been developed utilizing a more realistic volume current distribution instead of a filamentary (Delta function) type distribution. The outward force is caused by the increase of magnetic induction on the inside of the curve and a decrease on the outside, as in Figure 107. This is a "kink" force which is discussed in connection with plasma instabilities. This force is in addition to other forces due to magnetic fields from the same and/or external circuits.

Usually, this "kink" or self force is small for conductors carrying ordinary currents. However, for conductors carrying extremely large currents, such as those experienced in lighting simulation testing (200K amp), this force is no longer small.

In order to quantify this self force, the following model has been developed. The basic interaction is obtained from integrating the force density:

$$Fu = J \times B \tag{34}$$

where Fu is the force per unit volume, J the current density, and B the magnetic induction. The current density J is assumed as a uniform skin current, since high current lightning strikes have natural frequencies, and may be written as

$$J = \begin{cases} 0 & r < c \\ I/\pi \ (b^2 - c^2) & c \leq r \leq b \\ 0 & r > b \end{cases} \tag{35}$$

where I is the current carried by the wire conductor, b the wire radius, and c the inner radius for the skin current. The assumption of a uniform current density over the outer portions of the conductor (b-c) instead of a more complex form for J can be justified at the end of the calculation by examining the force dependence on c.

The magnetic induction over the curved current conductor is modified from the field of straight current carrying wire B, by

$$B = f \, B_{st} \tag{36}$$

where f is a function which modifies B_{st} to represent the magnetic induction of a curved current conductor. The lines of magnetic induction of a straight current carrying wire are circles concentric with the center of the current conductor and in a plane perpendicular to its axis. When the current conductor is curved, the density of magnetic flux lines are increased on the inside of the curve and decreased on the outside. The function f must represent this variation.

The form of f is determined as follows. Let a designate the radius of curvature of the curved current conductor, Figure 108, and p designate the distance from the center of curvature to some point r (measured from the axis of wire). Let

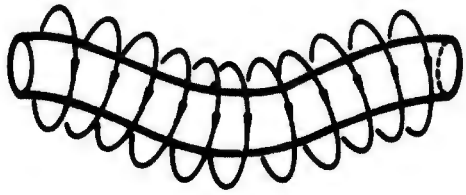

FIGURE 107
MAGNETIC FIELD ABOUT A CURVED CURRENT CONDUCTOR

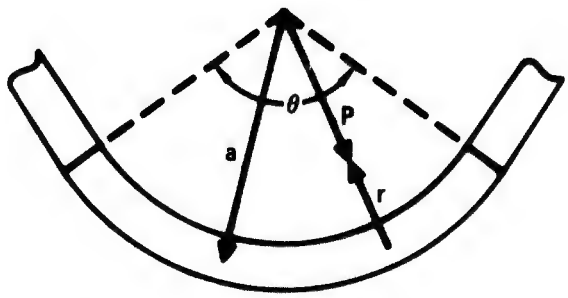

FIGURE 108
CURVED CURRENT CONDUCTOR WITH RADIUS OF CURVATURE a

$\phi(r)$ designate the magnetic flux at r, which is assumed to be constant for straight or curved current conductors. Then, since the magnetic induction is defined as the flux per unit area A, we have

$$f = |B|/|B_{st}| = A_{st}/A_p = a\theta dr/p\theta dr = a/p \tag{37}$$

This function has the required properties of

$$f = \begin{cases} >1 & p < a \\ =1 & p = a \\ <1 & p > a \end{cases} \tag{38}$$

The magnetic induction B_{st} from the current density assumed by (35) is found from the integral form of Amperes Law and is:

$$B_{st} = \begin{cases} 0 & r < c \\ \mu_o J(r^2 - c^2)/2r & c \leq r \leq b \\ \mu_o J(b^2 - c^2)/2r & r > b \end{cases} \tag{39}$$

From Figure 109, for a current into the page, the resulting force F is directed radially into the center of the conductor. For a uniform magnetic field (straight conductor), the net force would be zero. For a curved current conductor with radius of curvature a, laying in the x-z plane, the x component of force is

$$dF_x = JB \cos\alpha \; r \; \ell \; dr \; d\alpha \tag{40}$$

where ℓ is the length of the curved section. For the coordinate system of Figure 110, f is

$$f = a/p = a/(a + x) = a/(a + r\cos\alpha) \tag{41}$$

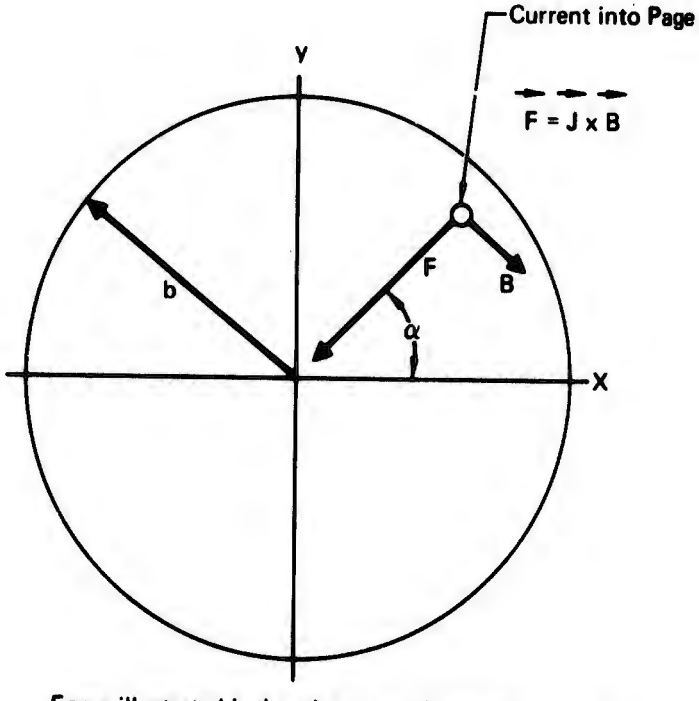

Force illustrated is that due to an elemental current element. For a curved current conductor, the elemental forces do not sum to zero, the result being a net outward force.

FIGURE 109
CONDUCTOR CROSS SECTION

The net outward force is thus

$$F_x = \frac{\mu_o I^2 \ell}{2\pi^2 (b^2 - c^2)^2} \int_c^b dr\ (r^2 - c^2) \int_o^{2\pi} d\alpha\ \frac{a \cos\alpha}{a + r\cos\alpha} \tag{42}$$

Equation 42 can be integrated in open or closed form, each of which illustrates certain features of the solution.

The series solution, obtained by expanding the angular portion of the integrand (since r < a), is

$$F = \frac{\mu_o I^2 \ell}{8\pi a} \sum_{n=o}^{\alpha} \frac{(2n+2)!}{(n+2)(n+1)!^2} \left(\frac{1}{2a}\right)^{2n} \left[(n+1)b^{2n} + nc^2 b^{2n-2} + \ldots + c^{2n}\right] \tag{43}$$

The first two terms of this expansion are explicitly:

$$F = \frac{\mu_o I^2 \ell}{8\pi a} \left[1 + \frac{2b^2 + c^2}{4a^2} + \ldots\right] \tag{44}$$

An examination of (44) shows that when the wire radius b is much less than the radius of curvature a, then: (1) the first term is sufficient and is accurate to 10% for b/a < .36; (2) the force is independent of wire radius and the assumed form of the current distribution.

The closed form solution, obtained by integrating in the complex plane to obtain the angular integral, is

$$F = \frac{\mu_o I^2 \ell a}{\pi (b^2 - c^2)^2} \left[(b^2 - c^2)/2 + a(a^2 - b^2)^{1/2} + c^2 \ln\left(\frac{a + (a^2 - b^2)^{1/2}}{a + (a^2 - c^2)^{1/2}}\right)\right] \tag{45}$$

Equation (45) is useful for evaluating the force for the case where the wire radius approaches the radius of curvature (sharp bend) for a uniform current distribution. Thus, for c = o, we have

$$F \xrightarrow[\substack{c = o \\ b \to a}]{} \frac{\mu_o I^2 \ell}{2\pi a} \tag{46}$$

A comparison of this result to the first term of Equation (44) shows that the outward force is four times greater for a sharp bend, b/a → 1, than for a gentle bend, b/a<<1.

For a gentle bend, the first term of Equation (44) can be interpreted as the outward force distributed over the length of the curved section. The total force is

$$F = \frac{\mu_o I^2 \theta}{8\pi} \tag{47}$$

since $\ell = a\theta$, where θ is the angle of the bend (Fig. 108).

To gain an idea of the magnitude of this force, for a gentle right angle bend, the current required for one pound of force is 7,550A. For 200K amp, the resulting force is 705 pounds.

Appendix VII

LIGHTNING SIMULATION FACILITY

The MCAIR Lightning Simulation Facility in St. Louis is equipped to conduct extensive studies of lightning mechanisms and phenomena, and lightning damage to aerospace systems and components, either on models or on full-scale flight systems. The facility uses an array of high-voltage, high-current, and high-coulomb sources to simulate the various aspects of lightning. The facility includes: (a) a 1.5 million volt Marx Surge Generator, (b) more than 100 kilojoules of current surge generators, (c) a 5,000 volt, 25 ampere dc power supply, and (d) a 300 volt, 500 ampere dc power supply. The 500 ampere supply is mated to a 30 kilojoule capacitor bank to produce a composite high peak current and high coulomb simulation, conforming to MIL-A-9094D. Additional capacitor banks are available with different current, voltage and discharge frequency characteristics. A 5-million volt Marx Surge Generator and a 600 kilojoule, 240 kilovolt High Current Generator have both been funded and will be available for full-scale aircraft testing early in 1972.

High Voltage Testing

The existing Marx Surge Generator has an energy storage capacity of 4,000 joules and is capable of generating a 8.5-foot spark to the test model. The generator can be used to study model attach points, dielectric surface flashover, and high electric field breakdown mechanisms. It consists of 66 stages of 25 kilovolt, 0.2 uF capacitors. The system is charged by a 0-30,000 volt, 5 mA dc power supply which contains the triggering and safety dump circuit controls. The output voltage and current waveforms are monitored by synchronized oxcilloscopes and cameras.

High Current Testing

The high current equipment was designed to meet or exceed all military and FAA specifications for lightning simulation tests. The Multi-Component Simulator is comprised of three subsystems, each of which produces a different strike component, and each of which can be operated individually or in timed sequence. The system is normally operated in an explosion proof concrete test cell which has remote viewing and control facilities. The system is designed to produce in a typical specimen the primary 200,000 ampere peak followed by a 2,000 ampere surge, followed in turn by the high coulomb dump as defined in MIL-A-9094D. If tests do not require all of the strike components, any combination of the components is available.

The primary current peak is generated by the discharge of a 60 kilojoule high-voltage capacitor bank. The secondary peak is generated by a capacitive-inductive circuit whose energy source is a 1,250 volt capacitor bank. The high coulomb surge is generated by a DC rectifier power supply with a surge capability of 500 amps at 200 volts (for several seconds).

The high peak current subsystem can meet the specifications of MIL-B-5087B. The design of the system was based on high-energy capacitor bank experience at MCAIR. The deactivated MCAIR Hypervelocity Impulse Tunnel capacitor bank, rated

at 7 megajoules, has been used as a source of capacitors for lightning tests. Preliminary testing has shown that 30,000 joules (0.4% of available energy) is adequate to produce 300,000 amperes with the desired wave shape, in a low impedance test article. Large high impedance structures and composite structures necessitate additional energy to produce the required current, but the additional capacitance is readily available and easily incorporated into the basic 60 kilojoule assembly.

The MCAIR Lightning Simulation Facility is located near a flight apron and can be used to conduct tests on full-sized vehicles as well as laboratory tests of models and components. In addition, a full array of laboratory support facilities is available, including conventional and precision machine shops, calibration and standards laboratories, service equipment supply cribs, damage analysis laboratories, and other conventional support.

Photographic equipment is available for monitoring and diagnostic studies. Still cameras, both polaroid and standard 35-mm, are supplemented by simultaneous high-speed streak and framing information. Our Beckman and Whitley Model 200 Simultaneous Streak and Framing Camera has a framing rate of 2.2 million frames per second and a streak writing rate of 28 mm/usec. In addition, a medium speed 35,000 frame per second framing camera is available for recording phenomena, such as swept-strokes, occuring in the millisecond time range.

REFERENCES

Cited References

1. R. Aston, "Scale Model Lightning Attach Point Study", MCAIR Report Number A0719 TIS CP020GF11.

2. A.S.T.M., "Standard Methods of Test for Dielectric Strength of Electrical Insulating Materials at Commercial Power Frequencies". U.S.A. Standard C59-68-1968 Designation D 149-64.

3. M. A. Uman, "A Comparison of Natural Lightning and the Long Laboratory Spare with Application to Lightning Testing". FAA Report Number NA-69-27 (DS-69-16).

4. J. D. Cobine, Gaseous Conductors, Dover Publications, 1958.

5. J. C. Anderson, Dielectrics, Reinhold Publishing Corporation, 1964.

6. J. H. Mason, "Breakdown of Solid Dielectrics in Divergent Fields", I.E.E. Proceedings Vol 102C, pp 254-263, 1955.

7. E. J. McMahon, "Surface and Volume Phenomena in Dielectric Breakdown of Polyethylene", A.I.E.E. Transactions, December 1963.

8. R. Cooper, "The Electric Strength of Solid Dielectrics", British Journal of Applied Physics, Vol. 17, 1966.

9. K. H. Stark and C. G. Garton, Nature Lond. Vol. 176, p. 1225 (1955).

10. R. A. Fava, Proceedings IEE. Vol. 112, pp 819-25, 1965

11. I.D.C. Ball, Proc. IEE. Vol. 98, pp 84-6, 1957

12. A. Charlesby, Proc. Royal Society A 218 00 245-55, 1953

13. J. Harrell and D. C. Voss, "High Temperature Transparencies". MCAIR Interim Report EMA-GEO-750, 1969.

14. Christopher and Fox, Polycarbonates, Reinhold Publishing Corporation, 1962.

15. W. R. Smythe, Static and Dynamic Electricity, McGraw Hill, 1968.

16. R. E. Orville, "A High Speed Time Resolved Spectroscopic Study of the Lightning Return Stroke", Journal of Atmospheric Sciences, Vol. 25, No. 5 Sept. 1968, pp 839-856.

17. W. E. Rogers, Electric Fields, McGraw Hill, 1954, p 34.

UNCLASSIFIED

Security Classification

DOCUMENT CONTROL DATA - R & D

Security classification of title, body of abstract and indexing annotation must be entered when the overall report is classified)

1. ORIGINATING ACTIVITY (Corporate author)

McDonnell Aircraft Company
St. Louis, Missouri

2a. REPORT SECURITY CLASSIFICATION

Unclassified

2b. GROUP

N/A

3. REPORT TITLE

LIGHTNING PROTECTION TECHNIQUES FOR LARGE CANOPIES ON HIGH SPEED AIRCRAFT

4. DESCRIPTIVE NOTES (Type of report and inclusive dates)

5. AUTHOR(S) (First name, middle initial, last name)

Robert Aston, Ronald Gorton, Gustave L. Weinstock

6. REPORT DATE	7a. TOTAL NO. OF PAGES	7b. NO. OF REFS
January 1972	106	17

8a. CONTRACT OR GRANT NO.	9a. ORIGINATOR'S REPORT NUMBER(S)
F33615-71-C-1581	
b. PROJECT NO.	
c.	9b. OTHER REPORT NO(S) (Any other numbers that may be assigned this report)
d.	AFAL-TR-72-49

Distribution limited to U.S. Gov't. agencies only; Test and Evaluation; 27 JUN 1972. Other requests for this document must be referred to

10. DISTRIBUTION STATEMENT ~~This document is subject to special export controls and each transmittal to foreign governments or foreign nationals may be made only with prior approval~~ of AFAL/AAA, Wright-Patterson AFB, Ohio 45433.

11. SUPPLEMENTARY NOTES	12. SPONSORING MILITARY ACTIVITY
N/A	Air Force Avionics Laboratory Air Force Systems Command Wright-Patterson Air Force Base, Ohio

13. ABSTRACT

The objectives of the work covered by this report were to determine by analysis and experimental evaluation the susceptibility of an F-15 canopy to a lightning strike and to develop lightning protection methods for large canopies.

The primary hazard from a lightning strike to an aircraft canopy occurs if the canopy punctures and the lightning strikes the pilot. This hazard was analyzed mathematically and extensively tested on flat polycarbonate sheets, a simulated canopy and an actual F-15 canopy. Both the analysis and lightning simulation tests showed that the F-15 canopy will not puncture but rather that the lightning would flashover to the canopy frame.

A detailed experimental investigation of corona inside the canopy due to the electric field from a lightning strike was performed. The investigation showed corona not to be a serious hazard but final assessment would require a medical study.

High current tests were performed on the canopy frame and proved that the canopy mounting and frame could withstand 200,000 amp currents. Three lightning diverter systems were designed and tested. Two of the designs proved effective for large canopy application.

The conclusion arrived at as the result of this program is that additional lightning protection for the F-15 canopy is not necessary. Furthermore, it should be noted that although an F-15 canopy was used in this study, the results are general enough that they can be usefully extrapolated to include the canopies and dielectric surfaces of other air vehicles.

DD FORM 1 NOV 68 1473

UNCLASSIFIED

Security Classification

14 KEY WORDS	LINK A		LINK B		LINK C	
	ROLE	WT	ROLE	WT	ROLE	WT
Lightning Protection						
Lightning Diverter						
Aircraft Canopy Protection						
LEXAN Breakdown						
Dielectric Breakdown						
Corona						
Pilot Hazard						
Flashover						